



TECHNISCHE UNIVERSITÄT MÜNCHEN

Integrative Research Center Campus Straubing für Biotechnologie und Nachhaltigkeit

# Chitin based composite materials

Yaqing Duan

Vollständiger Abdruck der von der promotionsführenden Einrichtung Campus Straubing für Biotechnologie und Nachhaltigkeit der Technischen Universität München zur Erlangung des akademischen Grades eines

**Doktors der Naturwissenschaften (Dr. rer. nat.)**

genehmigten Dissertation

Vorsitzender: Prof. Dr.-Ing. Jakob Burger

Prüfer der Dissertation: 1. Prof. Dr. Cordt Zollfrank

2. Prof. Dr. Werner Kunz

Die Dissertation wurde am 01.10.2020 bei der Technischen Universität München eingereicht und von der promotionsführenden Einrichtung Campus Straubing für Biotechnologie und Nachhaltigkeit am 04.12.2020 angenommen.



## **Foreword**

This cumulative dissertation is based on three original published papers with closely related topics. The author of the present dissertation authored two of the papers as the first author and one as co-author. All the three original published papers contain results and findings were obtained through own practical work.

A: Duan Y, Freyburger A, Kunz W, Zollfrank C. Cellulose and chitin composite materials from an ionic liquid and a green co-solvent. *Carbohydrate Polymers*, 192, 159-165 (2018). DOI: 10.1016/j.carbpol.2018.03.045.

B: Duan Y, Freyburger A, Kunz W, Zollfrank C. Lignin/chitin films and their absorption characteristics for heavy metal ions. *ACS Sustainable Chemistry and Engineering* 6, 6965–6973 (2018). DOI: 10.1021/acssuschemeng.8b00805.

C: Auriane Freyburger, Yaqing Duan, Cordt Zollfrank, Thomas Röder, and Werner Kunz. Chitin Coated Cellulosic Textiles as Natural Barrier Materials. *Lenzinger Berichte* 94, 105-113 (2018).



## Summary

The polysaccharide chitin is one of the most abundant biopolymers in nature. Due to its excellent properties such as biocompatibility, biodegradability, non-toxicity, and adsorptive abilities, chitin is of high commercial interest. However, the lack of a clear and accessible melting point, as well as insolubility in regular solvents hinder the development of chitin in creating high value-added materials both by solid and solution processing. To overcome these limitations, this work focus on the investigation and development of chitin based high performance biocomposite materials. The other two most abundant biopolymers cellulose and lignin are used in this thesis for the fabrication of biocomposite materials with chitin.

In this work, chitin based composite materials such as chitin/cellulose and chitin/lignin composite materials are primarily fabricated via solution processing. Several different solvents were investigated concerning their solubility on the biopolymers. Finally, the solvent system comprises from the ionic liquid 1-butyl-3-methylimidazolium acetate (BminOAc) together with a bio-based co-solvent,  $\gamma$ -valerolactone (GVL) is considered as the most efficient solvent for the dissolution of the three biopolymers.

The obtained composite chitin/cellulose materials from different solvent systems were characterized in detail employing spectroscopic, morphological, and mechanical analysis methods. The results illustrate that chitin/cellulose composites can be successfully obtained from the two solvent systems as BmimOAc-GVL and DMAc/LiCl. Compared to DMAc/LiCl, the solvent system of BmimOAc-GVL is more sustainable and environmentally benign. It is therefore considered as an efficient solvent for the fabrication of the chitin/cellulose composite materials. Furthermore, it should be noted that chitin is not deacetylated into chitosan during dissolving in BmimOAc-GVL, which is critical for the use of intact chitin in composite materials. Besides, the used BmimOAc can be fully recycled, which indicates that the dissolution process is sustainable and environmentally friendly. The wetting and permeability studies were additionally performed on the composite chitin/cellulose composite films as well as the chitin coated cellulosic materials. The analytical results confirm that the presence of chitin rendered all the composites, the surface of the wood and cellulosic textiles more hydrophobic. Because the chitin layer coated on the cellulosic textile slows down the penetration of water and oxygen (O<sub>2</sub>), it is considered to have potential applications as packaging materials or impregnating textiles.

The fabrication of chitin/lignin composite films is successfully performed via solution processing using the same solvent system (BmimOAc-GVL) as with chitin/cellulose composites. The potential application of the chitin/lignin composites as a bio-film sorbent for environmental remediation is studied in this work. The result illustrates that the chitin/lignin composite films exhibit a high adsorption capacity for Fe(III) and Cu(II) cations from aqueous solutions. Furthermore, some excellent properties of the composite film such as stability in aqueous solution, facile as well as reusability suggest that it might be utilized as a biosorbent in water purification.

## **Zusammenfassung**

Das Polysaccharid Chitin ist weltweit eines der häufigsten natürlichen Biopolymere. Aufgrund seiner herausragenden Eigenschaften wie der Biokompatibilität, der Bioabbaubarkeit, der Ungiftigkeit und seinem Potential als Adsorber, ist Chitin für die Industrie von besonderem Interesse. Aufgrund der Nichtvorhandensein ein definierten Schmelzpunktes und seine Unlöslichkeit in organischen Lösemitteln steht eine Herausforderung für die Entwicklung von chitinbasierten Hoheleistungswerkstoffen da. Um diese Einschränkungen zu überwinden, wurden in dieser Arbeit chitinbasierte Kompositmaterialien mit dem Ziel untersucht, neuartige Bioverbundwerkstoffe zu entwickeln. Cellulose und Lignin, ebenfalls sehr häufig in der Natur auftretende Biopolymere, wurden im Rahmen dieser Arbeit dazu verwendet, um Verbundwerkstoffe mit Chitin zu generieren.

Chitinbasierte Verbundwerkstoffe wie Chitin/Cellulose- und Chitin/Lignin-Komposite wurden im Wesentlichen aus einer Lösung hergestellt. Hierfür ist ein nachhaltiges Lösemittel für diese Biopolymere wünschenswert. In dieser Arbeit wurden verschiedene Lösemittelsysteme hinsichtlich ihrer Lösekraft von Biopolymeren untersucht. Als vielversprechendstes und zugleich umweltfreundlichstes Lösemittel stellte sich die ionische Flüssigkeit, 1-Butyl-3-methylimidazoliumacetat (BmimOAc) mit dem biobasierten Co-Lösungsmittel  $\gamma$ -Valerolacton (GVL) heraus.

Die so aus verschiedenen Lösemittelsystemen gewonnenen Chitin/Cellulose-Verbundwerkstoffe wurden genauer mittels spektroskopischer, morphologischer und mechanischer Analysemethoden detailliert untersucht. Die Analysen ergaben, dass Chitin nicht zu Chitosan deacetyliert wurde, was für die Verwendung von unmodifiziertem Chitin in Verbundwerkstoffen entscheidend ist. Es konnte weiterhin gezeigt werden, dass die mittels BmimOAc-GVL (8:1, mol:mol) hergestellten Komposite ebenso gute Ergebnisse zeigten wie die mittels DMAc/LiCl erzeugten. Allerdings ist die BmimOAc-GVL-Route nachhaltiger und umweltfreundlicher, weshalb die Chitin/Cellulose-Komposite in dieser Arbeit auf diese Weise gefertigt wurden. Darüber hinaus kann das verwendete BmimOAc recycelt werden, wodurch die ionische Flüssigkeit in mehreren Prozesszyklen eingesetzt werden kann, ohne dass sich dabei eine merkliche Verschlechterung der Eigenschaften der Komposite einstellte. Außerdem zeigten Benetzbarkeits- und Permeabilitätsversuche sowohl an Chitin/Cellulose-Verbundwerkstoffen als auch an mit Chitin beschichteten Cellulosegeweben, dass durch das Chitin die Oberflächen von Holz und Cellulosestextilien hydrophobisiert werden können. Zudem verringerte die

Chitinbeschichtung neben dem Eindringen von Wasser auch die Sauerstoffdiffusion, wodurch ein Potential für eine mögliche Anwendung als Verpackungsmaterial oder undurchlässige Gewebe für Hygieneartikel gegeben ist.

Die Herstellung von Chitin/Lignin-Kompositen erfolgte ebenfalls mittels BmimOAc-GVL (8:1, mol:mol). In dieser Arbeit wurde eine mögliche Anwendung dieses Verbundwerkstoffs als biobasiertes Adsorptionsmittel in Form einer Folie untersucht. Es zeigte sich, dass der Biosorptionsfilm ein hohes Adsorptionsvermögen für Fe(III)- und Cu(II)-Kationen in wässrigen Lösungen aufwies. Des Weiteren sind eine hohe Stabilität, eine einfache Anwendbarkeit, eine leichte Desorption und eine gute Wiederverwendbarkeit kennzeichnend für die Kompositfolie, weshalb eine mögliche Anwendung der Einsatz als neuartiges und erneuerbares Biosorptionsmittel für die Wasseraufbereitung sein kann.

# 1 Contents

Foreword.....	I
Summary.....	III
Zusammenfassung.....	V
List of Figures.....	IX
List of Tables.....	XI
Abbreviations .....	XIII
1 Introduction.....	1
1.1 Chitin based composite materials.....	1
1.2 Structures, properties and applications of the biopolymers.....	3
1.2.1 Chitin.....	3
1.2.2 Cellulose .....	6
1.2.3 Lignin .....	9
1.3 Processing technologies for chitin based composite materials .....	13
1.3.1 Chitin/cellulose composite materials.....	14
1.3.2 Chitin/lignin composite materials .....	16
1.4 Motivation and scientific work hypothesis .....	17
2 Experimental section.....	19
2.1 Materials and chemicals.....	19
2.1.1 Biopolymers .....	19
2.1.2 Chemicals .....	19
2.2 Preparation of solvents for the dissolution of biopolymers .....	20
2.2.1 DMAc/LiCl (8%, w:w).....	20
2.2.2 DES .....	20
2.2.3 Ionic liquids and co-solvent .....	21
2.3 Dissolution of biopolymers in various solvents.....	21
2.3.1 Dissolution of chitin and cellulose in DMAc/LiCl .....	21
2.3.2 Dissolution of chitin and cellulose in DES.....	22
2.3.3 Dissolution of chitin and cellulose in AmimBr and EmimOAc.....	23
2.3.4 Dissolution of chitin and cellulose in BmimOAc-GVL.....	23
2.3.5 Dissolution of chitin and lignin in BmimOAc-GVL .....	23
2.4 Fabrication of chitin based composite materials .....	24
2.4.1 Composite chitin/cellulose materials.....	24
2.4.2 Chitin coated cellulosic materials.....	25

2.4.3	Chitin/lignin composite materials .....	26
2.5	Characterization .....	27
2.5.1	Dissolution of the biopolymers.....	27
2.5.2	Scanning electron microscopy.....	27
2.5.3	Elemental analysis .....	27
2.5.4	Fourier transform infrared spectroscopy (FTIR).....	28
2.5.5	X-ray diffraction .....	28
2.5.6	Mechanical testing .....	28
2.5.7	Dimensional changes.....	28
2.5.8	Water contact angle and water absorption capacity of chitin/cellulose composites .....	29
2.5.9	Water and oxygen permeability of chitin coated cellulosic textiles .....	29
2.5.10	Ion adsorption/desorption of chitin/lignin composite.....	29
3	Results and discussion .....	31
3.1	Solubility of chitin, cellulose and lignin in various solvent systems.....	31
3.1.1	Dissolution of chitin and cellulose in DMAc/LiCl .....	33
3.1.2	Dissolution chitin and cellulose in DES.....	34
3.1.3	Dissolution of chitin in AmimBr and cellulose in EmimOAc.....	35
3.1.4	Dissolution of chitin and cellulose in BmimOAc-GVL.....	36
3.1.5	Dissolution of chitin and lignin in BmimOAc-GVL .....	37
3.2	Characterization of chitin based composite materials .....	38
3.2.1	Composite chitin/cellulose materials fabricated from DMAc/LiCl.....	38
3.2.2	Chitin/cellulose composite materials from AmimBr and EmimOAc .....	40
3.2.3	Chitin/cellulose composite materials from BmimOAc- GVL.....	41
3.2.4	Chitin film coated materials .....	45
3.2.5	Chitin/lignin composite films from BmimOAc-GVL.....	46
3.2.6	Chitin/lignin composite materials from melt compounding process .....	47
	Publication #A .....	49
	Publication #B .....	65
	Publication #C .....	85
4	Conclusion.....	97
	References:.....	101
	Appendices .....	109
	Acknowledgement.....	111

## List of Figures

<b>Figure 1.1:</b> Chitin source and the commercial powder. ....	4
<b>Figure 1.2:</b> Chemical Structure of chitin. ....	4
<b>Figure 1.3:</b> Partially deacetylated chitin (a), fully deacetylated chitin (b) and deacetylation of chitin (c). ....	6
<b>Figure 1.4:</b> Conversion of lignocellulosic plant source into cellulose powder.....	7
<b>Figure 1.5:</b> Chemical structure of cellulose and its intra molecular hydrogen bonds (a) and the crystalline and amorphous regions in cellulose (b). ....	8
<b>Figure 1.6:</b> Three essential components of wood. ....	10
<b>Figure 1.7:</b> The structures of the three monolignols and their subunits. ....	11
<b>Figure 1.8:</b> Kraft pulping process. ....	13
<b>Figure 1.9:</b> General scheme of the solution processing for the fabrication of chitin/cellulose composite materials. ....	15
<b>Figure 1.10:</b> Processing schemes for the fabrication of chitin/cellulose and chitin/lignin composites.....	18
<b>Figure 2.1:</b> Scheme of the activation process for chitin and cellulose .....	21
<b>Figure 2.2:</b> The preparing process of the chitin film coated on the surface of wood. ....	26
<b>Figure 3.1:</b> (i) Visual appearances of mixtures containing of (a) 3 wt% chitin, (b)1 wt% chitin and 3 wt% MCC, (c) 0,6 wt% chitin and 4 wt% MCC, (d) 0,4 wt% chitin and 5 wt% MCC, (e) 10 wt% MCC in DMAc/LiCl (8%, w:w) within 2h; (ii) Selected optical microscopy images of the mixtures containing (a) 3 wt% chitin, (b) 10 wt% MCC and (c)1 wt% chitin and 3 wt% MCC.....	34
<b>Figure 3.2:</b> Visual appearance of the mixtures containing (a) 1 wt% chitin and (b) 1 wt% MCC, in choline chloride/urea (molar ratio: 1:2); (c) 1 wt% chitin and (d) 1 wt% of MCC, in choline chloride/thiourea (molar ratio: 1:2).....	35
<b>Figure 3.3:</b> Visual appearance and corresponding light microscopy images of the obtained mixtures containing (a, b) chitin (2 wt%) in AmimBr; (c, d) MCC (8 wt%) in EmimOAc, .....	36
<b>Figure 3.4:</b> (i) Visual appearances and light microscopy images of the mixtures containing 1wt% chitin and 4 wt% MCC in solvent with different molar ratios of BmimOAc to GVL (without GVL (a), 4:1(b), 8:1 (c)). (ii) Light microscopy images of mixtures containing 2 wt% chitin in BmimOAc-GVL (molar ratio: 8:1) within (a) 1h, (b) 2h, (c) 3h under the selected experimental conditions.....	37

**Figure 3.5:** Photographs (i) and SEM micrographs (ii) of the chitin/cellulose composite films fabricated from DMAc/LiCl (8%, w:w) (a) chitin, (b) cellulose, (c) composite film with 25 wt% chitin concentration. .... 38

**Figure 3.6:** ATR-FTIR spectra of the films prepared from DMAc/LiCl (8%, w:w): (a) cellulose, (b) chitin, (c) composite film with 25 wt% chitin concentration. .... 39

**Figure 3.7:** Water contact angles of the chitin/cellulose composite films with different concentrations of chitin regenerated from DMAc/LiCl. .... 40

**Figure 3.8:** (i) Photographs of films (a) cellulose, (b) composite film with 20 wt% chitin concentration, (c) composite film with 33 wt% chitin concentration, (d) unsuccessfully regenerated chitin; (ii) the SEM micrographs of (a) cellulose, (b) composite film with 20 wt% chitin concentration, (c) composite film with 33 wt% chitin concentration. .... 41

**Figure 3.9:** Visual appearances of the obtained gel and films before drying (pure chitin (a, d) pure cellulose (b, e) and (b) composite film with 20 wt% chitin concentration, (c) composites with 20 wt% chitin concentration (c, f)). .... 42

**Figure 3.10:** Composite gel (i) and film (ii) with 50 wt% chitin concentration with different drying methods (a) wet; (b) drying with scCO<sub>2</sub>; (c) drying at ambient conditions; (d) drying with compressed air. .... 44

**Figure 3.11:** The photographs of the spruce cubes coated with chitin film and without chitin film (a,) and SEM micrographs of the surface of spruce cubes coated with chitin film (b, c). ... 45

**Figure 3.12:** Water absorption time and contact angles of the wood samples non-coated and coated with chitin film. .... 46

**Figure 3.13:** Chitin/lignin composite material (CL\_3) fabricated by melt compounding. .... 47

**Figure A.1:** Teflon mould for preparing the chitin based composite gel (a) and film (b). .... 105

**Figure A.2:** Light microscopy images of mixtures containing (a) 30 wt%, (b) 35 wt% Kraft lignin in BmimOAc-GVL (mass ratio: 4:1) under the selected experimental conditions. .... 105

## List of Tables

<b>Table 2.1:</b> Preparation of composite materials with different cellulose to chitin molar ratios with DMAc/LiCl (8%, w:w). CC: chitin/cellulose composite. ....	22
<b>Table 2.2:</b> Mixtures with different chitin to cellulose molar ratios in choline chloride/urea and choline chloride/thiourea. CC: chitin/cellulose composite. ....	22
<b>Table 2.3:</b> Preparation of composite materials with different cellulose to chitin molar ratios with AmimBr and EmimOAc. CC: chitin/cellulose composite. ....	23
<b>Table 2.4:</b> Composite chitin/lignin materials with different concentrations of chitin, lignin and BmimOAc solvent prepared .....	27
<b>Table 3.1:</b> Maximum solubility of $\alpha$ -chitin and microcrystalline cellulose native powders in various solvent systems as well as their dissolution conditions (NS: Not soluble; *: incompletely dissolution). ....	32
<b>Table 3.2:</b> Maximum solubility of Kraft lignin in various solvent systems as well as its dissolution conditions (NS: Not soluble). ....	33
<b>Table 3.3:</b> Measured absorption bands of samples with assignment to the type of atomic vibration. ....	39
<b>Table 3.4:</b> Linear shrinkage of the composite chitin/cellulose composite gels/films after drying with three different drying methods. ....	44



## **Abbreviations**

AmimBr	1-Allyl-3-methylimidazolium bromide
BmimOAc	1-Butyl-3-methylimidazolium acetate
AGU	Anhydroglucose unit
ATR	Attenuated total reflectance
CI	Crystallinity index
DA	Degree of acetylation
DES	Deep eutectic solvent
DMAc	N,N-Dimethylacetamide
DP	Degree of polymerization
EmimOAc	1-Ethyl-3-methylimidazolium acetate
EtOH	Ethanol
FTIR	Fourier transform infrared spectroscopy
GVL	$\gamma$ -Valerolactone
IL	Ionic liquid
IR	Infrared
LiCl	Lithium chloride
MCC	Microcrystalline cellulose
NMMO	N-Methylmorpholine N-oxide
NMR	Nuclear magnetic resonance
PTFE	Polytetrafluoroethylene
RTIL	Room temperature ionic liquid
SEM	Scanning electron microscopy
TGA	Thermogravimetric analysis
wt%	Weight percentage



# 1 Introduction

## 1.1 Chitin based composite materials

Within the last decade, the plastic pollution has drawn increasing public and scientific attentions. Especially in marine systems, plastic pollution represents the dominant type of anthropogenic debris [1]. Around 75–80 million tons of packaging plastics used globally each year end up in the oceans, which can have a significant impact on marine ecosystems [2,3]. Furthermore, those plastic wastes can be degraded into secondary microplastic, which consists of particles less than 5 mm in size and is therefore hard to be detected. Additionally, due to the large adsorbent surface, the microplastic can also easily transport the pollutants into fish and other marine organisms so that worse the pollution [4]. Hence, development of alternative materials, which are renewable, environmentally benign and sustainable in terms of resourcing, production and end-use-applications have attracted more and more attentions [5]. Products made from renewable and sustainable natural polymers are increasingly demanded from consumers, industry, and governments. Especially in recent years, much attention has been focused on research to replace petroleum-based commodity plastics, in a cost-effective manner, using biodegradable materials offering competitive mechanical properties [6,7]. The natural polymers from annually renewable agricultural and biomass feed stocks can offer an alternative to fossil based non-biodegradable polymers where recycling is impractical or not economical [8]. Biopolymers as chitin, cellulose and lignin are considered as the most promising materials for this purpose [9].

Considering the current demand for reducing environmental impact, concern is being placed on not only renewable resource but also new technologies for development of innovation sustainable materials [7]. A polymeric composite material is usually defined as the combination of two or more different components, in which one plays the role of polymer matrix material while the other performs as a filler or reinforcement [10]. Progress in the field of materials technology has given birth to a fascinating and novel class of material called biocomposites [11]. Biocomposites consist of low-cost, biodegradable and sustainable polymers, which are considered as an environmental waste management option [12]. Furthermore, biocomposites might yield improved properties such as higher mechanical strength and stiffness by overcoming the shortcomings of the single biopolymer [13]. Therefore, biocomposites are considered as a promising alternative to conventional fossil based materials. For example, natural/biofiber

composites are emerging as a viable alternative to glass fibre reinforced composites especially in automotive and building product applications [14]. Biofiber-filled derived thermoplastics and thermosetting polymers have been extensively used for composites manufacturing [15,16]. Biocomposites applied as medical tissue materials, which have been adopted and developed by many industrial companies since 1990s [17].

According to the different compositions, biocomposites can be mainly classified as i) bio-based composites and ii) green composites [18]. Bio-based composite materials are composite materials made from natural/bio fibre and fossil oil derived non-biodegradable polymers. Whereas green composite material is made from all biodegradable polymers, which are obtained from natural renewable resources by fractionation, fermentation or genetic modification and chemical synthesis process [18]. The bio-based composite materials present the comparable properties to the conventional petroleum-based materials. Additionally, they are environment benign to a large extent [19]. However, the bio-based composite materials are not completely degradable and recycling is often impractical. On the other side, the green composites can be completely decomposed without any environmental impact [20]. Hence, green composites are considered more eco-friendly and are therefore attracting more and more scientific and industrial attention. Accordingly, green composites with further developments and improvements in performance would be the most viable alternative materials to conventional petroleum based materials in the near future.

Chitin is considered as an optimal natural polymer for obtaining green composites due to its characteristics such as chemical stability and non-toxicity [21-23]. Over the past several decades, there has been extensive research on chitin based composite materials. It was reported that composite materials from chitin and polylactic acid show significantly improved properties such as higher tensile strengths and lower coefficient of thermal expansion [24]. Several research reports suggested potential applications for chitin based composite materials such as barrier films, antimicrobial films, transparent films, flexible displays reinforcing fillers, biomedical implants, drug delivery, fibres and textiles, separation membranes, electro-active polymers, and many others [25-27]. Although some researchers have investigated the potentials of green composite materials from chitin with the other two most abundant natural polymers as cellulose and lignin [25,26,28], the development of a sustainable and environmentally friendly process for the chitin based green composite materials with high performance is still required. Especially, there are almost no research reports regarding the deacetylation of chitin from the dissolution process [29,30]. Hence, the development of a green process for utilizing chitin persists as a crucial interest for researchers.

## **1.2 Structures, properties and applications of the biopolymers**

### **1.2.1 Chitin**

Chitin is an amino-polysaccharide, which consists of a glucose polymer linked through  $\beta$  (1 $\rightarrow$ 4) glycosidic linkages bearing acetamido groups at the C-2 positions as Figure 1.2 shown. It is synthesized from units of N-acetyl-D-glucosamine as 2-(acetamino)-2-deoxy-D-glucose [31]. This allows for increased hydrogen bonding between adjacent polymers, giving the chitin-polymer matrix increased strength [32]. On the other hand, the rigid molecular structure of chitin forms a strong inter- and intramolecular hydrogen bond, which leads to a lack of solubility in water and common organic solvents [25].

Chitin in its native form is a slightly yellow and brittle polysaccharide. In its pure, unmodified form, chitin is translucent, pliable, resilient and tough [21]. Chitin was first isolated by Bracnot in the year of 1811. He isolated chitin from mushrooms with diluted warm alkali solution and found it was the distinct substance, which is responsible for the abundance of nitrogen in fungi [33]. Then, Odler found that there is the same substance in the structure of insect and plant in 1823. He named this substance as chitin, which is derived from the Greek term  $\chi\iota\tau\acute{\omega}\nu$  (chiton), meaning covering and refers to a marine animal with a protective shell [33, 34]. Since 1844, chitin is considered as one of the most abundant natural polysaccharides [21]. The chemical structure of chitin was elucidated by Ledderhose in 1878 as the composition of glucosamine and acetic acids [33]. In 1929, Hofmann first determined the specific chemical structure of chitin through an enzymatic degradation method [32].

Chitin occurs primarily as a characteristic component of the cell walls of fungi, the exoskeletons of arthropods such as crustaceans (e.g. crabs, lobsters and shrimps), and insect cuticles as well as in the internal structure of invertebrates. It serves in many functions where reinforcement and strength are required [21]. Chitin is produced in large quantities as a by-product (secondary resource) in the course of shrimp meat production [35,36]. One of the industrial processes for producing chitin is by fermentation [37]. Another is to extract chitin from crustaceans by acid treatment in order to dissolve the high concentration of calcium carbonate present in shrimps or crab shells, which is followed by alkali treatment for removing proteins [21, 36]. After that, a decolourization step is often applied to remove the pigments to obtain a colourless chitin product [27].

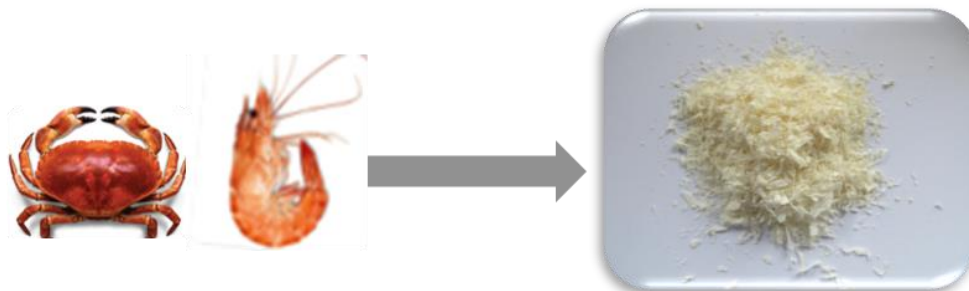


**Figure 1.1:** Chitin source and the commercial powder.

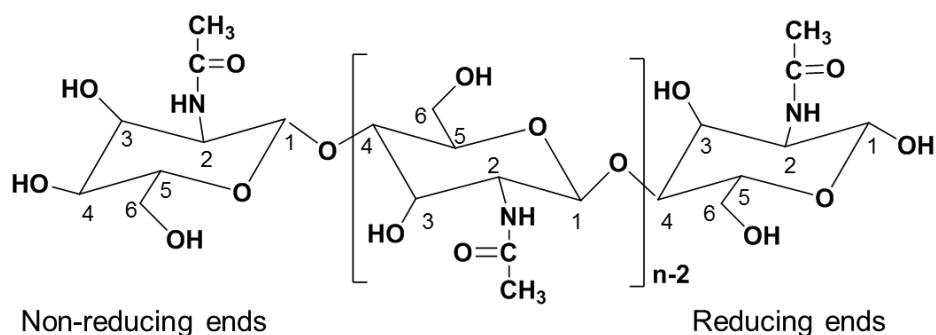


**Figure 1.2:** Chemical Structure of chitin.

Chitin can be classified as  $\alpha$ -,  $\beta$ - and  $\gamma$ -chitin according to its crystalline structures (polymorphs). The polymer chains are actually arranged in sheets or stacks. In  $\alpha$ -chitin, the adjacent sheets along the c-axis exhibit an opposite direction and they are antiparallel with respect to the reducing ends of the polysaccharide chain. In  $\beta$ -chitin, adjacent sheets along the c-axis show the same direction and they are parallel. In  $\gamma$ -chitin, every third sheet exhibits the opposite direction regarding the two preceding sheets [37,38].  $\alpha$ -Chitin is the most common polymorph and has been investigated more extensively than the two other polymorphs.  $\alpha$ -Chitin is mostly present in crabs, shrimps shells, krill, lobsters, insect cuticle, as well as fungal and yeast cell walls. It is also found in some marine living organisms such as cone snails [21].  $\alpha$ -Chitin usually presents a remarkably high crystallinity and high purity. In addition to native chitin, it is possible to obtain  $\alpha$ -chitin through recrystallization from solution, in vitro biosynthesis and enzymatic polymerization [38]. The polymorph  $\beta$ -chitin is mainly found in chitin samples isolated from squid pens and tubeworms. It also occurs in some seaweeds and protozoa. A pure form of  $\beta$ -chitin is rare and only found in the monocrystalline spines excreted by the diatom *Thalassiosira fluviatilis* [33,39]. Opposed to  $\alpha$ -Chitin,  $\beta$ -chitin is impossible obtain via a solution process or through in-vitro

biosynthesis [21]. Very few studies have been carried out on  $\gamma$ -chitin. Some reports suggested that  $\gamma$ -chitin might only be a distorted version of either  $\alpha$ - or  $\beta$ -chitin rather than a true third polymorphic form [27,35,40].

Chitin is the most abundant polymer after cellulose in the world, the main commercial sources of chitin are crab and shrimp shells until now [21]. Additionally, the chitin waste from shrimp meet production is a major source of surface pollution in coastal areas. For instance, the annually amounts of chitin waste in India was estimated to about 60,000–80,000 ton [41]. Chitin has unique properties including polyoxysalt formation, the ability to form films, to chelate metal ions and optical characteristics [6]. Those properties allow the efficient use of chitin as a biodegradable new functional material, which could be used as a high potential alternative for replacing of the petrochemical based materials in various fields [21,23]. For instance, chitin is of commercial interest as a chelating agent used in food and cosmetic industries [22]. Chitin and chitin derivatives have been reported over the last three decades that they could be used to inhibit fibroplasia in wound healing and to promote tissue growth and differentiation in tissue culture [21]. Chitin films and fibres have been developed in medical and pharmaceutical applications as drug release and carrier materials [21,27,33]. Furthermore, chitin based materials have found applications as biosensor and for the remediation of industrial pollutants [27].

Chitin is mainly produced commercially in India, Poland, Japan, the US, Norway and Australia. Although chitin has an annual production of more than  $10^7$  tons, it has long been underutilized [21,30,42]. There is considerable research in progress on biopolymers such as chitin worldwide [21]. However, due to its insolubility in ordinary solvents, chitin is difficult to characterize and process. Furthermore, the diversity sources and the organization state in solid state of chitin is responsible for the quality of the commercial chitin available. Therefore, this results cause many difficulties for chitin transformation and chemical modification. Furthermore, the high cost of purification and modification of chitin is also one of the factors that hinder its industrial development in industries. Though much work has been performed on the exploration of chitin in its utilization, difficulties remain in the development of new applications [27,42,48].

Recent progress of chitin chemistry is mostly focusing on chemical modification including acylation, alkylation and reductive alkylation, carboxyalkylation, phthaloylation, silylation, tosylation, quaternary salt formation, and sulfatation and thiolation [43]. Deacetylation of chitin yields chitosan, which is known as a main commercial product with applications as biomaterial in biomedicine, agriculture, food, and cosmetics. Since it has be described as the N-deacetylated

derivative of chitin, it is also a linear polymer of  $\beta$  (1, 4)-linked 2-amino-2-deoxy- $\beta$ -D-glucopyranose [21]. Chitosan is usually characterized by the degree of acetylation [21]. The degree of acetylation (DA) of chitin is close to 0.90. Chitosan is the fully or partially N-deacetylated derivative of chitin with a DA of less than 0.50 (Fig 1.3) [37]. Usually, chitosan is obtained by hydrolysis of chitin with alkaline hydroxide solution at a concentration of 30-50% (w/v) and high temperature (100 °C) for 1-3h (Fig. 1.3) [44]. Because chitosan is water soluble in acidic or neutral media, it can be much easier processed than chitin. However, compared to chitin, chitosan materials exhibit lower chemical stability as well as decreased mechanical properties [21]. The deacetylation processing of chitin for yielding chitosan mostly exhibits disadvantages such as high energy loss, high cost and so on [45,46]. Some solvent systems such as aqueous NaOH/urea, strong acids could also lead to accumulation of pollutants [47,48]. Therefore, a fabrication process for biocomposites by directly using chitin as a raw material instead of modified or deacetylated chitin would be quite favourable.

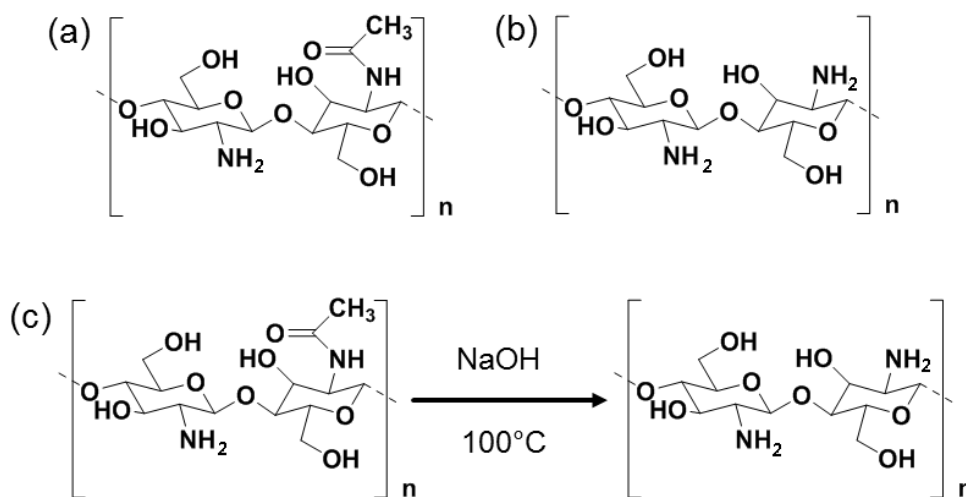


**Figure 1.3:** Partially deacetylated chitin (a), fully deacetylated chitin (b) and deacetylation of chitin (c).

## 1.2.2 Cellulose

The natural polysaccharide cellulose is one of the most abundant biopolymers and renewable natural resource in the world with an annual production of around  $1.5 \times 10^{12}$  tons [49]. As the primary source of biofuels and value-added product, cellulose is considered as a promising alternative to non-renewable natural resources for the sustainable supply of fuel and chemicals in the future [50]. The composition of cellulose, isolated from plant cell walls, was first

determined and described by Anselme Payen (1795–1871) [51]. Cellulose is mainly produced from lignocellulosics, such as wood and lignified higher plants and is the main constituent of the plant cell walls [52]. Additionally, it also can be produced in some algae, fungi and bacteria species. Due to the promising properties of cellulose such as mechanical strength, biocompatibility, biodegradability, hydrophilicity, relative thermal stability and high sorption capacity for water, it has significant industrial applications [50,51]. For instance, the cellulose-containing materials and their derivatives have been widely used in humanity for the production of paper, textiles, cosmetics and many other industrial products [53]. Furthermore, extensive research has been carried out world-wide to convert cellulose into biofuels, feedstock chemicals and bio-based materials [54].

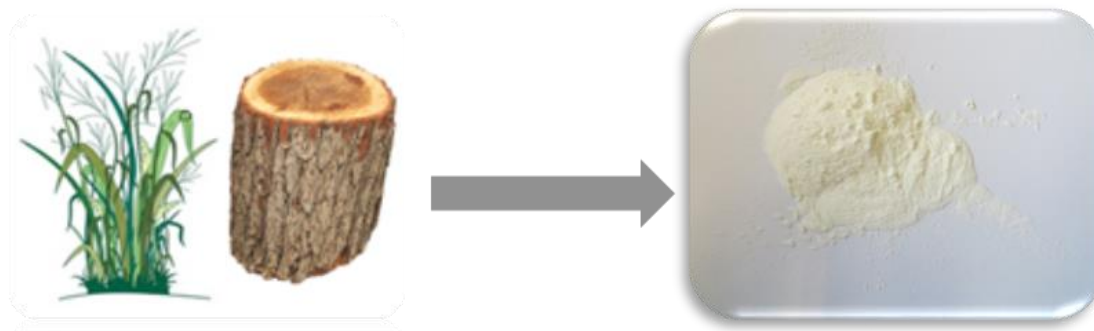


**Figure 1.4:** Conversion of lignocellulosic plant source into cellulose powder.

Cellulose is a colourless, odourless, and nontoxic solid polymer. Its chemical structure is a glucose based homopolymer linked through  $\beta$ -(1 $\rightarrow$ 4) glycosidic bonds, Figure 1.5 [52]. Cellulose can be regarded as a linear polymer composed from a repeating unit of cellobiose and each unit bears six hydroxyl groups. The large number of hydroxyl groups present in the structure leads to a highly hydrophilic cellulose chain. Furthermore, these hydroxyl groups and their ability to form intermolecular hydrogen bonds play a major role in directing the crystalline packing of cellulose [55]. Infrared spectroscopy and X-ray diffraction studies of cellulose organization in plants have shown that the main portion of cellulose is constituted of highly structured crystalline regions (highly ordered) with amorphous regions (less ordered) [56,57]. Generally, the crystallinity index CI of cellulose in wood-based fibres is about 60–70% and in other plant-based fibres is about 90–99% [58]. The crystallinity of cellulose is one of the key characteristics affecting its properties, including its reactivity, mechanical performance, water absorption, and biodegradability. The cellulose amorphous region can absorb water more easily due to its facile accessibility [59]. This

means that, the amorphous regions are more prone to acid hydrolysis and result in shorter and crystalline fragments such as microcrystalline cellulose [60].

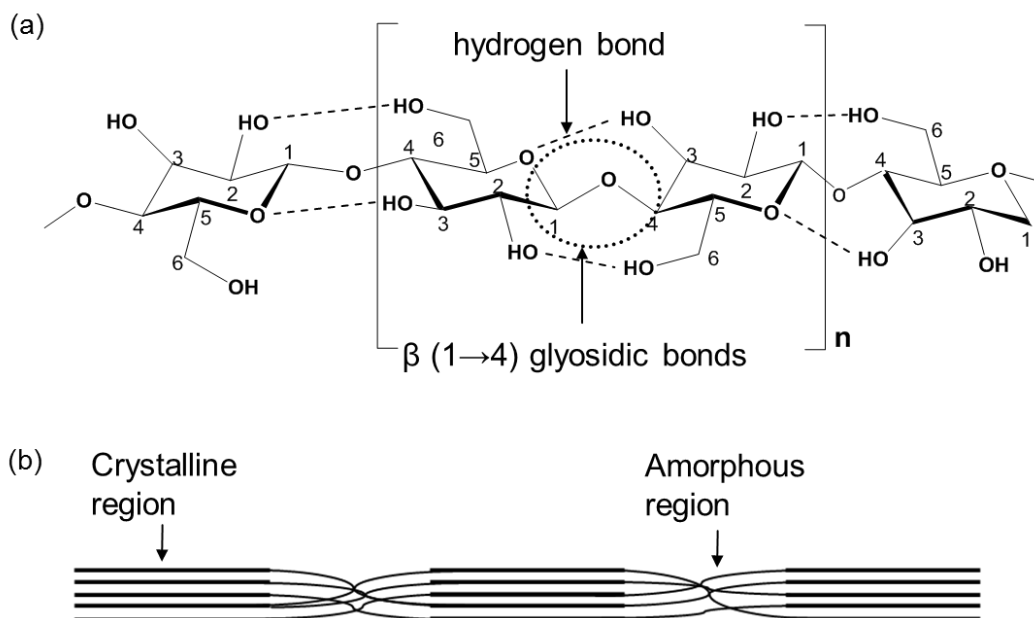


**Figure 1.5:** Chemical structure of cellulose and its intra molecular hydrogen bonds (a) and the crystalline and amorphous regions in cellulose (b).

Cellulose-I is the crystalline type in native cellulose while cellulose-II, -III, and -IV are the other common allomorphs of cellulose. The existence of two different crystalline forms in native cellulose, I $\alpha$  and I $\beta$ , was first demonstrated from nuclear magnetic resonance (NMR) experiments with cross polarization/magic angle spinning (CP-MAS) [56,61]. The cellulose I $\alpha$  crystal has a triclinic unit cell and is predominantly found in algal-bacterial celluloses, while the cellulose I $\beta$  exhibit a monoclinic unit cell and is the allomorph present in the cellulose typically derived from annual plants (ramie and cotton) [56,62]. Both of the two forms are present in native cellulose but with a different fraction according to the various source of cellulose. It was reported that the cellulose from tunicates (a sea animal) consists of I $\beta$  phase with around 90%, whereas freshwater algal consist of nearly pure I $\alpha$  cellulose (approximately 90%) [56,63]. It should be noted that cellulose-I $\alpha$  is a metastable form and can be converted into the I $\beta$  form by an annealing treatment [56]. Cellulose-II is generally formed by mercerization or regeneration from its solutions [57,64]. Cellulose-III can be formed from either cellulose-I or cellulose-II by treatment with liquid ammonia. Cellulose-IV is obtained from the corresponding form of cellulose-III by heating in glycerol [65,66].

The degree of polymerization (DP) indicates the number of glucose units AGU ( $(C_6H_{10}O_5)_n$ ) in the cellulose chain [60]. The DP of native cellulose in wood is about 10,000 glucose units and is around of 15,000 glucose units in cotton. The DP varies not only according to the sources of cellulose, but also within the extraction methods [50, 56]. However, the DP is reduced under hydrolysis condition, which includes temperature, acid concentration and time [60]. It was reported that a DP of native cellulose in cotton is reduced from 14,000 to about 2,500 by purification processes [56,60].

Microcrystalline cellulose (MCC) is purified, partially depolymerized cellulose, where the fraction of the amorphous regions is reduced by acid hydrolysis. The DP of MCC is below 350 glucose units [56,60]. MCC is obtained at an industrial scale through hydrolysis of wood and cotton cellulose by using dilute mineral acids [56]. Different properties of MCC (crystallinity, moisture content, surface area and molecular weight, etc.) vary within the cellulose sources and the conditions of hydrolysis [67]. The degree of crystallinity index (CI) of MCC is reported between 60% and 80% according to different determination methods as X-ray diffraction and infrared spectroscopy as well as the other data evaluation methods and analysis. Due to the higher crystallinity, MCC presents relatively higher mechanical strength but lower chemical reactivity [66,68]. It is a very promising cellulosic reinforcement for composite materials for plastic industries [69]. Furthermore, because of the relatively low bulk density, broad particle size distribution, high surface area of MCC, it presents unique binding properties. Therefore, MCC is one of the preferred direct compression binders [56,70]. MCC has been widely applied in medical tablets as an efficient binder for pharmaceutical ingredients and as a fat replacer and stabilizer in food industries [66]. Additionally, MCC is lubricant sensitive, strain rate sensitive and cohesive. It therefore also finds applications in cosmetics industry [66,68]. Last but not least, some other advantages as broad compatibility, physiological inertness, and facile handling of MCC makes it as an optimum source for the development of a new generation of biodegradable composite materials [57].

### **1.2.3 Lignin**

Lignin is one of the three basic biopolymeric components from wood and also one of the most abundant biopolymers next to cellulose and chitin [71]. Lignin constitutes about 15-30 wt% of all lignocellulosic biomass. It is abundant in the cell walls of terrestrial plants, which is typically contain 16–33 wt% of plant biomass and it serves as the matrix or binding agent for cellulose and polyoses [72]. The amount of total lignin biomass was estimated about 300 billion tons in the

year of 2012 and around 20 billion tons of lignin is formed every year. In 2010, 50 million tons of lignin was produced in the paper and pulp industry, of which only two percentages were used in commercial applications [39]. However, it should be noted that this is only estimated data. Because most of the lignin is thermally converted into energy after production, there are almost no reliable statistics on this issue [71].

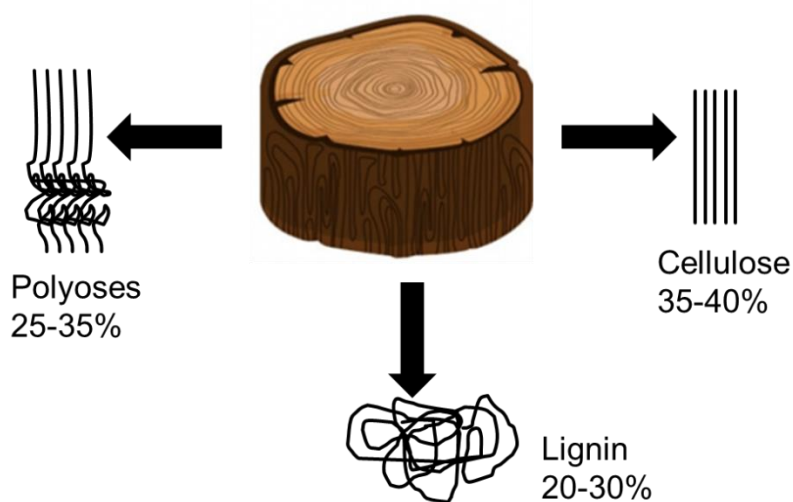


**Figure 1.6:** Three essential components of wood.

Lignin is a complex aromatic heteropolymer derived mainly from three hydroxycinnamyl alcohol monomers differing in their degree of methoxylation. The three monolignols are p-hydroxyphenyl H, guaiacyl G, and syringyl S phenylpropanoid units, respectively, Figure 1.7 [73,74]. The chemical structure of lignin is complex. It is referred to as a three-dimensional amorphous polymer composed of monolignin structures [75]. The empirical formula for lignin was reported as  $C_9H_{10}O_2(OCH_3)_n$ , with n being the ratio of MeO to  $C_9$  groups:  $n = 1.4, 0.94$  and  $1.18$  for hardwood, softwood and grasses, respectively [73]. The amount and composition of lignin varies among taxa, cell types, and as well as the individual cell wall layers and they are influenced by developmental and environmental cues [76]. For instance, lignin extracted from hardwood consists principally of guaiacyl G and syringyl S units, whereas lignin from softwood is composed mostly of guaiacyl G with low levels of p-hydroxyphenyl H units. Lignin from grasses has equivalent level of guaiacyl G and syringyl S units and more hydroxyphenyl H units than the former [75].

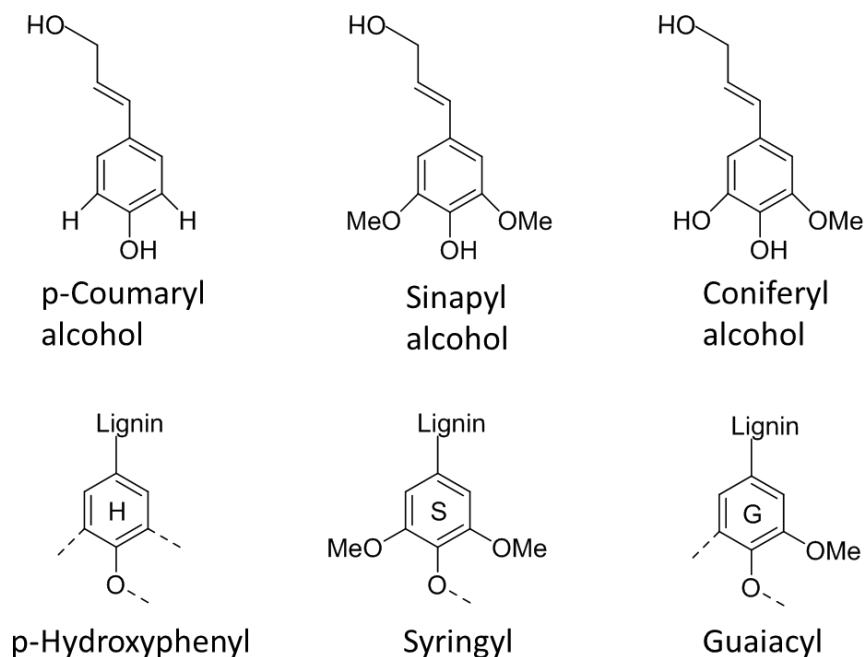


**Figure 1.7:** The structures of the three monolignols and their subunits.

The main role of lignin is to provide mechanical strength to the cell walls in the plants. Furthermore, it also functions as regulator for the water transport. Additionally, lignin also plays an important role in plant defence with its anti-bacterial properties against microorganisms [76]. Because of the complex molecular structure and the large heterogeneity of its feedstock, the applicability of lignin for high-valued applications is limited. Lignin is currently mainly used in low value-added applications as waste or low-grade burning fuel. Only a small amount is utilized in concrete additives, stabilizing agents or dispersants and surfactants in paper industry [77]. Lignin is mainly extracted through pulping chemical processes, which produce technical lignin [78]. According to different lignin source and pulping processes, technical lignin can be classified into Kraft lignin, liginosulfonates, soda lignin and organosolv lignin. The Kraft pulping is the dominant process for industrial lignin production [72]. Chemical modification of lignin occurs during cooking of wood chips in an aqueous solution of sodium hydroxide and sodium sulphide at 170 °C for about two hours [79]. During this treatment, the hydroxide and hydrosulphide anions from the solvent are react with lignin and leads the biopolymer to fragment into smaller water/alkali-soluble fragments. As a result, the linkages between the phenylpropanoid units are cleaved. Therefore, the resulting Kraft lignin is hydrophobic and has a high sulphur content (1 to 2 wt%) [77]. The sulphite process is similar as the Kraft process except using the acidic medium instead of the alkaline one. The obtained liginosulfonates are water-soluble and with sulfonate

groups present on the aliphatic side chains [77]. The main industrial uses of lignosulfonates are as binders, cement adhesives, and tanning leather [80]. Different from the previous two processes, the soda process uses non-wood raw material for chemical pulping and without additional sulphur in the pulping process. Compared to Kraft lignin and lignosulfonates, soda lignin is much closer to the composition of natural lignin and can be used directly without purification. Furthermore, it can be reapplied in many industrial applications after chemical modification [77]. The organosolv pulping process was invented by Theodor Kleinert in 1968 as an environmentally benign alternative to Kraft pulping [81]. The organosolv pulping process applies a solvent fractionation technique to separate lignin molecules into fractions with low polydispersity and defined properties [72]. The processes includes: 1) The use of a variety of organic solvents for successively dissolving lignin fractions with specific properties [81,82]; 2) precipitation of lignin by using hexane, aqueous ethanol, acetone or water [83]. It has to be noted that many solvents used for precipitation fractionation are non-toxic and environmental benign [84]. The organosolv lignin might be applied in pulp and paper manufacturing and for bioethanol fuel productions [85]. However, due to the low molecular weight and hydrophobicity, organosolv lignin shows a poorer quality on the pulp productions than Kraft lignin [77,86].

Although Kraft lignin is utilized as an energy source for a modern Kraft mill for many years, many reports have indicated that this pulp mill also has the potential to be reengineered into a production, which would not only contribute to paper, energy, chemical feedstock but could also serve as renewable bio-based materials [87,88]. The broad visions of the biomaterials are including renewable biobased polymers, biocomposites, and biofuels, which are synthesized by utilizing lignin as a bioresource. Because lignin is considered to mechanically support plant cell walls in nature, extensive studies have been carried out on lignin-reinforced polymer composites by using lignin as a reinforcing agent in the polymer matrix [77]. For instance, it was reported that lignin-based polyurethane foams are widely studied materials with porous structures by utilizing of lignin as a reinforcing agent [78,80,89]. Furthermore, lignin has been used as reinforcing agent for the rubber thermoplastic systems [77]. Meanwhile, lignin-based phenol-formaldehyde resins were presented for potential applications in electronics, railways, building and construction products such as coatings, insulation, lamination, and wood bonding systems [90]. Due to the aromatic rings with hydroxyl and methoxy functional groups, lignin was reported to have antioxidant properties in composites with other polymers [77,90]. Studies were also carried on for developing lignin based materials requires for antioxidation activity in food packaging applications [80]. Last but not least, there were also various reports on lignin based copolymers applied as UV-absorbent coating materials [77].

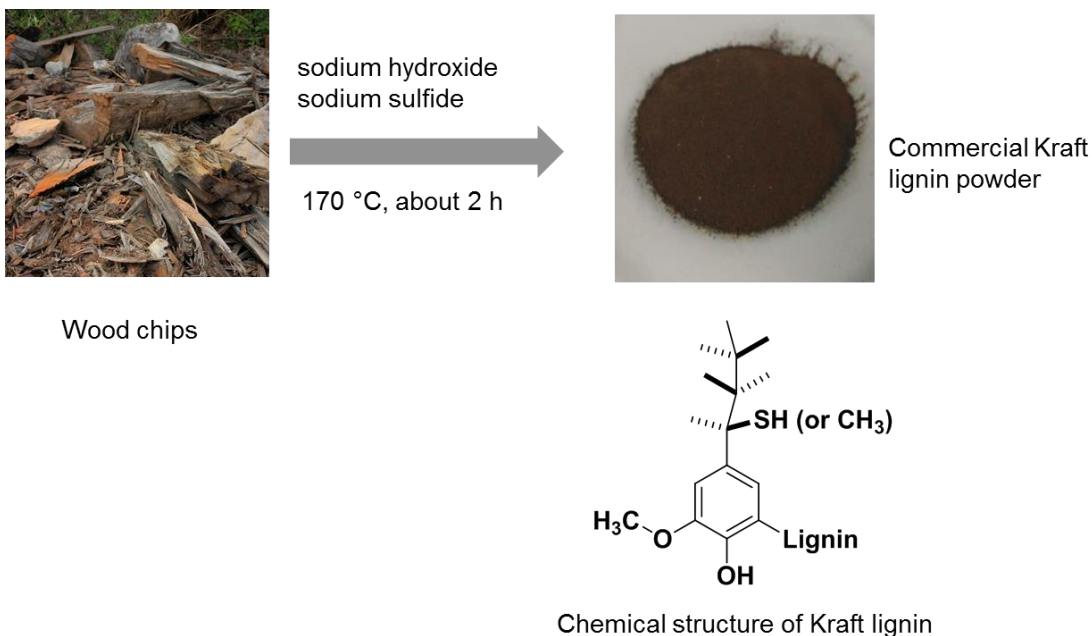


**Figure 1.8:** Kraft pulping process.

However, raw lignin, without any chemical modification, shows a brittle and immiscible characteristic, which hinders its wide application [77,91]. Most utilization of raw lignin was the incorporation of inexpensive lignin into industrial polyolefin for reducing the costs of the final products [92,93]. Indeed, lignin-based materials might have a bright future as a promising alternative to traditional petroleum based materials [94]. Since the current improvement of chemical processing today, chemical markets might be open for lignin products, which can meet the needs of these new end products and develop them with novel properties [95]. Along with the concerns of the increasing environmental issues, the development of lignin-based polymeric materials by utilizing unmodified lignin is a rational start to the wide use of this sustainable biopolymer [96-98].

### 1.3 Processing technologies for chitin based composite materials

The commonly processing technologies for manufacture green composite materials include physical and chemical techniques. Processing such as press moulding, lamination, filament winding, pultrusion, extrusion, moulding and compounding belong to physical techniques [99]. Chemical techniques include fractionation, fermentation, chemical modification or synthesis and

solution processing, etc. [6]. Compared to physical techniques, chemical processing techniques show more contributions for the development of novel sustainable biopolymer composite materials [18,30].

### **1.3.1 Chitin/cellulose composite materials**

The development of efficient solvents is considered to have a crucial impact on the processing of chitin/cellulose composites. The solution processing can provide access to new composite and hybrid materials in the form of fibres, films, nanomaterials, gels, and membranes with a high performance in various applications [6,25,28,47].

Figure 1.9 illustrates the solution process route for the production of composite chitin/cellulose materials. The first step is the dissolution of the two biopolymers in a suitable solvent. Then, the resulting mixtures are shaped into the required form by using e.g. a mould. After that, an anti-solvent such as water or ethanol is added for the regeneration of the biopolymers from the solution. At last, the obtained composite is repeatedly washed with water or ethanol until the solvent is completely removed. It should be noted that, the dissolution of the two biopolymers in an efficient solvent is the crucial step in the whole process. However, according to various research reports on fabrication of chitin/cellulose composites by solution processing, only a few solvents can be used for the dissolution of native cellulose or chitin [25,30].

Suitable solvents for dissolving chitin and cellulose are the conventional polar solvent systems as N-methylmorpholine-N-oxide (NMMO) [100], dimethylacetamide/lithium chloride (DMAc/LiCl) [101], lithium chloride/N-methyl-2-pyrrolidone (LiCl/NMP) [102], paraformaldehyde/dimethyl sulfoxide (PF/DMSO) [103], and calcium chloride dihydrate/methanol ( $\text{CaCl}_2 \cdot 2\text{H}_2\text{O}/\text{MeOH}$ ) [104]. However, the toxicity or corrosive properties of these solvent systems can inhibit batch production and potential application of the resulting composite materials [105].

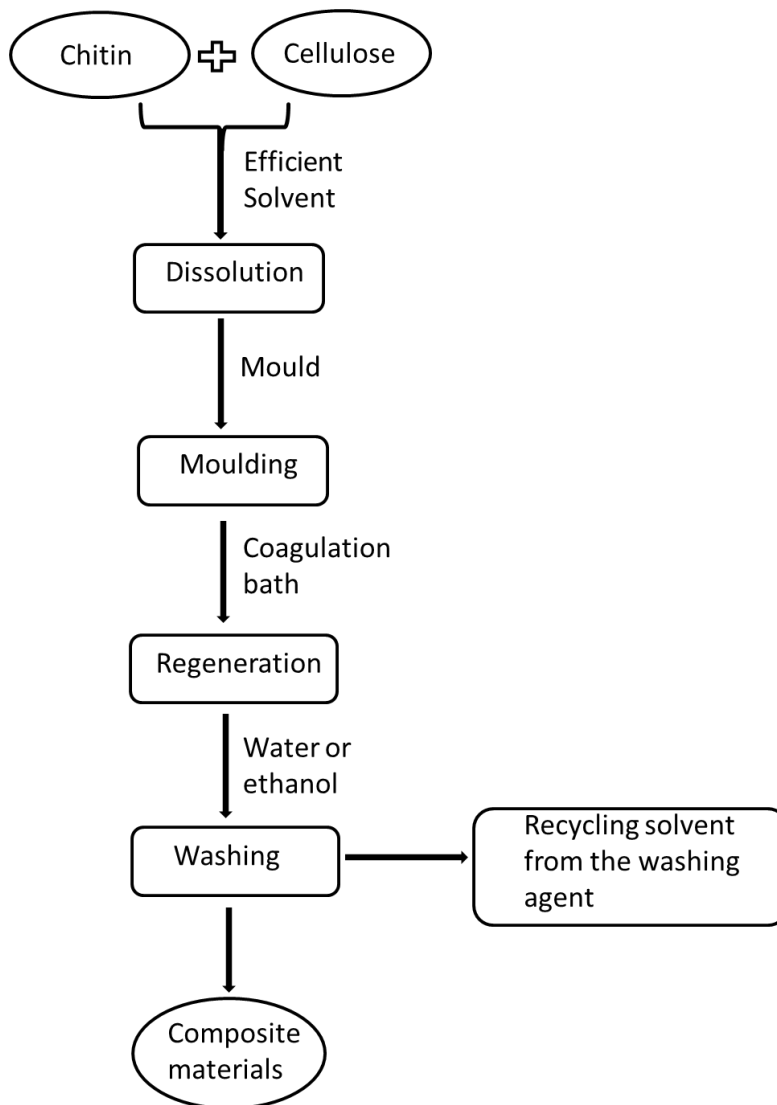


**Figure 1.9:** General scheme of the solution processing for the fabrication of chitin/cellulose composite materials.

Two other solvent systems, which present a considerable good solubility for biopolymers are deep eutectic solvents (DES) and alkali/urea (thiourea) aqueous systems. DES is obtained by heating two or three components that are capable of self-association through hydrogen bonding [105]. For instance, the combination of choline chloride (m.p 302 °C) with urea (m.p 133 °C) can form a DES with an mp of 12 °C [106]. Alkali/urea (thiourea) aqueous systems were developed for the dissolution of biopolymers, i.e. [107]. They utilized an entropy-driven processing involving a low treatment temperature for the dissolution of the biopolymers, which reduces the processing energy [107,108]. However, it was found that the DES solvent can only yield a soft chitin gel and no research reports exist for cellulose gelation up to now [109]. Nevertheless, both

DES and alkali/urea (thiourea) aqueous systems, often require the use of solvents with non-recyclability properties. Hence, the two solvent systems were also considered not reach the requirement to be environmentally benign.

Given the concerns of the increasing environmental issues, it is worthwhile to develop advanced solvent systems not only with environmental benign properties but also with a good solubility for biopolymers such as chitin and cellulose. Ionic liquids (ILs) have been thoroughly investigated as direct and powerful solvents for cellulose and chitin and are therefore frequently used for material processing [25,28,110]. ILs consist of an imidazolium, pyridinium, ammonium or phosphonium cation paired with a strongly basic, hydrogen bond accepting anion (e.g., OAc<sup>-</sup>, HCOO<sup>-</sup>, HSCH<sub>2</sub>COO<sup>-</sup>, (MeO)HPO<sub>2</sub><sup>-</sup>, (MeO)MePO<sub>2</sub><sup>-</sup>, Cl<sup>-</sup>, or Br<sup>-</sup>) The most commonly used ILs are 1-allyl-3-methylimidazolium bromide (AmimBr), 1-ethyl-3-methylimidazolium acetate (EmimOAc) and 1-butyl-3-methylimidazolium acetate (BmimOAc) [30,105,111,112]. Because of the large size and conformational flexibility of the ions, most of the ILs melt below 100 °C [113]. Some ILs with a melting temperature below room temperature is called Room-Temperature Ionic Liquids (RTILs). They have several advantages over classical volatile solvents due to their negligible vapour pressure, non-inflammability, high thermal and chemical stability. Therefore, ILs are often considered as “green” solvents [25,30]. Furthermore, a variety of anion and cation combinations allow the adaptation of ILs for specific purposes. There are also called “designer solvents”. They have been considered as an alternative to conventional solvents in reaction media (e.g. chemical synthesis, biocatalysts) and separation processes [114-116]. In addition, it was found that ILs show effective solubility for the dissolution and processing of biopolymers such as cellulose, chitin and chitosan [117-122]. There are literature reports on the preparation of chitin/cellulose composite materials by dissolving the two biopolymers in two different ILs separately [25]. However, it is found that not all the ILs is environmentally friendly. The most extensively used imidazolium and pyridinium-based ILs are toxic and poorly biodegradable [123,124]. Hence, the improvement of ILs for good solubility on biopolymers and environmental benign properties might play an important role on the fabrication of composite biopolymers.

### **1.3.2 Chitin/lignin composite materials**

Composite materials from chitin and lignin have been scarcely studied in the literature. There are only few reports on the combination of lignin and modified chitin, which present specific adsorption abilities for hydrophobic organic and inorganic compounds [26,125,126]. One report suggested that the composite chitin/lignin powders, which were fabricated by modified chitin and

Kraft lignin using solid process, could be applied as a promising biosorbent for the removal of cadmium and nickel ions [26]. However, the chemical modification process can bring some drawbacks such as high costs, leaching of undesired organic compounds as well as difficulties in recycling operations, which would not meet the requirements for a sustainable routine process [127].

The fabrication of composite chitin/lignin materials by solution processing was scarcely reported. Since ILs, composed of anions such as chloride, acetate have been considered as effective solvents for both chitin and lignin, the development of a sustainable solution processing is expected to yield new advanced composite chitin/lignin materials directly using chitin and lignin native powders [44,128].

## **1.4 Motivation and scientific work hypothesis**

Chitin, cellulose and lignin are three abundant biopolymers on earth. However, some of their characteristics such as low reactivity and solubility lead limitations regarding their fabrication process of advanced composite materials. Chitin wastes are mostly discarded into the sea and lingo-cellulosic (cellulose and lignin) waste is largely incinerated [33]. Considering the fact that chitin is commonly used as a chelating agent food and cosmetic industries, development of chitin based cellulose and lignin composite materials might be a good solution for overcome their application limitations [22,25,30,129].

Although there are already some literature reports on the fabrication of chitin composite materials using solution processing, they have difficulties in recycling of the solvents by using different separate solvents. Furthermore, there are no evidences in these literatures regarding the deacetylation of chitin during the dissolution process [25,29,30]. Therefore, the development of chitin based composite materials with intact unaltered chitin in a sustainable and environmental friendly process is still a challenge nowadays.

In this work, we investigate and develop mainly two different processing methods for the fabrication of chitin based biocomposites, Fig 1.10. First, different variants of solvent systems are performed on the dissolution of the biopolymers [130]. The solubility of the three biopolymers in these solvent systems as well as the degree of acetylation of chitin during the dissolution process will be studied. A sustainable solvent system, which can directly dissolve the native powders of the three natural biopolymers without drastically changing their properties and

without deacetylated chitin into chitosan, will be considered as the optimum solvent. Then, a method, which can successfully produce the chitin based biocomposites in a facile and sustainable processing associated with low-cost and low energy consumption, would be detail described. At last, the potential commercial applications of the obtained chitin based composite materials are going to be evaluated.

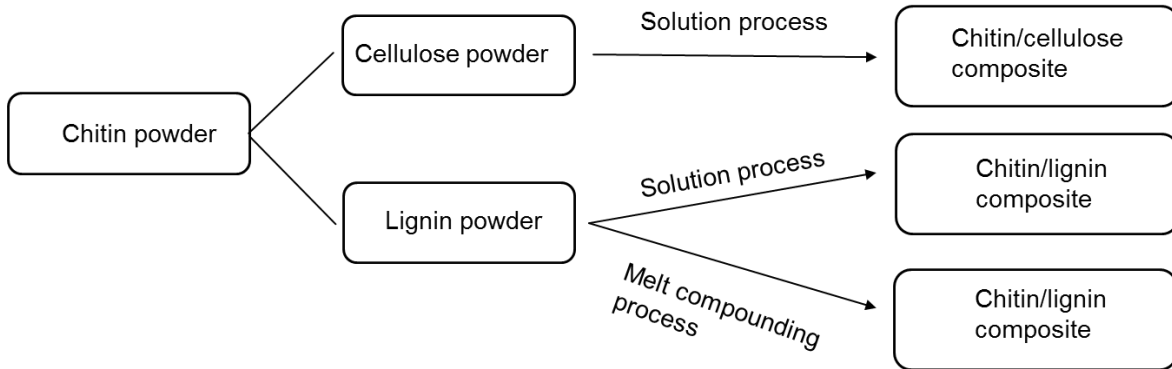


**Figure 1.10:** Processing schemes for the fabrication of chitin/cellulose and chitin/lignin composites.

## **2 Experimental section**

### **2.1 Materials and chemicals**

#### **2.1.1 Biopolymers**

Chitin powder from the shell of shrimps (Sigma Aldrich) was used. The DP of native chitin powders was 1691, as determined by dissolving it in DMAc/LiCl (5%, w:w) solvent. Detailed information of the experimental procedure is present in the enclosed Publication #A.

Microcrystalline cellulose powder (MCC) with a degree of DP of 124 was obtained from Merck (Germany). The DP was determined according to DIN 54 270 as described in the enclosed Publication #A.

Kraft lignin powder (Indulin AT) was purchased from MeatWestVaco (USA). Its number average molecular weight ( $M_n$ ) and weight average molecular weight ( $M_w$ ) is 600 g/mol and 4540 g/mol, respectively, as determined by gel permeation chromatography (GPC). Prior to use, the Kraft lignin was first washed with ethanol by Soxhlet extraction at 90 °C for 48 h. The solid residue was subsequently collected and dried as described in the enclosed Publication #B.

All the three biopolymers were dried at 90 °C for one day and stored in a desiccator charged with silica gel prior to use.

#### **2.1.2 Chemicals**

N,N-Dimethylacetamide (DMAc) and lithium chloride (LiCl) were obtained from Sigma Aldrich (Germany). Prior to use, LiCl was oven-dried at 110°C for overnight and then stored in a desiccator charged with silica gel. DMAc was heated at 100-110°C for 10 minutes in order to remove the residual moisture. After that, it was immediately filtered through a 0.45 µm PTFE-membrane filter for removing impurities. The treated DMAc solvent was then stored in a flask at 4 °C and was used within one week.

Choline chloride (purity ≥ 98%) was obtained from Alfa Aesar (Germany). Urea (purity ≥ 99%) and thiourea (purity ≥ 98%) were purchased from Sigma Aldrich (Germany). The chemicals were dried under vacuum ( $10^{-6}$  mbar) for 5 days before use. They were stored in a nitrogen-filled

glove box to avoid water uptake. The water content of the chemicals were found to be lower than 500 ppm determined with coulometric Karl Fischer titration (Mitsubishi CA-02, Japan) [130].

1-Allyl-3-methylimidazolium bromide (AmimBr, purity  $\geq$  97%), 1-ethyl-3-methylimidazolium acetate (EmimOAc, purity  $\geq$  98%) and 1-butyl-3-methylimidazolium acetate (BmimOAc, purity  $\geq$  98%) were all obtained from Sigma-Aldrich (Germany). Prior to use, they were dried using a high vacuum setup ( $10^{-6}$ - $10^{-7}$  mbar) for 5 days. The residual water content of the ILs was determined using coulometric Karl Fischer titration (Mitsubishi CA-02, Japan). All the investigated ILs contained very low water fraction ( $<1.2$  wt%) [130]. The co-solvent:  $\gamma$ -valerolactone (GVL, purity  $\geq$  99%) was obtained from Sigma Aldrich (Germany) and dried by adding dried molecular sieve (3 Å) before use. They were all stored in sealed vials in a desiccator over silica gel after drying prior to use.

The biopolymers and reagents were used without any further chemical modification or purification, other than stated above.

## **2.2 Preparation of solvents for the dissolution of biopolymers**

### **2.2.1 DMAc/LiCl (8%, w:w)**

The solution of DMAc/LiCl (8%, w:w) was prepared by dissolving the dried LiCl powder (2 g) into DMAc (23 g) at 40 °C under magnetic stirring for one hour. The obtained clear solution was stored at 4 °C before use.

### **2.2.2 DES**

The DES solutions were prepared by mixing the dried components choline chloride and urea (molar ratio: 1:2) and choline chloride with thiourea (molar ratio: 1:2), respectively in glass vials. Then the mixtures were heated and stirred in an oil bath until the colourless liquids were obtained, respectively. The whole processing were performed in a nitrogen-filled glove box in order to avoid oxidation. The obtained DES solutions were stored in sealed glass containers in a glove box in a nitrogen atmosphere.

### 2.2.3 Ionic liquids and co-solvent

The ILs AmimBr, EmimOAc and BmimOAc were directly used after drying. Two molar ratios of BmimOAc and GVL namely 8:1 and 4:1 were obtained by mixing BmimOAc and GVL in desired amounts. Detailed preparation procedures of BmimOAc-GVL solvent system were described in enclosed Publication #A.

## 2.3 Dissolution of biopolymers in various solvents

### 2.3.1 Dissolution of chitin and cellulose in DMAc/LiCl

Chitin and cellulose native powders can be dissolved in DMAc/LiCl after an activation step [131,132]. First, chitin or cellulose powders were covered with water for one hour to ensure full swelling (Figure 2.1). Then the expanded powders were filtered and transferred into acetone for one hour in order to remove water. The polymer powders were subsequently filtered again and immediately transferred to the solvent DMAc for a one hour activation. Finally, the activated chitin and cellulose powders were obtained by drying the DMAc activated biopolymers in oven at 80 °C for 4 hours [132]. Prior to use, the obtained activated chitin and cellulose powders were stored in a desiccator charged with silica gel.

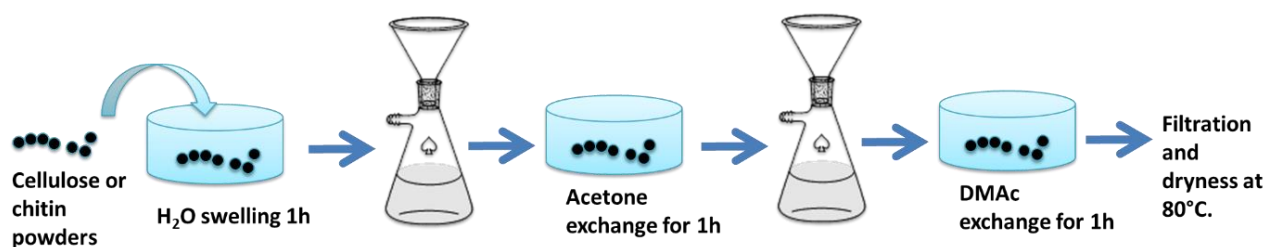


**Figure 2.1:** Scheme of the activation process for chitin and cellulose

The dissolution of the activated chitin and cellulose powders in DMAc/LiCl (8%, w:w) solvent was performed at room temperature under magnetic stirring for 2 hours. It was noticed that chitin and cellulose are dissolved simultaneously in the solvent. Several mixtures with different chitin concentrations were prepared as shown in Table 2.1. The dissolution of pure chitin and cellulose in DMAc/LiCl (8%, w:w) were prepared, respectively, as references.

**Table 2.1:** Preparation of composite materials with different cellulose to chitin molar ratios with DMAc/LiCl (8%, w:w). CC: chitin/cellulose composite.

Sample	Chitin: cellulose/ (DMAc:LiCl) (molar ratio) In solution	Chitin concentration in solution (wt%)	Chitin concentration in film (wt%)
CC_1	1: 3.2/ 9.5	1	25
CC_2	1: 5.1/ 9.5	0.6	15
CC_3	1: 6.4/ 9.5	0.4	8
Pure chitin	0: 1/ 15.1	3	100
Pure cellulose	1: 0/ 5.6	0	0

### 2.3.2 Dissolution of chitin and cellulose in DES

Based on the reports on the solubility of biopolymers in some DES solvents [134, 135], the dissolution of chitin and cellulose native powders in two selected solvents choline chloride/urea (molar ratio: 1:2) and choline chloride/thiourea (molar ratio: 1:2) were investigated in this work. The dissolution procedure was as follows: first, the request amounts of dried chitin and cellulose powders were added in respective amounts of the two DESs in a nitrogen-filled glove box. Then, they were heated at 100 °C for approximately 6 hours with magnetic stirring, respectively. Finally, they were stored in sealed glass containers. Table 2.2 shows the molar ratios of chitin and cellulose with the two DESs in the prepared mixtures.

**Table 2.2:** Mixtures with different chitin to cellulose molar ratios in choline chloride/urea and choline chloride/thiourea. CC: chitin/cellulose composite.

Sample	Chitin:cellulose/ (choline chloride: urea) (molar ratio)	Chitin concentration in solution (wt%)	Chitin:cellulose/ (choline chloride: thiourea) (molar ratio)	Chitin concentration in solution (wt%)
CC_4	1:2/74:148	1	1:2/72:144	1
Pure chitin	0:1/76:152	1	0:1/74:148	1
Pure cellulose	0:1/76:152	0	0:2/74:148	0

### 2.3.3 Dissolution of chitin and cellulose in AmimBr and EmimOAc

In this work, the dissolution of chitin and cellulose in AmimBr and EmimOAc were designed as follows: First, chitin/AmimBr solution with a chitin concentration of 1 wt% was obtained by dissolving chitin powders (0.05 g) in AmimBr solvent (5 g) at 100 °C for ca 6 hours with magnetic stirring. Cellulose/EmimOAc solution with 5 wt% of cellulose was prepared by dissolving cellulose powders (0.53 g) in EmimOAc (10 g). The dissolution of the two biopolymers in the two ionic liquids was visually monitored until all the aggregated powder disappeared and two clear mixtures were visually observed. Then, the two obtained chitin and cellulose solutions were mixed according to the request amounts together at 100 °C for 30 min until a homogeneous solution was formed. Table 2.3 shows the different molar ratios of chitin to cellulose in the prepared solutions as well as different concentrations of chitin in the solutions and corresponding regenerated films.

**Table 2.3:** Preparation of composite materials with different cellulose to chitin molar ratios with AmimBr and EmimOAc. CC: chitin/cellulose composite.

Sample	Chitin: cellulose/ AmimBr: EmimOAc (molar ratio) in solution	Chitin concentration in solution (wt%)	Chitin concentration in film (wt%)
CC_5	1:2 / 98.4:17.8	0.5	33
CC_6	1:4 / 98.4:17.8	0.2	20
Pure chitin	0:1 / 98.4:0	1:0	1
Pure cellulose	1:0 / 0 :17.8	0:1	0

### 2.3.4 Dissolution of chitin and cellulose in BmimOAc-GVL

Dissolution process of chitin and cellulose native powders in the BmimOAc-GVL solvent system were described in detail in the enclosed Publication #A.

### 2.3.5 Dissolution of chitin and lignin in BmimOAc-GVL

Detailed information on the dissolution process of chitin and Kraft lignin in the BmimOAc-GVL solvent system can be found in the enclosed Publication #B.

## **2.4 Fabrication of chitin based composite materials**

### **2.4.1 Composite chitin/cellulose materials**

#### **2.4.1.1 Composite chitin/cellulose films from DMAc/LiCl**

The chitin/cellulose composite films prepared from DMAc/LiCl were as follows: First, the resulting mixtures (approximately 1 g) with different mass ratios of chitin to cellulose in DMAc/LiCl (8%, w:w) were casted on a glass plate with a syringe (d = 1 cm)) at room temperature, respectively (Table 1). After the mixtures cooled down, they were soaked in an ethanol coagulation bath and subsequently kept in a hood at room temperature for overnight until the gel-like films were obtained and could be easily removed. Then, the obtained composite films were subjected to the successive Soxhlet extractions with ethanol (150 mL) for 20 hours and with water (150 mL) for another 20 hours, respectively, in order to completely remove the DMAc/LiCl. The complete removal of DMAc/LiCl was confirmed by adding silver nitrate (AgNO<sub>3</sub>) into the final ethanol and water extracts. The absence of a white precipitation (AgCl) indicated the DMAc/LiCl solvent was completely removed from the composite films by Soxhlet extraction. At last, the chitin/cellulose films were sandwiched between two Teflon plates and left to dry for approximately two days at ambient temperature. The obtained composite films with different chitin concentrations are presented in Table 2.1.

#### **2.4.1.2 Composite chitin/cellulose films from AmimBr and EmimOAc**

The fabrication of composite chitin /cellulose films from AmimBr and EmimOAc was as follows: First, chitin/AmimBr and cellulose/EmimOAc were mixed in different chitin concentrations at 100 °C, Table 3. Then, the resulting mixtures (around 1 g) were casted in a petri dish (d = 4 cm) with a syringe (d = 1 cm) at room temperature. After the mixtures cooled down to room temperature, they were soaked with water in a coagulation bath at room temperature for one day until the gel-like films were obtained. The films were subsequently removed and subjected to Soxhlet extraction with ethanol (150 mL, 12 h) and followed water (150 mL, 12 h) in order to completely remove the two ILs in the composite films. The residual films were sandwiched between two Teflon plates and dried at ambient conditions for two days. The obtained composite films with different chitin concentrations are presented in Table 2.3.

### **2.4.1.3 Composite chitin/cellulose materials from BmimOAc-GVL**

The composite chitin/cellulose materials fabricated from the BmimOAc-GVL solvent system were described in detail in the enclosed Publication #A. The Teflon moulds using for preparing composite materials in forms of gel and film are shown in Figure A.1.

The obtained composite chitin/cellulose materials from BmimOAc-GVL were dried with supercritical carbon dioxide (scCO<sub>2</sub>), at ambient conditions and with compressed air, respectively. The scCO<sub>2</sub> drying method utilized a critical point dryer (E3100, United Kingdom) operated at 38 °C and 83 bar for 3 hours. The ambient condition drying method was carried out by sandwiching the composite samples between two Teflon plates at room temperature for 48 h. The compressed air drying was using a laboratory compressed air at a low pressure (ca. 7 bar) at room temperature.

The recycling of the used BmimOAc-GVL was performed as follows: first, all washing agent in the coagulation bath and Soxhlet extractions were collected after the composite chitin/cellulose materials were generated. Then, the collected solutions were first filtrated with a 0.2 µm polytetrafluorethylene (PTFE) membrane filter to remove residues. Afterwards, ethanol was evaporated from these solutions for two hours under reduced pressure (100 mbar) at 40 °C using a rotary evaporator. The recycled solutions were subsequently further dried at 40 °C at 10<sup>-6</sup> mbar using the high vacuum setup for 5 days. The purity of the recycled solvent was identified by 1H- and 13C-NMR measurements in d<sub>6</sub>-dimethyl sulfoxide recorded with a nuclear magnetic resonance spectrometer (NMR, ECA400, Jeol Inc, USA) at 300 MHz.

## **2.4.2 Chitin coated cellulosic materials**

### **2.4.2.1 Chitin film coated on the surface of wood**

The preparation of chitin films coated on the surface of wood is shown in Figure 2.2. First, a 1 wt% chitin solution (5 g) was prepared by dissolving chitin powder (0.05 g) in BmimOAc–GVL solvent (4.95 g) at 90 °C (detail info see above). Then, five samples (spruce, picea abies) with an axial length of 0.5 cm and a radial length of 1 cm were oven dried at 80 °C for 12 h before use. Afterwards, they were soaked into the resulted chitin solution for about one hour to yield the coagulation of the chitin layer on the wood surface. Each sample was subsequently soaked in an ethanol bath for 24 h and then in water bath for 24 h to remove BmimOAc and GVL. Finally, the obtained samples were dried with compressed air at room temperature.

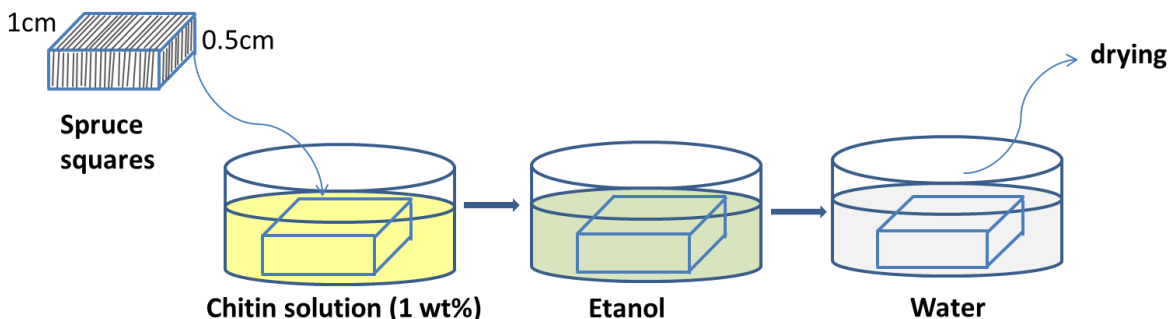


**Figure 2.2:** The preparing process of the chitin film coated on the surface of wood.

#### 2.4.2.2 Chitin film coated on the cellulosic textiles

In this work, four different cellulosic textiles as TENCEL®, Lenzing Viscose®, Lenzing Modal® and cotton fibres were employed as substrates for coating with chitin thin layer. This work was performed in cooperation with our project partner and detailed information can be found in the enclosed Publication #C.

### 2.4.3 Chitin/lignin composite materials

#### 2.4.3.1 Composite chitin/lignin materials from BmimOAc-GVL

Detailed information on preparation of the composite chitin/lignin films from BmimOAc-GVL solvent system can be found in the enclosed Publication #B.

#### 2.4.3.2 Composite chitin/lignin materials from melt compounding process

The preparation of composite chitin/lignin materials using melt compounding process was as follows: First, requested amounts of dried chitin, Kraft lignin and BmimOAc were mixed in desired mass ratios (Table 2.4). Then, the mixture (ca. 7 g) was processed with a laboratory extruder with two tapered screws (HAAKE Minilab II, Thermo Fischer Scientific, Germany). The extrusion was carried out at 130 °C with a screw speed of 150 rpm for 10 minutes. The molten mixture was subsequently ejected through a preheated cylinder to the Haake Minijet II mini injection mould (Thermo Scientific, Germany). After demoulding of the composite sample, it was immediately soaked in an ethanol bath at room temperature for 24 h in order to remove BmimOAc. The obtained composite chitin/lignin materials were subsequently dried at room

temperature. The resulting composites with different chitin concentrations can be found in Table 2.4.

**Table 2.4:** Composite chitin/lignin materials with different concentrations of chitin, lignin and BmimOAc solvent prepared using melt compounding process. CL: chitin/lignin composite.

Sample	Chitin concentration (wt%)	Lignin concentration (wt%)	BmimOAc concentration (wt%)
CL_1	40	20	40
CL_2	45	30	25
CL_3	35	40	25
CL_4	30	50	20

## 2.5 Characterization

### 2.5.1 Dissolution of the biopolymers

The dissolution of the three biopolymers in different solvent systems was first visually monitored and the total dissolution of the biopolymers was confirmed by a light microscopy (Leitz, Germany).

### 2.5.2 Scanning electron microscopy

The morphology of the obtained composite samples was analysed by scanning electron microscopy (SEM). Dried samples were placed on carbon tape and coated with Au/Pd. SEM images were obtained with a digital scanning electron microscope (DSM 940 A, Zeiss, Germany) in secondary imaging mode at an acceleration voltage of 10 kV.

### 2.5.3 Elemental analysis

The elemental compositions of the prepared chitin based composite materials were investigated in an element analyser Euro EA (HEKAtech GmbH, Germany). After oxidation at 1000 °C, the gaseous products were separated by gas chromatography and detected with a thermal conductivity detector. Carbon (C), hydrogen (H) and nitrogen (N) relative contents were

determined using tin capsules, containing 1-3 mg of sample. Oxygen (O) content was measured using silver capsule within 1-2 mg of sample.

#### **2.5.4 Fourier transform infrared spectroscopy (FTIR)**

Infrared spectra of chitin based composites were obtained by using an attenuated total reflectance-Fourier transform infrared spectrometer (ATR-FTIR, Nicolet 380, Thermo Fisher Scientific, USA) equipped with a diamond crystal. The measurements were conducted directly on the powder and film samples in the wavenumber region of 4000-400  $\text{cm}^{-1}$ .

#### **2.5.5 X-ray diffraction**

X-ray diffraction (XRD) patterns of chitin/cellulose composites regenerated from BmimOAc-GVL were obtained with an X-ray diffractometer (Rigaku, MiniFlex 600, Tokyo, Japan) equipped with a high-speed one-dimensional detector (Rigaku, D/teX Ultra, Tokyo, Japan) and a  $\text{K}\beta$ -filter. Detailed description and evaluation of the crystallinity index (CI) can be found in enclosed Publication #A.

#### **2.5.6 Mechanical testing**

The mechanical properties of the composite chitin/cellulose gels regenerated from BmimOAc-GVL were evaluated with a universal tensile tester (Smar Tens 010, Karg Industrietechnik, Krailing, Germany) with an initial grip separation of 1 mm and crosshead speed of 10 mm/min. Detailed measurements were described in enclosed Publication #A.

#### **2.5.7 Dimensional changes**

The linear dimensional change of the chitin/cellulose composites obtained from BmimOAc-GVL after drying with three different drying methods was evaluated by the following equation:

$$D = (A_0 - A_1) / A_0 \times 100$$

Where D is the dimensional change (%),  $A_0$  is the initial area of the composites before drying ( $\text{cm}^2$ ) and  $A_1$  is the final area of the composite samples after drying ( $\text{cm}^2$ ).

### **2.5.8 Water contact angle and water absorption capacity of chitin/cellulose composites**

The water contact angle of the samples as composite chitin/cellulose films and chitin coated cellulosic materials were measured using a P1 goniometer (Erna Inc, Japan) equipped with a microscope and a back light. A 2  $\mu\text{L}$  drop of deionized filtrated water droplet formed by an automated micrometer pipette (Hamilton Company, USA) was slowly placed on the surface of the samples. The tangent of the drop profile at the contact point with the surface of the sample was observed through an optical system. The measurements were repeated ten times for each sample and the mean values with standard deviations were calculated. In addition, the absorption time of the water droplet was recorded for the chitin coated cellulosic samples. The measurements of water absorption time were repeated ten times for each sample and the mean values with standard deviations were evaluated.

### **2.5.9 Water and oxygen permeability of chitin coated cellulosic textiles**

The water and oxygen permeability of the chitin coated cellulosic textiles were determined by our project partner and described in detail in the enclosed Publication #C.

### **2.5.10 Ion adsorption/desorption of chitin/lignin composite**

The adsorption/desorption experiments of chitin/lignin composite films on Fe(III) or Cu(II) ions from aqueous solutions as well as the investigation of the kinetics of the adsorption process were described in detail in the enclosed Publication #B.



## **3 Results and discussion**

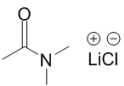
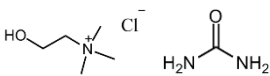
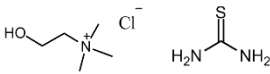
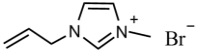
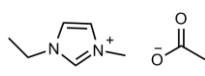
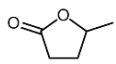
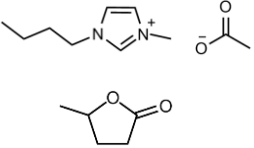
### **3.1 Solubility of chitin, cellulose and lignin in various solvent systems**

The investigation of different solvent systems for the dissolution of the biopolymers was a cooperation work with Dr. Auriane Freyburger from the Institute of Physical and Theoretical Chemistry at the University of Regensburg [130]. In this work, we mainly discussed some selected representative solvent systems: i) conventional polar solvent systems (DMAc/LiCl); ii) deep eutectic solvents (cholinchloride/urea or thiourea) and iii) ILs (AmimBr, EmimOAc and BmimOAc) for the dissolution of the biopolymers. Because of the high viscosity of an IL solution with biopolymer content, their solubilisation is challenging [111,136]. Therefore, a less viscous co-solvent,  $\gamma$ -valerolactone (GVL), which is a readily available and a sustainable solvent derived from lignocellulosic biomass, was selected as a co-solvent for BmimOAc to support the biopolymer dissolution [133].

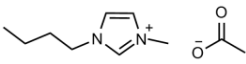
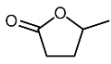
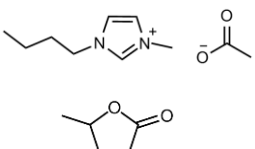
In this work,  $\alpha$ -chitin from shrimp shells was used as main chitin substrate because of its commercial facility. The low degree of polymerization (i.e. 124) of MCC results of a relatively fast dissolution, therefore, it was selected as the cellulose substrate. Kraft lignin with pretreatment was used as the lignin substrate in this work, because it is insoluble in ethanol, which can ensure the successfully regeneration of the chitin/lignin composites from the ethanol coagulation bad.

The solubility of chitin and cellulose in the above mentioned solvent systems including DMAc/LiCl, DES, ILs as well as ILs mixed with co-solvent were observed by optical microscopy. Then, the solvent system, which presents good solubility on chitin and cellulose, was applied for the dissolution of chitin and lignin. Maximum solubility of  $\alpha$ -chitin, MCC and Kraft lignin as well as their dissolution conditions in the selected solvent systems are show below (Table 3.1; 3.2). In addition, the polymers are considered insoluble when the addition of desired amounts of biopolymers to the solvent yielded turbid mixtures under the selected experimental conditions.

**Table 3.1:** Maximum solubility of  $\alpha$ -chitin and microcrystalline cellulose native powders in various solvent systems as well as their dissolution conditions (NS: Not soluble; \*: incompletely dissolution).

Solvent variant	Solvent name	Chemical structure	Maximum Solubility (wt%)		Dissolution conditions
			MCC $\alpha$ -chitin		
Conventional polar solvent system	DMAc/LiCl 8% w:w		10	3	magnetic stirring at room temperature for 2 h
DES	Choline chloride/urea (molar ratio: 1:2)		NS	NS	magnetic stirring at 100 °C for 24 h
	Choline chloride/thiourea (molar ratio: 1:2)		NS	NS	magnetic stirring at 100 °C for 24 h
ILs	1-Allyl-3-methylimidazolium bromide (AmimBr)		NS	2*	magnetic stirring at 100 °C for 6 h
	1-Ethyl-3-methylimidazolium acetate (EmimOAc)		15	NS	magnetic stirring at 90 °C for 6 h
	1-Butyl-3-methylimidazolium acetate (BmimOAc)		10	3	magnetic stirring at 110 °C for 4 h
Co-solvent	$\gamma$ -Valerolacton (GVL)		NS	NS	magnetic stirring at 100 °C for 6 h
Mixtures	BmimOAc: GVL (molar ratio: 3:1)		6	NS	magnetic stirring at 90 °C for 4 h
	BmimOAc: GVL (molar ratio: 5:1)		8	2	magnetic stirring at 90 °C for 4 h
	BmimOAc: GVL (molar ratio: 8:1)		12	3	magnetic stirring at 90 °C for 3 h

**Table 3.2:** Maximum solubility of Kraft lignin in various solvent systems as well as its dissolution conditions (NS: Not soluble).

Solvent variant	Solvent name	Chemical structure	Maximum Solubility (wt%) Kraft lignin	Dissolution conditions
IL	1-Butyl-3-methylimidazolium acetate (BmimOAc)		10	magnetic stirring at 110 °C for 4 h
Co-solvent	$\gamma$ -Valerolactone (GVL)		NS	magnetic stirring at 100 °C for 6 h
Mixtures	BmimOAc: GVL (mass ratio: 1:1)		15	magnetic stirring at 90 °C for 4 h
	BmimOAc: GVL (mass ratio: 2:1)		20	magnetic stirring at 90 °C for 4 h
	BmimOAc: GVL (mass ratio: 4:1)		30	magnetic stirring at 90 °C for 3 h

### 3.1.1 Dissolution of chitin and cellulose in DMAc/LiCl

It is observed that about 3 wt% activated chitin and 10 wt% activated MCC can be dissolved in DMAc/LiCl (8%, w:w) at room temperature within two hours, respectively, Table 3.1. As shown in Figure 3.1, the obtained transparent mixtures are clear and homogeneous, which can be observed from both from the visual appearance and in the light microscope. The results indicate a complete dissolution of the two biopolymers in the solvent of DMAc/LiCl (8%, w:w) under the selected experimental conditions. Furthermore, it clearly proves that DMAc/LiCl has the ability to dissolve both chitin and cellulose simultaneously.

The reason for the good solubility of the two biopolymers in DMAc/LiCl is the activation process can weaken the hydrogen bonds among the molecules of the biopolymers. It can be explained as the molecules of the biopolymers can be separated due to charge-charge exclusion and expansion effects from solvent exchange process. Correspondingly, the solvent will penetrate into crystalline regions of biopolymers to destroy the association hydrogen bonding among molecules [101,132].

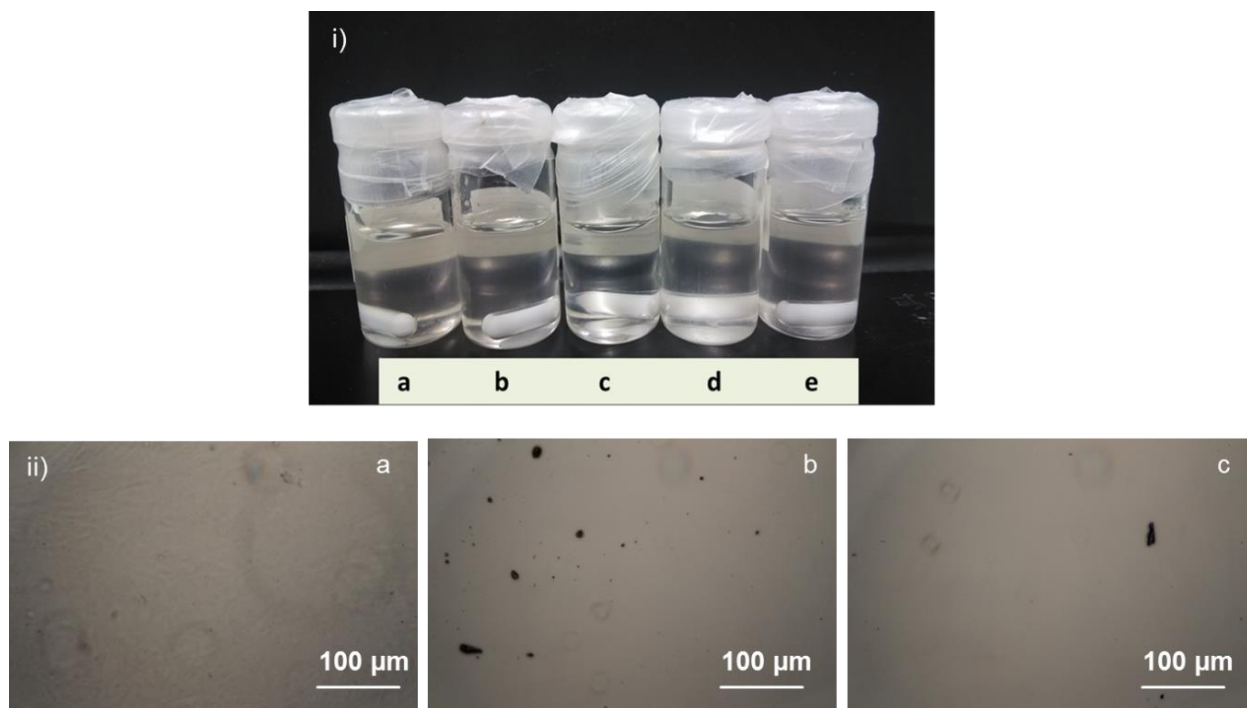


**Figure 3.1:** (i) Visual appearances of mixtures containing of (a) 3 wt% chitin, (b) 1 wt% chitin and 3 wt% MCC, (c) 0,6 wt% chitin and 4 wt% MCC, (d) 0,4 wt% chitin and 5 wt% MCC, (e) 10 wt% MCC in DMAc/LiCl (8%, w:w) within 2h; (ii) Selected optical microscopy images of the mixtures containing (a) 3 wt% chitin, (b) 10 wt% MCC and (c) 1 wt% chitin and 3 wt% MCC.

### 3.1.2 Dissolution chitin and cellulose in DES

Figure 3.2 shows turbid solutions are obtained from the mixtures containing 1 wt% chitin and 1 wt% MCC in choline chloride/urea (molar ratio: 1:2) and choline chloride/thiourea (molar ratio: 1:2), respectively. Therefore, it can be considered that both  $\alpha$ -chitin and MCC are insoluble in the two prepared DES solvents as choline chloride/urea (molar ratio: 1:2) and choline chloride/thiourea (molar ratio: 1:2) under the selected experimental conditions. The phenomenon suggests that the two DES solvents cannot be used for the direct dissolution of  $\alpha$ -chitin and MCC. The insoluble behaviour of chitin and cellulose in DESs could result from the high viscosity of the solvent systems [108,134,137].

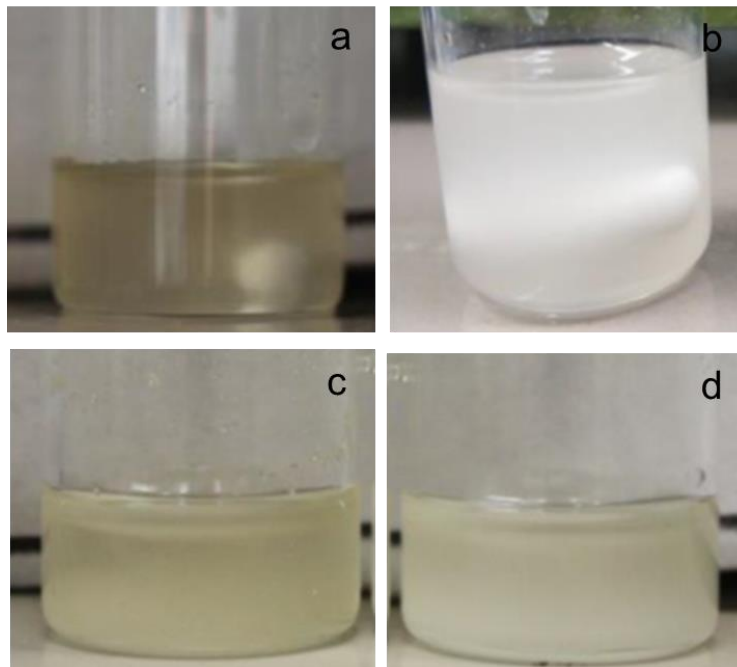


**Figure 3.2:** Visual appearance of the mixtures containing (a) 1 wt% chitin and (b) 1 wt% MCC, in choline chloride/urea (molar ratio: 1:2); (c) 1 wt% chitin and (d) 1 wt% of MCC, in choline chloride/thiourea (molar ratio: 1:2).

### 3.1.3 Dissolution of chitin in AmimBr and cellulose in EmimOAc

Table 3.1 illustrates that the IL AmimBr shows certain solubility for chitin, while cellulose is found to be insoluble. It is considered that the solubility of chitin in AmimBr is caused by some specific interactions formed by the solvent with the chitin chains as well as the relatively lower viscosity of the IL [30]. However, it can be observed from Figure 3.3 that although the visual appearance of the obtained mixture with 2 wt% chitin in AmimBr seems transparent and clear, some incompletely dissolved particles of chitin were observed in light microscopy. The result indicates an incomplete dissolution of chitin in AmimBr under the selected experimental conditions. On the contrary, it can be observed that up to 15 wt% cellulose can be dissolved in EmimOAc, while chitin shows insoluble. The good solubility of EmimOAc for MCC can be caused by the interactions of its anion with cellulose hydroxyl group [110,138]. On the other side, the insolubility of chitin in EmimOAc might result from the high viscosity of the solvent [25,130].

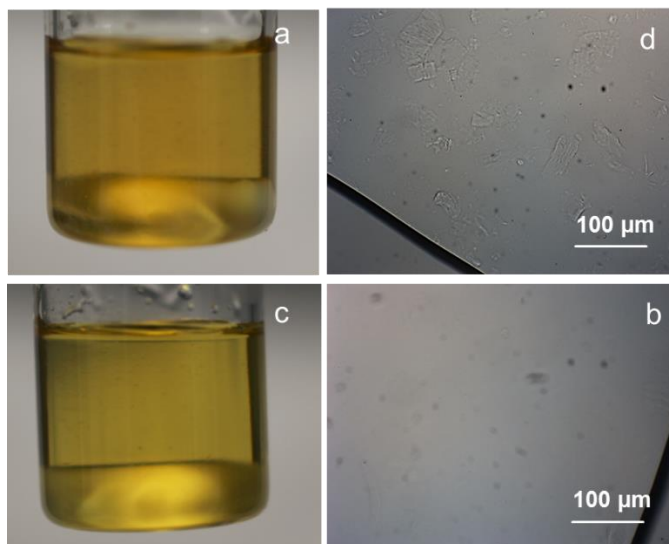


**Figure 3.3:** Visual appearance and corresponding light microscopy images of the obtained mixtures containing (a, b) chitin (2 wt%) in AmimBr; (c, d) MCC (8 wt%) in EmimOAc,

### 3.1.4 Dissolution of chitin and cellulose in BmimOAc-GVL

It is shown that up to 10 wt% MCC and 3 wt% chitin can be dissolved in BmimOAc under the selected experimental conditions, Table 3.1. The good dissolving power of BmimOAc for the two biopolymers can result from its acetate anion, which disrupts the complex hydrogen bond network of chitin or cellulose during the dissolution process. This strong hydrogen bonding acceptor and coordinating anion is supposed to interact strongly with the protons of the amino and hydroxyl groups for chitin and with the protons of hydroxyl group for cellulose [30,138,139].

The dissolution capacity of BmimOAc for chitin and cellulose can be improved by adding the co-solvent GVL, Figure 3.4. Furthermore, Table 3.1 shows that the solvent system with a molar ratio of BmimOAc to GVL as 8:1 can dissolve about 13 wt% MCC and 2 wt% chitin at 90 °C. The result illustrates that although GVL alone can dissolve neither chitin nor cellulose (Table 3.1), when applied as a co-solvent, it brings up some advantages for the dissolution of the biopolymers as follows: GVL presents a positive influence on the dissolution of chitin and MCC, because lower temperatures and shorter times can be applied. Furthermore, GVL facilitates further processing by decreasing the viscosity of the biopolymer solutions [130]. Therefore, compared to the sole ILs, BmimOAc-GVL solvent system is more environmentally benign. The investigation of GVL as a co-solvent was a cooperation work with our project partner. More detailed information of the

dissolution chitin and MCC in BmimOAc-GVL solvent can be found in the enclosed Publication #A and corresponding appendices [131].

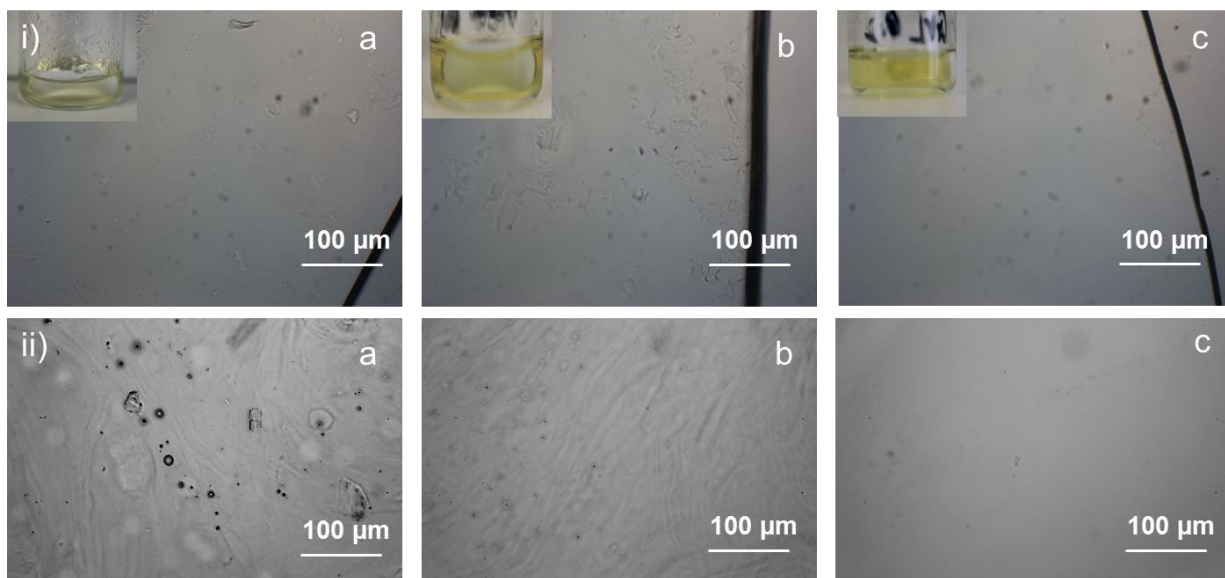


**Figure 3.4:** (i) Visual appearances and light microscopy images of the mixtures containing 1wt% chitin and 4 wt% MCC in solvent with different molar ratios of BmimOAc to GVL (without GVL (a), 4:1(b), 8:1 (c)). (ii) Light microscopy images of mixtures containing 2 wt% chitin in BmimOAc-GVL (molar ratio: 8:1) within (a) 1h, (b) 2h, (c) 3h under the selected experimental conditions.

### 3.1.5 Dissolution of chitin and lignin in BmimOAc-GVL

Due to the good solubility of BmimOAc-GVL for chitin and MCC as mentioned above, this solvent system was also employed for the dissolution of Kraft lignin. Table 3.2 shows that a maximum of 30 wt% Kraft lignin can be dissolved in BmimOAc-GVL at a mass ratio of 4:1. The confirmation of the solubility of Kraft lignin in BmimOAc-GVL can be found in Figure S3 (enclosed Publication #B). Detailed description of the dissolution of chitin and lignin in BmimOAc-GVL can be found in the enclosed Publication #B.

## 3.2 Characterization of chitin based composite materials

### 3.2.1 Composite chitin/cellulose materials fabricated from DMAc/LiCl

#### 3.2.1.1 Visual appearance and SEM analysis

All the obtained films fabricated from DMAc/LiCl present a transparent and homogeneous appearance, Figure 3.5 (i). Furthermore, it should be noted that all the regenerated films were with a certain strength, which could be easily handled both in wet and dry state. The SEM micrographs illustrates that the morphology of the composite film containing chitin is rougher than the pure cellulose film, Figure 3.5 (ii).

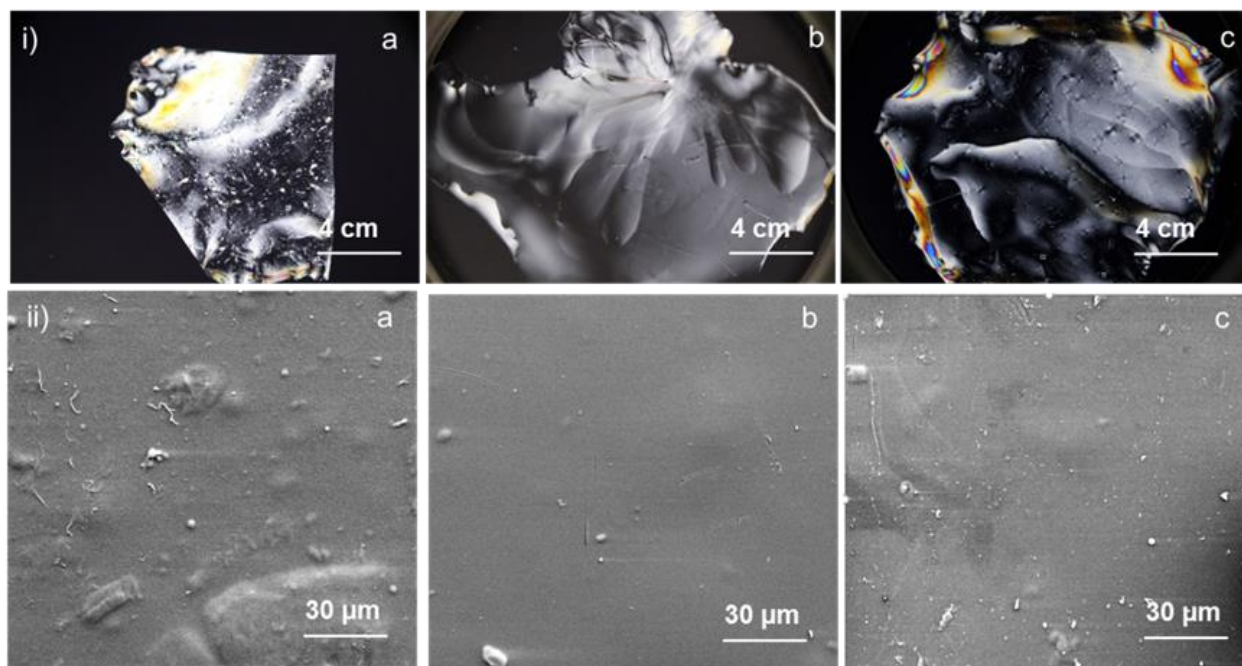


**Figure 3.5:** Photographs (i) and SEM micrographs (ii) of the chitin/cellulose composite films fabricated from DMAc/LiCl (8%, w:w) (a) chitin, (b) cellulose, (c) composite film with 25 wt% chitin concentration.

#### 3.2.1.2 ATR-FTIR measurement

In order to confirm the composition of chitin and cellulose in the composite films fabricated from DMAc/LiCl, composite chitin/cellulose films as well as the pure chitin and cellulose films were characterized by FTIR-ATR spectroscopy, Figure 3.6. The ATR-FTIR results illustrate that composite chitin/cellulose film shows the characteristic bands for both chitin and cellulose, Table

3.3. A chemical reaction between the biopolymers and the solvents during dissolution, which occurred as new absorption peaks, was not detected. The results demonstrate the successful fabrication of chitin/cellulose composite materials from the solvent system of DMAc/LiCl under the selected experimental conditions.

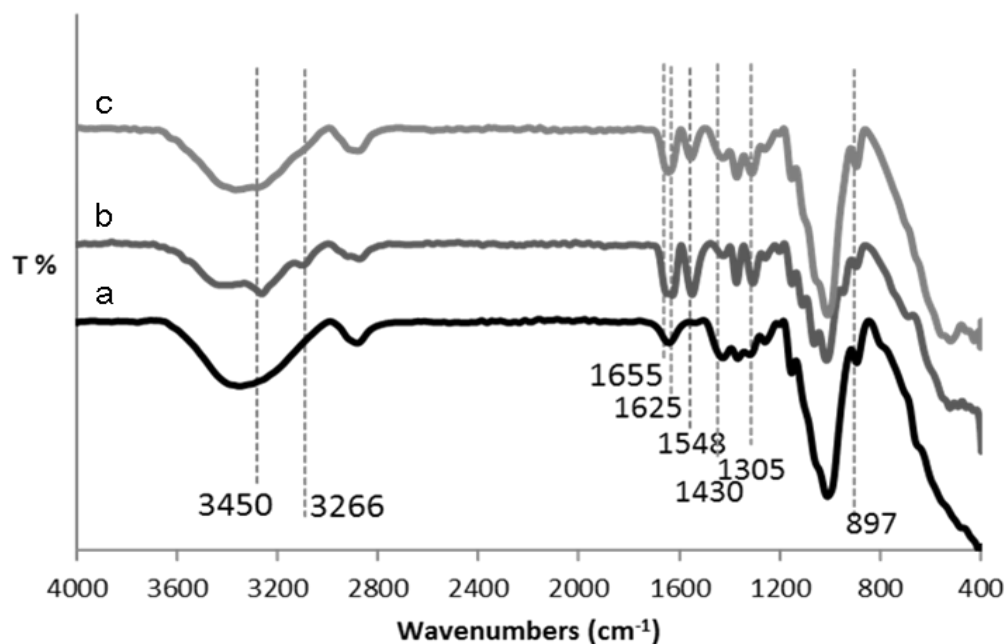


**Figure 3.6:** ATR-FTIR spectra of the films prepared from DMAc/LiCl (8%, w:w): (a) cellulose, (b) chitin, (c) composite film with 25 wt% chitin concentration.

**Table 3.3:** Measured absorption bands of samples with assignment to the type of atomic vibration.

Absorption bands	Type of atomic vibration	Reference
3405 $\text{cm}^{-1}$	stretching vibration of O-H in the structure of chitin	[26]
3266 $\text{cm}^{-1}$	vibrational mode of the N-H	[26]
1655, 1625 $\text{cm}^{-1}$	vibration mode of amide-I double bands for distinguishing chitin from chitosan	[26], [35]
1650	adsorbed water in cellulose	[140]
1548 $\text{cm}^{-1}$	bending vibrations of amide-II band	[35]
1430 $\text{cm}^{-1}$	a mixture of cellulose-II and amorphous cellulose	[141]
1305 $\text{cm}^{-1}$	bending vibrations of amide-III band	[35]
897 $\text{cm}^{-1}$	C <sub>1</sub> at the $\beta$ -1,4 glycosidic linkages	[49]

### 3.2.1.3 Water contact angle measurements

The wetting performance of the composite chitin/cellulose film fabricated from DMAc/LiCl was evaluated using water contact angle measurement. The contact angle is defined by the angle between a water droplet and the sample interface, which describes the wetting behavior of materials. Water contact angles lower than  $90^\circ$  correspond to a hydrophilic surface, whereas hydrophobic surface induce contact angles higher than  $90^\circ$  [142]. The water contact angle of the pure cellulose film is of  $23.5^\circ$ , which is considered hydrophilic, Figure 3.7. The water contact angles of the chitin/cellulose composite films increased with the increasing of chitin concentration. It should be noted that water contact angle of the composite with 25 wt% chitin concentration is about 90% large of pure chitin film, Figure 3.7. The result illustrates that chitin renders the composite materials more hydrophobic, even in a relatively low percentage of content.

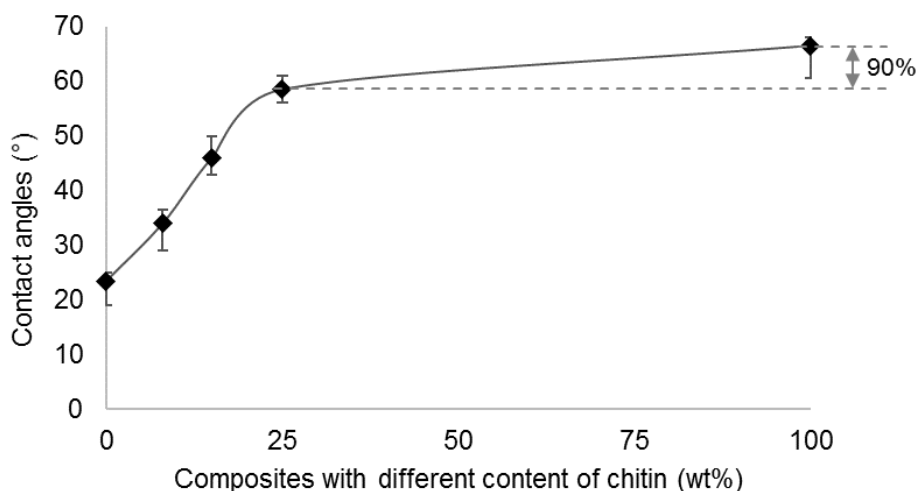


**Figure 3.7:** Water contact angles of the chitin/cellulose composite films with different concentrations of chitin regenerated from DMAc/LiCl.

## 3.2.2 Chitin/cellulose composite materials from AmimBr and EmimOAc

### 3.2.2.1 Visual appearance and SEM analysis

The obtained materials from the two ILs as AmimBr and EmimOAc present different appearances compared to the one from DMAc/LiCl. It can be observed that the obtained the pure cellulose film were transparent, whereas the composite chitin/cellulose film with 20 wt % of chitin content show

a more or less white and partly opaque appearance. The composite materials become more translucent with increasing content of chitin (Figure 3.8 (i)). Furthermore, the composite chitin/cellulose films are quite weak and almost cannot be completely removed from the coagulation bath. Especially, it should be noted that the pure chitin film is not successfully regenerated, Figure 3.8 (i (d)). The phenomenon confirms the good solubility of MCC in EmimOAc, whereas chitin is partly dissolved in AmimBr under the selected experimental conditions. The SEM micrographs of the pure cellulose film present a homogeneous morphology, while the composite films exhibit a rough surface, which might due to the chitin content (Figure 3.8 (ii)). No further characterizations were conducted on composite chitin/cellulose films prepared from AmimBr and EmimOAc, because stable composite films could not be successfully obtained.

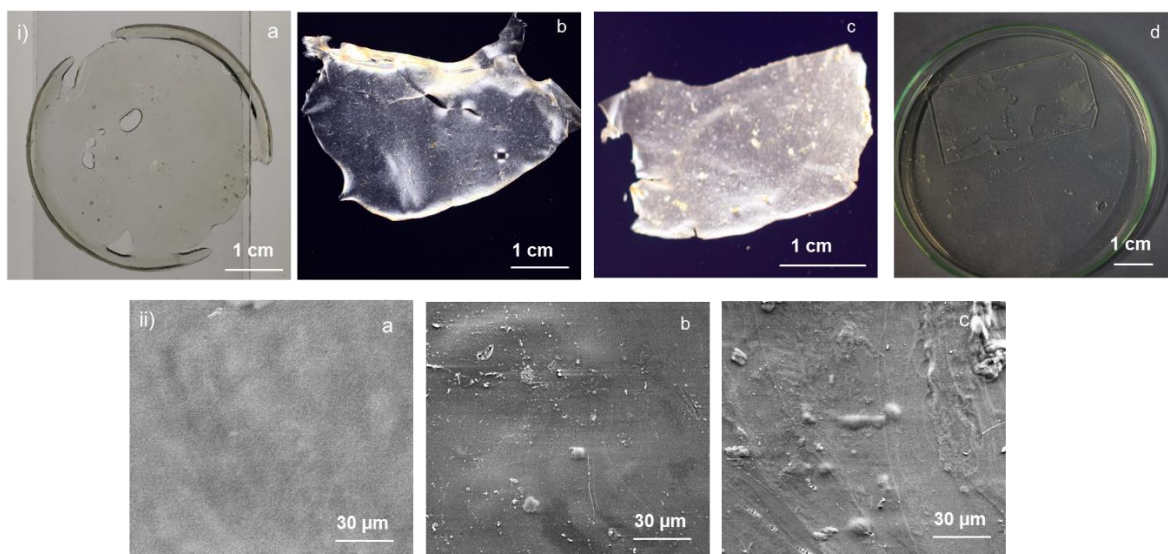


**Figure 3.8:** (i) Photographs of films (a) cellulose, (b) composite film with 20 wt% chitin concentration, (c) composite film with 33 wt% chitin concentration, (d) unsuccessfully regenerated chitin; (ii) the SEM micrographs of (a) cellulose, (b) composite film with 20 wt% chitin concentration, (c) composite film with 33 wt% chitin concentration.

### 3.2.3 Chitin/cellulose composite materials from BmimOAc- GVL

All the composite chitin/cellulose materials with different chitin concentrations can be successfully regenerated from the BmimOAc-GVL solvent system. Therefore, characterizations of the composite chitin/cellulose fabricated from BmimOAc-GVL solvent system including morphology analysis, polymer compositions, crystal structures, thermal analysis, as well as mechanical properties were investigated. In order to confirm that chitin was not deacetylated into chitosan by dissolving in BmimOAc, the degree of acetylation of the regenerated chitin was determined using

element analysis (EA) and ATR-FTIR spectroscopy. It is found that chitin is not deacetylated into chitosan, which is critical for the use of intact chitin in composite materials. In addition, the water absorption capacity and wetting behaviour of the obtained composite chitin/cellulose materials were studied. All the referred characterizations as well as the purity examination of the recycled BmimOAc can be found in the enclosed Publication #A and its supplementary materials.

### 3.2.3.1 Drying method investigation

#### 3.2.3.1.1 Visual appearances of the obtained composite chitin/cellulose materials before dry

The visual appearance of the pure chitin, pure cellulose and composite chitin/cellulose with 20 wt% of chitin content gels (about 7 mm thick) and films (about 1 mm thick) before drying are shown in Figure 3.9. It is found that the appearance of pure chitin gels is partly opaque, while films are almost transparent before drying. The wet pure cellulose gel and film show a white and opaque appearance. Compared to pure cellulose, the wet composite chitin/cellulose gel and film are lighter white and partly opaque.

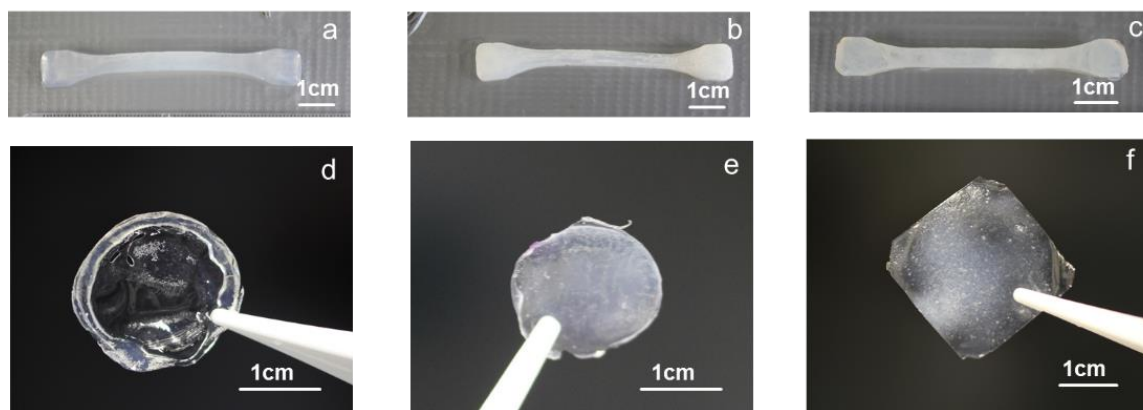


**Figure 3.9:** Visual appearances of the obtained gel and films before drying (pure chitin (a, d) pure cellulose (b, e) and (b) composite film with 20 wt% chitin concentration, (c) composites with 20 wt% chitin concentration (c, f)).

#### 3.2.3.1.2 Composite chitin/cellulose materials drying with supercritical carbon dioxide (scCO<sub>2</sub>)

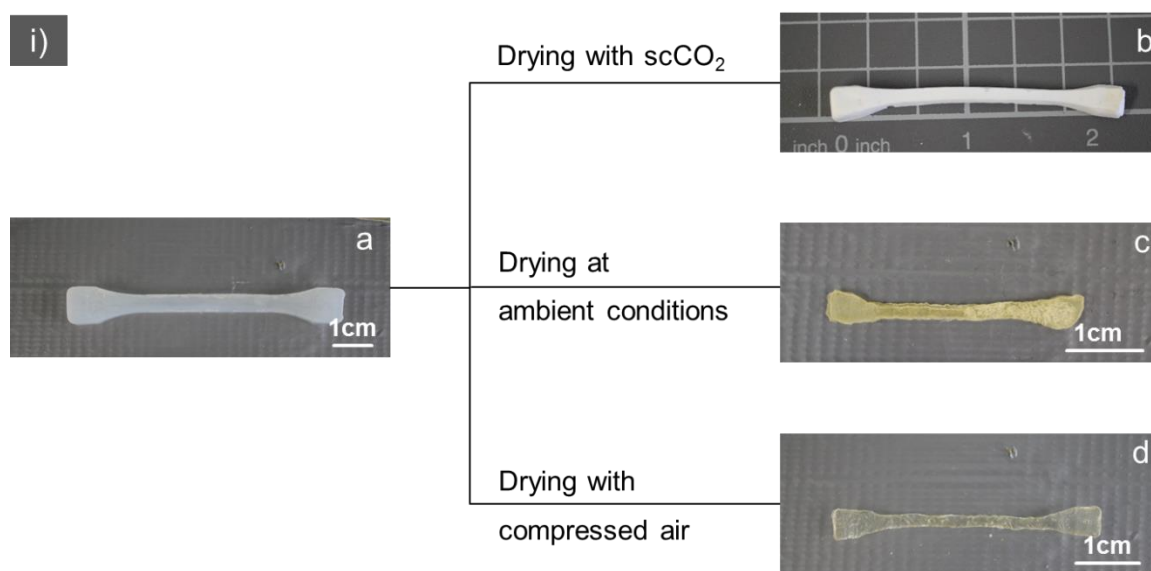
It is observed that both of the composite gels/films converted from aquogels to aerogels with white appearances after drying with scCO<sub>2</sub>, Figure 3.10. Almost no shrinkage occurred on the dried composites, Table 3.4. The phenomenon can be caused by scCO<sub>2</sub> drying, which is applied to avoid pore collapse of the porous structures of material [143].

### 3.2.3.1.3 Composite chitin/cellulose material drying at ambient conditions.

It is observed that the obtained composite chitin/cellulose film and gel dried at ambient conditions show yellow appearance, which can be caused by oxidizing from oxygen ( $O_2$ ) by exposing in the air for two days, Figure 3.10. Furthermore, the dried composite gels and films are not uniform with an extensive linear shrinkage between 73% and 78%, Table 3.

### 3.2.3.1.4 Composite chitin/cellulose materials dried with compressed air

It is found that both of the composite gels/films show a slight opaque appearance after drying with compressed air, Figure 3.10. It should be noted that the composite chitin/cellulose materials dried with compressed air are uniform and of even shape. Only a slight linear dimensional changes ranging from 9-12% is observed, Table 3.4. In addition, compared with the above two other drying methods, the dryness time of the chitin/cellulose composites drying with compressed air is shorter. For instance, a composite gel (thickness: 5 mm) costs around 60 min to be dry, while film with a thickness of 1 mm needs only around 20 min for drying.



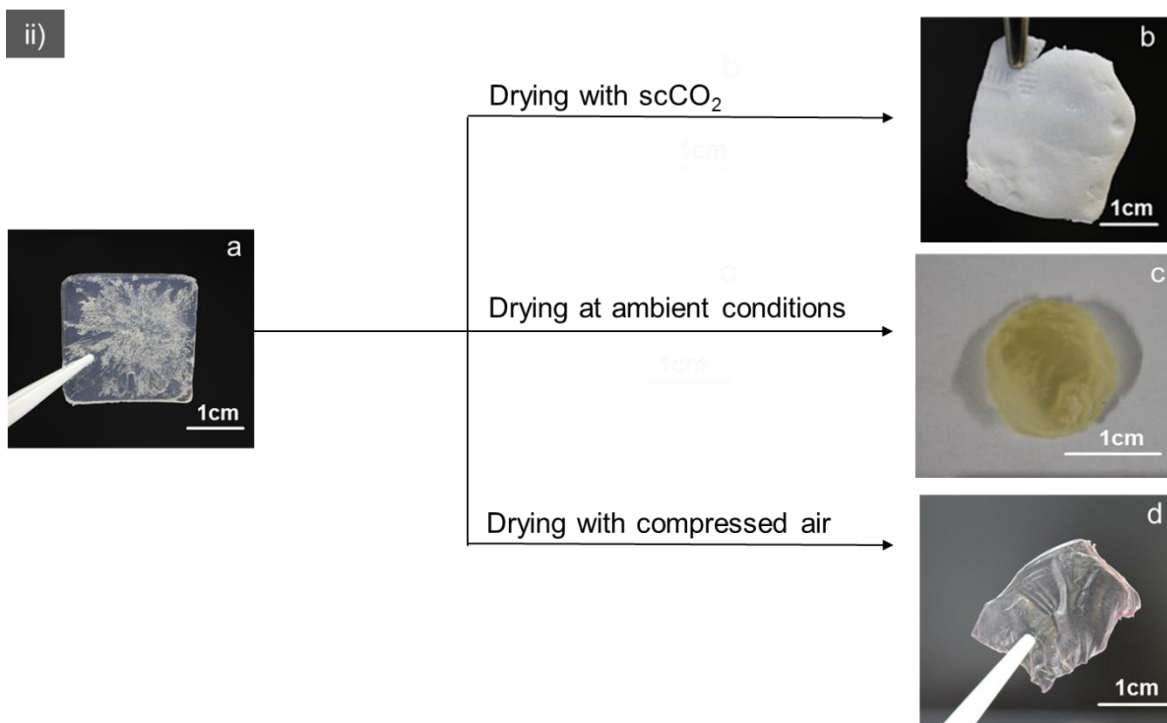


**Figure 3.10:** Composite gel (i) and film (ii) with 50 wt% chitin concentration with different drying methods (a) wet; (b) drying with scCO<sub>2</sub>; (c) drying at ambient conditions; (d) drying with compressed air.

**Table 3.4:** Linear shrinkage of the composite chitin/cellulose composite gels/films after drying with three different drying methods.

Composite Samples	Chitin concentration (wt%)	Linear shrinkage (%) with different drying method		
		ScCO <sub>2</sub>	Ambient condition	Compressed air
gel	20	0	77	11
	50	0	78	12
	80	0	78	12
film	20	0	73	9
	50	0	73	9
	80	0	75	10

### 3.2.3.2 Recycling of BmimOAc

The recycled solvent was analysed by using  $^1\text{H}$ - and  $^{13}\text{C}$ -NMR to evaluate the sustainability and environmental benign of the solution process for the fabrication of chitin/cellulose composite materials using BmimOAc-GVL. The analysis result of the obtained extract reveals that the solvent remained unaltered after dissolving the two biopolymers. Detailed information can be found in the enclosed Publication #A (Fig. A5).

## 3.2.4 Chitin film coated materials

### 3.2.4.1 Chitin film coated on wood

#### 3.2.4.1.1 Visual appearance and SEM analysis

The appearance of the untreated wood and the coated wood is shown in Figure 3.11. A homogeneous chitin layer can be clearly detected on the surface of spruce sample, The SEM micrographs illustrate that chitin is not only successfully coated on the surface of the wood but also partly infiltrates into the pores of wood sample.

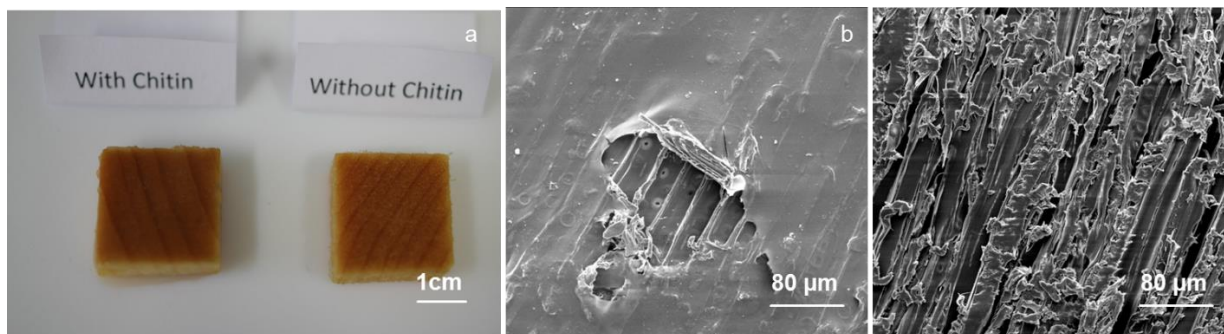


**Figure 3.11:** The photographs of the spruce cubes coated with chitin film and without chitin film (a,) and SEM micrographs of the surface of spruce cubes coated with chitin film (b, c).

#### 3.2.4.1.2 Water contact angles

Figure 3.12 shows the measured contact angles of water as well as the water absorption time on the samples. The contact angle of wood coated with chitin film is  $72.6^\circ$  (quite close to hydrophobic) and without chitin is  $125.2^\circ$ . However, the penetration time of a water droplet into the sample was about 16.8 min for a coated with chitin sample, whereas it is around 8.1 min for the wood sample without chitin.

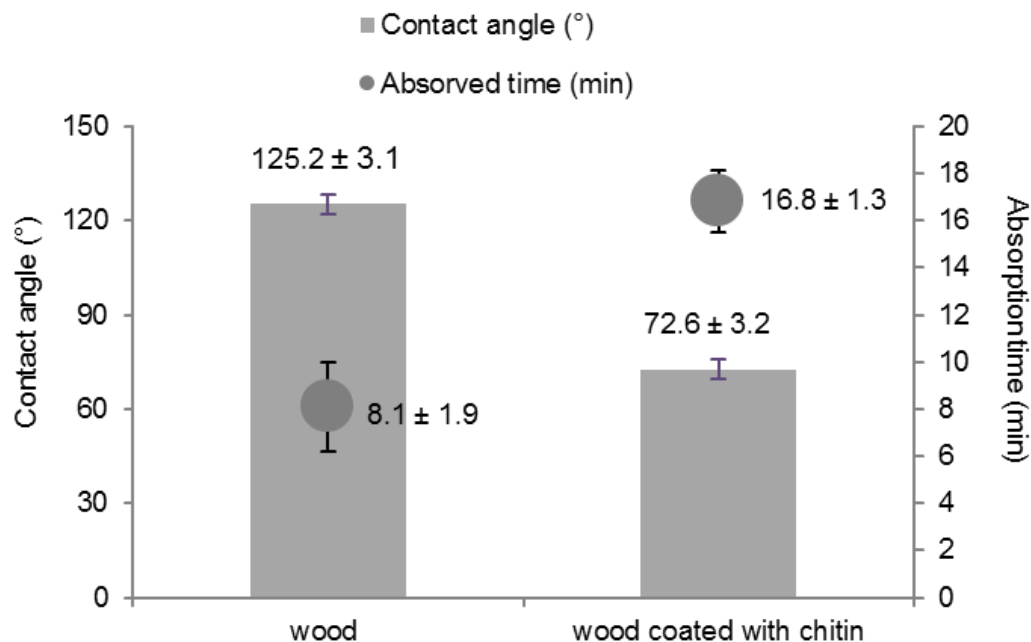


**Figure 3.12:** Water absorption time and contact angles of the wood samples non-coated and coated with chitin film.

According to literature report, the natural wood is hydrophilic due to the hygroscopic properties [144]. The observed large contact angle of the natural wood might originate from the rough wood surface structure. Due to the large pores of the natural wood surface, the water droplet is quickly absorbed. The phenomenon proves that the coated chitin layer rendered the wood surface more hydrophobic. Furthermore, the chitin film significantly retarding the water infiltration into wood.

#### 3.2.4.2 Chitin film coated on the cellulosic textiles

The characterization on the chitin coated cellulosic textiles was mainly performed with our project partner and detailed information can be found in the enclosed Publication #C.

#### 3.2.5 Chitin/lignin composite films from BmimOAc-GVL

Chitin/lignin composite films with different mass ratio of lignin were successfully obtained from the BmimOAc-GVL solvent system. The detailed characterization of the composites including morphology analysis and polymer compositions was performed. Especially, the specific properties of the composite chitin/lignin material as a biofilm sorbent for Fe(III) and Cu(II) ions from aqueous

solutions at room temperature were evaluated. All the detailed information is present in the enclosed Publication #B.

### **3.2.6 Chitin/lignin composite materials from melt compounding process**

It is found that all the chitin/lignin composite samples fabricated from melt compounding process are severely deteriorated after soaking in an ethanol bath. None of them formed an intact specimen for tensile testing, Figure 3.13. After drying, all the composite samples are considerably brittle and friable, which made them problematic for further characterization. Due to the unsuccessful generation of the chitin/lignin composite material, no further characterizations are carried on the chitin/lignin composite from melt compounding process.



**Figure 3.13:** *Chitin/lignin composite material (CL\_3) fabricated by melt compounding.*



## **Publication #A**

### **Cellulose and chitin composite materials from an ionic liquid and a green co-solvent**

Yaqing Duan, Auriane Freyburger, Werner Kunz, Cordt Zollfrank

Carbohydrate Polymers 192 (2018) 159-165; <http://doi.org/10.1016/j.carbpol.2018.03.045>

This work represents the first report on a sustainable method for the preparation of cellulose/chitin composite materials from the ionic liquid 1-Butyl-3-methylimidazolium acetate and  $\gamma$ -valerolactone as a biosourced sustainable co-solvent. Element analysis and attenuated total reflectance Fourier transform infrared spectroscopy show that the average degree of acetylation of chitin in the composite materials was around 82.5%. This indicates that chitin is not deacetylated to chitosan during the dissolution process. The X-ray diffraction results show that the degree of crystallinity of the composite materials increases from amorphous to 59% with increasing chitin concentration accompanied by a developing crystallite size up to 3 nm. Mechanical testing yielded a maximum tensile stress of 4.7 MPa, an elastic modulus of 27.4 MPa and a breaking elongation of 78.7% for the composites with 80 wt% chitin. In addition, water contact angle measurements indicated that the presence of chitin rendered the materials more hydrophobic.

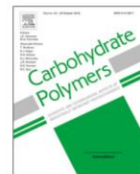
The work was performed under the supervision of Prof. Dr. Cordt Zollfrank, Biogenic Polymers, TUM and Prof. Dr. Werner Kunz, Institute of Physical and Theoretical Chemistry, University of Regensburg (UR). The solvent for the dissolution of the two biopolymers were developed in collaboration with Dr. Auriane Freyburger (UR). The preparation, measurement, characterization and evaluation of the composite samples were carried out by the author of this dissertation.





Contents lists available at ScienceDirect

Carbohydrate Polymers

journal homepage: [www.elsevier.com/locate/carbpol](http://www.elsevier.com/locate/carbpol)

## Cellulose and chitin composite materials from an ionic liquid and a green co-solvent



Yaqing Duan<sup>a</sup>, Auriane Freyburger<sup>b</sup>, Werner Kunz<sup>b</sup>, Cordt Zollfrank<sup>a,\*</sup>

<sup>a</sup> Chair for Biogenic Polymers, TUM Campus Straubing for Biotechnology and Sustainability, Technical University of Munich, Straubing, Germany

<sup>b</sup> Institute of Physical and Theoretical Chemistry, University of Regensburg, Regensburg, Germany

### ARTICLE INFO

#### Keywords:

Cellulose/chitin composite  
Ionic liquid  
Gamma-valerolactone  
Degree of acetylation  
Crystallinity index  
Mechanical property

### ABSTRACT

We report on a method for the preparation of cellulose/chitin composite materials from the ionic liquid 1-butyl-3-methylimidazolium acetate and  $\gamma$ -valerolactone as a biosourced sustainable co-solvent. Element analysis and attenuated total reflectance Fourier transform infrared spectroscopy show that the average degree of acetylation of chitin in the composite materials was around 82.5%. This indicates that chitin is not deacetylated to chitosan during the dissolution process. The X-ray diffraction results show that the degree of crystallinity of the composite materials increases from amorphous to 59% with increasing chitin concentration accompanied by a developing crystallite size up to 3 nm. Mechanical testing yielded a maximum tensile stress of 4.7 MPa, an elastic modulus of 27.4 MPa and a breaking elongation of 78.7% for the composites with 80 wt% chitin. In addition, water contact angle measurements indicated that the presence of chitin rendered the materials more hydrophobic.

### 1. Introduction

Composite materials based on biopolymers have gained special attention due to their biocompatibility and environmentally benign properties (Shen, Shamshina, Berton, Gurau, & Rogers, 2016). Biopolymer based materials can be applied in numerous fields such as medical applications (Qiu & Park, 2001), pollutant adsorbents (Houghton & Quarmby, 1999), packaging materials (Gontard et al., 2011), and many more. As the two most important and abundant natural biomass resources (Kadokawa, Hirohama, Mine, Kato, & Yamamoto, 2012; Takegawa, Murakami, Kaneko, & Kadokawa, 2010) cellulose and chitin are both commercially available with an annual production of more than  $10^7$  and  $10^{11}$  tons, respectively (Deguchi, 2017; Khalaf, 2016; Park & Kim, 2010; Varshney & Naithani, 2011). Cellulose is a renewable resource from lignocellulosics, such as wood and lignified higher plants and is the main constituent of the plant cell walls (Klemm, Heublein, Fink, & Bohn, 2005). This biopolymer is widely used for the production of paper, textiles and cosmetics and in many other industrial processes (Shokri & Adibkia, 2013). It is a glucose based homopolymer linked through  $\beta$  (1  $\rightarrow$  4) glycosidic bonds (Klemm et al., 2005). Chitin has a similar structure to cellulose, but bears an acetamido group ( $-\text{NHAc}$ ) at the C-2 positions instead of the hydroxyl group. It is the characteristic structural component of cell walls of fungi, the exoskeletons of arthropods such as crustaceans (e.g., crabs, lobsters and shrimps) and insects (Kurita, 2001). Chitin is produced in large quantities as a

byproduct during shrimp meat production (Wu, Sasaki, Irie, & Sakurai, 2008).

Both polysaccharides cellulose and chitin form rigid molecular structures caused by strong inter- and intramolecular hydrogen bonds. This leads to a lack of solubility of these polysaccharides in water and common organic solvents (Takegawa et al., 2010). Despite their huge availability, cellulose and chitin in composite materials remain unutilized. This is primarily due to the fact that only a few solvents are capable of dissolving chitin without deacetylation into chitosan (Wu et al., 2008). In order to directly prepare composite materials from cellulose and chitin, a solvent, which has the ability to dissolve both polymers without undesired derivatization and without being altered itself, is required. Over the last decade, ionic liquids (ILs) have been thoroughly investigated and proposed as promising solvents with negligible vapor pressure, non-inflammability and high thermal and chemical stability (Heinze & Koschella, 2005). Among them, some have been found to dissolve unmodified cellulose and chitin (Kadokawa et al., 2012). The preparation of cellulose/chitin composite materials was recently performed by preparing two separate solutions of the biopolymers in two different ILs during for four days at elevated temperatures (Kadokawa et al., 2012; Takegawa et al., 2010). The main drawback of this method is the high amount of ILs still present in the final composite materials. The separation of the two ILs after washing remains a problem concerning efficient recycling procedures. However, the IL 1-butyl-3-methylimidazolium acetate (BmimOAc) is capable of

\* Corresponding author.

E-mail address: [cordt.zollfrank@tum.de](mailto:cordt.zollfrank@tum.de) (C. Zollfrank).

<https://doi.org/10.1016/j.carbpol.2018.03.045>

Received 15 December 2017; Received in revised form 15 March 2018; Accepted 16 March 2018

Available online 18 March 2018

0144-8617/ © 2018 Elsevier Ltd. All rights reserved.

dissolving both cellulose and chitin from different origin and molecular weight at 110 °C (Wu et al., 2008). Since ILs are partly toxic and poorly biodegradable (e.g. imidazolium and pyridinium-based ILs; Stolte et al., 2007; Wood & Stephens, 2010), reducing the amount of an IL applied for dissolution would be desirable.  $\gamma$ -Valerolactone (GVL), which is a readily available biosourced solvent derived from renewable lignocellulosic biomass (Alonso, Wettstein, & Dumesic, 2013), was selected as a co-solvent to improve solution processing and to reduce environmental issues. We report on the simultaneous dissolution of native cellulose and chitin in a solvent system composed of the IL BmimOAc and the biosourced co-solvent GVL. We hypothesize that the dissolution of both polysaccharides in a single phase solvent is required to prepare cellulose and chitin composite materials without chemical modification or alteration of the two biopolymers. The obtained materials were characterized by optical microscopy, element analysis (EA), attenuated total reflectance Fourier transform infrared spectroscopy (ATR-FTIR), X-ray diffractometry (XRD) and mechanical testing. Special attention was paid to the evaluation of the degree of acetylation of the regenerated chitin to confirm that chitin was not deacetylated into chitosan during processing. We further anticipate that the wetting behavior and water absorption capacity of the cellulose/chitin composites can be tuned as a function of molar ratio cellulose to chitin.

## 2. Experimental

### 2.1. Chemicals and materials

Microcrystalline cellulose was purchased from Merck (Germany).  $\alpha$ -Chitin extracted from shrimp shells was obtained from Sigma Aldrich (Germany). The degree of polymerization (DP) of cellulose was 124 and of chitin was 1691 as determined by solution viscosimetry, Table S1. Both biopolymers were dried at 90 °C for one day and stored in a desiccator over silica gel prior to use. 1-Butyl-3-methylimidazolium acetate (BmimOAc, purity  $\geq$  98%, Sigma Aldrich, Germany) was dried with a high vacuum set-up at  $10^{-7}$  mbar for 5 days.  $\gamma$ -Valerolactone (GVL, Reagent Plus<sup>®</sup>, purity  $\geq$  99%, Sigma Aldrich, Germany) was dried by adding dried molecular sieve (3 Å). The solvents were stored in a desiccator over silica gel after drying. The biopolymers and reagents were used without any further chemical modification or purification.

### 2.2. Preparation of solvents to dissolve chitin and cellulose

The solvent system was obtained by mixing desired amounts of BmimOAc and GVL in a glove box at room temperature. Two molar ratios of BmimOAc to GVL, namely 8:1 and 4:1, were mixed in glass vials and immediately stirred to obtain clear and homogenous mixtures.

### 2.3. Dissolution of cellulose and chitin in BmimOAc-GVL solvent system

First, solutions of 8 wt% cellulose and 2 wt% chitin were prepared by dissolving the biopolymers in the respective BmimOAc/GVL mixture at 90 °C under mechanical stirring for 3 h. Then, the two solutions were mixed together to obtain the desired molar ratio of cellulose to chitin. The composition of the prepared samples and mixtures are summarized in Table 1.

### 2.4. Preparation of cellulose/chitin composite films and gels

Composite cellulose/chitin thin films were prepared by pouring the respective hot solution (1 g) into a petri dish ( $d = 4$  cm) with a syringe. They were subsequently kept at room temperature until the mixtures cooled down. Then, they were carefully covered with ethanol and left for about 4 h at room temperature until the composite films could be easily removed. Finally, the composite films were subjected to Soxhlet extraction with ethanol (100 mL) for 24 h in order to completely remove BmimOAc and GVL. The complete solvent removal was confirmed

**Table 1**

Preparation of composite materials with different cellulose to chitin molar ratios; Cs: composite polymer solution, Cf: composite films, Cg: gel films.

Sample code (solution)	Cellulose:chitin/BmimOAc:GVL (molar ratio)	Sample code (composites)	Cellulose:chitin (molar ratio)	Chitin concentration (wt%)
Cs_1	3.2:1/8:1	Cf_1 (Cg_1)	3.2:1	20
Cs_2	1.9:1/8:1	Cf_2 (Cg_2)	1.9:1	30
Cs_3	1:1.3/8:1	Cf_3 (Cg_3)	1:1.3	50
Cs_4	1:2.9/8:1	Cf_4 (Cg_4)	1:2.9	70
Cs_5	1:5.0/8:1	Cf_5 (Cg_5)	1:5.0	80

by ATR-FTIR measurements, as will be detailed in Section 3.4. The residual films were sandwiched between two Teflon plates and left to dry for approximately one day at ambient temperature.

A similar process was performed for the preparation of the composite cellulose/chitin gels. Approximately 2 g of the polymer solutions were cast into a square Teflon mold ( $4 \times 4 \times 1$  cm<sup>3</sup>). The composite gels were subjected to Soxhlet extraction with ethanol (100 mL) for 24 h in order to completely remove BmimOAc and GVL. After washing they were dried with compressed air at room temperature.

### 2.5. Determination of the degree of acetylation DA of chitin

The DA of chitin in the composites was determined using element analysis (EA) and ATR-FTIR spectroscopy. Pure regenerated chitin materials (called chitin-R1, chitin-R2 and chitin-R3) were prepared from three BmimOAc/GVL solutions with different chitin concentrations ranged from 1%, to 3% (wt:wt). The DA value from the native chitin powder (called chitin-NP) was determined under identical conditions and was taken as reference. The DA of chitin (%) was determined using the element composition of the samples from EA analysis and was calculated with the following Eq. (1) (Sajomsang & Gonil, 2010; Xu, McCarthy, Gross, & Kaplan, 1996)

$$DA = (C/N - 5.14)/1.72 \times 100 \quad (1)$$

where C/N is the mass ratio (w/w) of carbon to nitrogen. The DA of chitin (%) determined from the ATR-FTIR spectra was calculated by evaluation of three absorbance area ratios of the samples from Eq. (2). This equation is generally applicable for chitin samples, where DA values range from 50 to 100 (Kasaai, 2008; Shigemasa et al., 1996):

$$DA (\%) = (A_{1655} + A_{1625})/A_{3450} \quad (2)$$

where  $A_{1655}$ ,  $A_{1625}$  and  $A_{3450}$  are related to the baseline corrected amide-I absorbance area and O–H absorbance area of samples (Fig. 2).

### 2.6. Characterization

The elemental composition of cellulose and chitin as well as of the prepared composite materials was investigated in an element analyzer Euro EA (HEKAtech GmbH, Germany). After oxidation at 1000 °C, the gaseous products were separated by gas chromatography and detected with a thermal conductivity detector. Carbon (C), hydrogen (H) and nitrogen (N) relative contents were determined using tin capsules, containing 1–3 mg of sample. Relative content of oxygen (O) was measured using silver capsule within 1–2 mg of sample.

Infrared spectra of the samples were obtained by using an attenuated total reflectance-Fourier transform infrared spectrometer (ATR-FTIR, Nicolet 380, Thermo Fisher Scientific, USA) equipped with a diamond crystal. The measurements were conducted directly on native powder and film samples in the wavenumber region of 4000–400 cm<sup>-1</sup>.

X-ray diffraction (XRD) patterns were obtained with an X-ray diffractometer (Rigaku, MiniFlex 600, Tokyo, Japan) equipped with a high-speed one-dimensional detector (Rigaku, D/teX Ultra, Tokyo, Japan) and a K $\beta$ -filter. XRD spectra were recorded in the 2 $\theta$  range of

5°–40°, with a step width of 0.02°, a scanning speed of 2°/min and a CuK $\alpha$  radiation ( $\lambda = 0.1541$  nm) generated at 40 kV and 15 mA at room temperature. The crystallinity index (CI) of the samples was evaluated using Eq. (3) (El-Nesr, Raafat, Nasef, Soliman, & Hegazy, 2013; Foche, Beltrame, Naggi, & Torri, 1990; Shankar, Reddy, Rhim, & Kim, 2015):

$$CI\% = (I_{110} - I_{am})/I_{110} \times 100\% \quad (3)$$

where  $I_{110}$  is the maximum intensity of the peak at  $2\theta = 22.5^\circ$  for cellulose and  $2\theta = 19.1^\circ$  for chitin.  $I_{am}$  is the intensity of the amorphous region, which is at  $2\theta = 18^\circ$  for cellulose (Park, Baker, Himmel, Parilla, & Johnson, 2010), and at  $2\theta = 16^\circ$  for chitin (Herrera, Salaberria, Mathew, & Oksman, 2016; Shankar et al., 2015). The crystallite size (D) for some samples was evaluated using the Scherrer Eq. (4) (Das et al., 2009):

$$D = K\lambda/B(2\theta) \cos \theta \quad (4)$$

where  $K$  is a constant (0.94),  $\lambda$  is the wavelength of the X-ray (0.1541 nm),  $B(2\theta)$  is the full width at the half maximum of the respective peak (FWHM) after subtraction of the values measured with standard material ( $B_s(2\theta) = 0.001745$  rad) and  $\theta$  is Bragg's angle (Shankar et al., 2015).

The mechanical properties of the composite gels were evaluated with a universal tensile tester (Smar Tens 010, Karg Industrietechnik, Krailing, Germany) with an initial grip separation of 1 mm and cross-head speed of 10 mm/min. Pure cellulose, pure chitin and composite gels were cut into rectangular strips ( $1 \times 2$  cm<sup>2</sup>). The thickness of the gels was determined using an electronic digital caliper with an accuracy of 0.01 mm. Three random measurements of the thickness and width were taken from each gel sample. Tensile stress, elastic modulus and the elongation at break were obtained by the measurement of three specimens and the mean values with standard deviations were provided.

### 2.7. Water absorption capacity and water contact angle of cellulose/chitin composite materials

Water absorption capacity of the pure cellulose, pure chitin and composite materials were measured as follows: First, composite samples were dried at 100 °C for 12 h. Then, the samples were cut into small square pieces ( $1 \times 1$  cm<sup>2</sup>) and weighed. Subsequently, each sample was directly placed into a small beaker containing deionized water (15 mL) at room temperature for 48 h. Samples were removed, superficially dried with a tissue paper and weighed after 24 h soaking in water. Three specimens from each sample were measured and the mean values with standard deviations were calculated. The water absorption capacity of the sample was evaluated by the following Eq. (5):

$$A\% = (M_1 - M_0)/M_0 \times 100 \quad (5)$$

where  $A\%$  is the percentage of water absorption;  $M_1$  the weight (g) of sample with absorbed water in the respective test time;  $M_0$  the initial weight (g) of dry sample.

The wetting behavior of the composite cellulose/chitin films was evaluated by measuring the contact angle of a water droplet on the films using a P1 goniometer (Erna Inc, Japan). To this purpose, a water droplet formed with a micrometer pipette was slowly placed on the surface of the samples. The tangent of the drop profile at the contact point with the surface of the sample was observed through an optical system. The measurements were repeated ten times for each sample and the mean values with standard deviations were calculated.

## 3. Results and discussion

### 3.1. Solvent system for cellulose and chitin

The IL BmimOAc is capable of dissolving both cellulose and chitin

from different origins and molecular weights at 110 °C (Wu et al., 2008). As mentioned above, ILs are partly toxic and poorly biodegradable (Stolte et al., 2007; Wood & Stephens, 2010). As a consequence, it would be desirable to reduce the amount of IL applied for dissolution. We selected GVL, a biosourced solvent derived from renewable lignocellulosic biomass (Alonso et al., 2013). Unfortunately, GVL alone does not dissolve cellulose or chitin. However, a mixture of BmimOAc with GVL is capable of dissolving both biopolymers. To find the optimum molar ratio of BmimOAc and GVL, 2 wt% cellulose and 0.5 wt% chitin were simultaneously dissolved in solely BmimOAc, and in BmimOAc-GVL mixtures of 8:1 and 5:1 (mol:mol) ratios. All obtained solvent mixtures were clear (Fig. S1). However, complete dissolution of cellulose and chitin were only obtained with BmimOAc and GVL with an optimum molar ratio 8:1. Hence, the BmimOAc/GVL mixture with a molar ratio of 8:1 was chosen as the solution system for preparing the composite materials. An advantage of this solvent system is that it has a lower viscosity compared to pure BmimOAc (Fig. S2). A low viscosity is beneficial for the dissolution of polymers with high molecular weight such as chitin to improve processing capabilities. Secondly, the solvent system allowed a relatively low temperature (90 °C) and shorter time (3 h) to dissolve chitin and cellulose compared to other solvents previously reported (Kadokawa et al., 2012; Takegawa et al., 2010; Wu et al., 2008).

### 3.2. Preparation of cellulose/chitin composite materials

Fig. 1(i) shows the preparation process of the cellulose/chitin composite materials. The prepared composite films were transparent, whereas the gels showed a more or less white and partly opaque appearance. After drying, the composite films (with a thickness of 10  $\mu$ m) were translucent, while the opacity of composite gels (about 2 mm thick) decreased with increasing chitin concentration (Fig. 1(ii), Table 1).

In addition, both composite films and gels exhibited a homogeneous surface, which was observed using scanning electron microscopy. Furthermore, the morphology of composite gels showed an increasing surface roughness with increasing chitin content (Fig. S4).

### 3.3. Determination of the DA of chitin

Table 2 shows the DA values of the chitin native powder and of the regenerated chitin films determined from EA and ATR-FTIR analysis. The DA values of the samples evaluated by both methods showed a comparable good correlation. Chitin from regenerated films showed a slight decrease of the DA compared to the chitin native powder. The average DA values of the regenerated chitin films were 81% from EA and 83% according to the ATR-FTIR evaluation. This indicated that the regenerated material is still chitin (Pillai, Paul, & Sharma, 2009; Rinaudo, 2006, Table 2).

The ATR-FTIR spectra showed that the regenerated chitin films chitin\_R1, chitin\_R2, chitin\_R3 exhibited similar peaks corresponding to the native chitin powder, Fig. 2. The vibration mode of amide-I double bands at 1655 and 1625 cm<sup>-1</sup>, which are the important bands for distinguishing chitin from chitosan, were detected in all the samples. The bending vibrations of amide-II band at 1548 cm<sup>-1</sup> and amide-III band at 1305 cm<sup>-1</sup> all confirmed that chitin was not deacetylated to chitosan, which is in good agreement with the EA result. The peak at 897 cm<sup>-1</sup> confirmed the presence of  $\beta$ -1,4 glycosidic linkages and the band located at 3450 cm<sup>-1</sup> is ascribed to the stretching vibration of O–H in the structure of chitin (Wysokowski et al., 2014). However, a decrease of absorption band at 1655 cm<sup>-1</sup> of the regenerated chitin films indicated a decrease of the DA during the regeneration process (Kasaai, 2008), which was in good agreement with the aforementioned EA result.

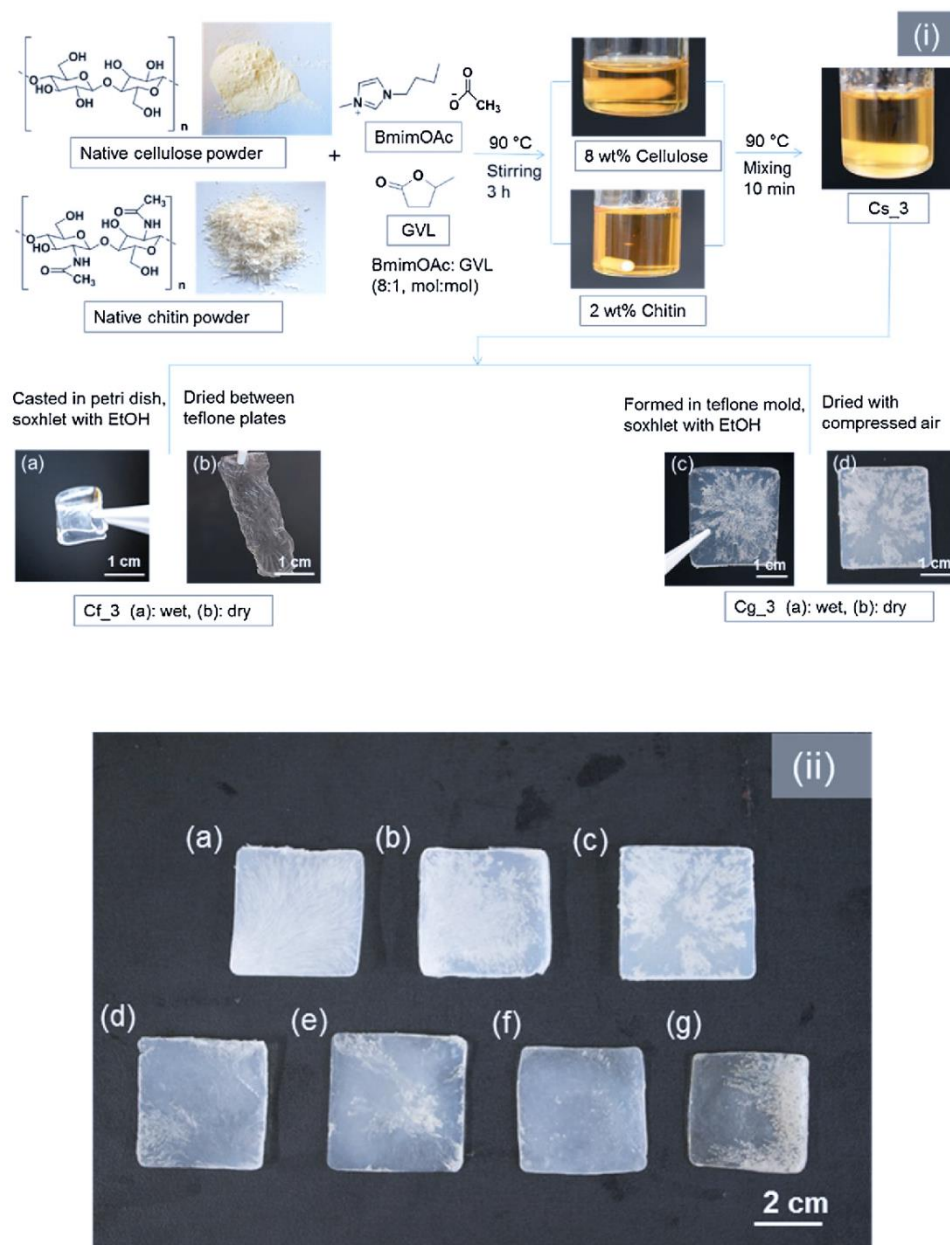


Fig. 1. (i): Preparation procedure for composite chitin/cellulose films and gels from BmimOAc-GVL solution; (ii): Composite gels prepared with different cellulose/chitin molar ratios (pure cellulose (a), Cg1 (b), Cg2(c), Cg3 (d), Cg4 (e), Cg5 (f), pure chitin (g)).

### 3.4. ATR-FTIR measurement of composite cellulose/chitin materials

To examine the composition of cellulose and chitin in the prepared films/gels and to confirm whether BmimOAc and GVL have been completely removed from the composite materials, samples were characterized by ATR-FTIR (Fig. 3a). The band located at  $1650\text{ cm}^{-1}$  in the cellulose film could be resulting from adsorbed water (Pang et al., 2014) and the band at  $1430\text{ cm}^{-1}$  indicated that the film consists of a mixture of cellulose-II and amorphous cellulose (Nelson & O'Connor, 1964a). The small sharp band at  $894\text{ cm}^{-1}$  is characteristic for the  $\beta$ -

glycosidic linkages between glucose (Jin et al., 2009). The detailed spectra for chitin were described above. The splitting of the amide-I, and the bands at  $3266$  and  $3106\text{ cm}^{-1}$  (vibrational mode of the N-H) indicated that the native chitin is  $\alpha$ -chitin (Cárdenas, Cabrera, Taboada, & Miranda, 2004). Hence, a decrease of these absorbance bands might suggest a change of the crystalline structures after regeneration. The composite samples showed the spectral characteristics in both cellulose and chitin. The characteristic absorption peaks of chitin were stronger with increasing concentration in chitin as expected. For instance, sample of Cf\_1 did not show absorption band at  $3266$  and  $3106\text{ cm}^{-1}$

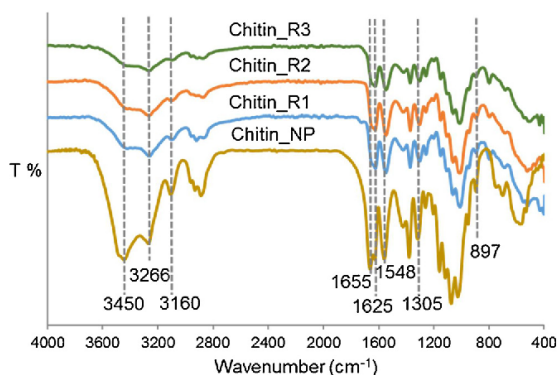


Fig. 2. ATR- FTIR spectra of native chitin powder and regenerated chitin films prepared from different chitin concentrations.

Table 2

Elemental analysis of regenerated chitin films as well as chitin native powder and the corresponding degree of acetylation (DA) values evaluated by EA and ATR-FTIR respectively (wt% is the mass ratio of the examined element in the samples).

Sample	C (wt%)	H (wt %)	N (wt %)	O (wt%)	DA% (EA)	DA% (ATR-FTIR)
Chitin_NP	39.0	6.1	5.8	37.6	88.9	90.7
Chitin_R1	39.3	6.3	6.0	34.5	82.2	85.4
Chitin_R2	39.2	7.4	5.9	32.5	82.1	82.7
Chitin_R3	39.0	7.8	5.9	41.3	79.7	80.2

(vibrational mode of the N–H) and exhibited only weak amide-II and -III bands. Those bands were comparably stronger in sample Cf\_3, which contain more chitin. No reaction between the biopolymers and the solvents occurred as new absorption peaks could not be observed. Furthermore, absorption peaks derived from BmimOAc and GVL were not observed in any spectra of the composite samples (Fig. 3b). These results demonstrated the successful fabrication of cellulose/chitin composite materials from the solvent system of BmimOAc-GVL.

3.5. Crystallinity of cellulose/chitin composite materials

The crystal structure of native cellulose and chitin powders and of the composite films was analyzed by XRD, Fig. 4. Native micro-crystalline cellulose powder exhibited the typical peaks of cellulose-I at 2θ of 15.0°, 16.0° and 22.6° (Herrera et al., 2016; Nelson & O'Connor, 1964b). The chitin powder showed the characteristic crystalline peaks of α-chitin (around 9.1°, 18.9° and 26.3°) (Wu et al., 2008).

The regenerated cellulose film showed only flat and broad

diffraction peaks from 10° to 25°, which indicated the expected formation cellulose-II in an apparently amorphous state (Park et al., 2010). The diffraction peaks of the chitin film appearing at 2θ = 9.1° and 18.9° were weaker and broader than those of the native powders and the peaks at 18.9° and 26.3° almost disappeared. This phenomenon suggests a transition from the α-chitin to the β-chitin polymorph after regeneration (Cárdenas et al., 2004). The XRD patterns of the cellulose/chitin composite films showed both diffraction peaks from cellulose and chitin and the intensity of the chitin peaks increased with chitin content. This result suggests that chitin is the predominant crystalline form in the composite films. The crystallinity index (CI) and crystallite size (D) were determined by using Eq. (1) and the Scherrer Eq. (2). The calculated values are listed in Table 3. The cellulose regenerated from solution appeared as an amorphous solid. The CI of chitin was also strongly decreased from 82% to 54%. This phenomenon is caused by the dissolution process, where crystalline structures of cellulose and chitin were destroyed. Furthermore, all composite films exhibited relatively lower crystalline degrees compared to the pure chitin film. However, their CI increased with increasing chitin content (Table 3). The crystallite size of native cellulose and chitin was 5 and 7 nm, respectively, These values are similar to those previously reported (Ardizzone et al., 1999; Shankar et al., 2015). The comparably smaller crystallite size of chitin in the composite film (6 nm) illustrated a slight decrease induced by the regeneration process. Furthermore, the crystallite size of the composite samples became smaller with decreasing chitin content. For instance, the composite sample with higher cellulose content Cf\_1 was apparently amorphous. The determined crystallite size of Cf\_2 and Cf\_3 were 1 nm and 2 nm, respectively, which also indicated an almost amorphous state. Only Cf\_4 with a crystallite size of 3 nm showed a developing crystallinity.

3.6. Mechanical properties of composite cellulose/chitin gels

The mechanical properties of the composite cellulose/chitin gels were determined by tensile testing. Table 4 shows that the tensile stress values of the composite samples increased linearly with the increase of chitin content from 20 to 80 wt% from 0.5 to 4.7 MPa. However, composite samples with lower than 70 wt% of chitin exhibited lower tensile stress values than the pure cellulose and chitin gels. On the other hand, the elastic modulus of the composite samples increased from 13.3 to 27.4 MPa with increasing chitin content. The hydrogen bonding between cellulose and chitin might be stronger with the increasing concentration of chitin in the composite gels. This might be the reason for the observed increased stiffness and strength of the composite samples. Additionally, the composite gels exhibited a higher elongation at break than the cellulose gels. The higher breaking elongation with increasing chitin concentration indicated the contribution of chitin to the elastic properties of the composite materials (Fig. S5). Furthermore, the relatively higher tensile strength (4.7 MPa) and breaking elongation

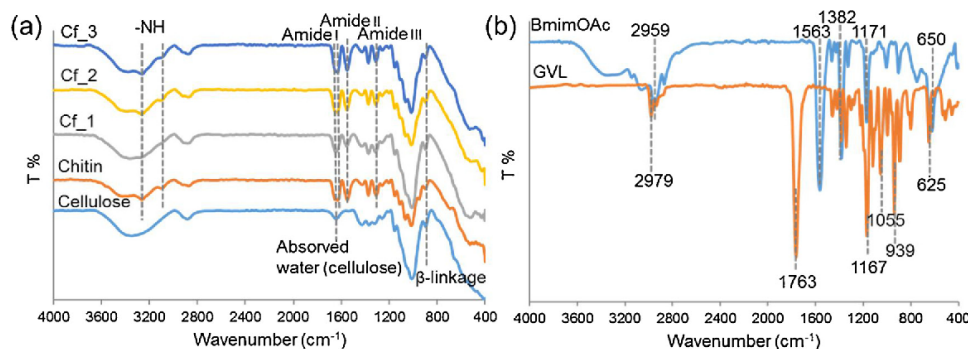


Fig. 3. ATR- FTIR spectra of (a) cellulose, chitin and selected composite films and (b) the components of the solvent system BmimOAc and GVL.

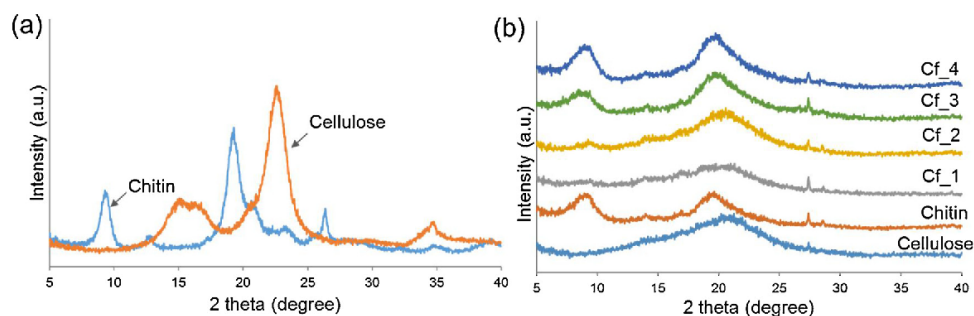


Fig. 4. XRD diagrams of (a) cellulose and chitin and (b) the regenerated cellulose, chitin and selected composite films.

**Table 3**  
Crystallinity index (CI) and crystallite size (D) of cellulose, chitin and selected composite samples.

Sample	CI (%)	D (nm)	sample	CI (%)	D (nm)
Cellulose, reference	81	5	Cf_1	–	–
Chitin, reference	89	7	Cf_2	45	(1)
Cellulose film	–	–	Cf_3	56	(2)
Chitin film	54	6	Cf_4	59	3

**Table 4**  
Results of the mechanical properties, water absorption and contact angles for the cellulose, chitin and the composite gels.

Sample	Tensile stress (MPa)	Elastic modulus (MPa)	Breaking elongation (%)	Water absorption (wt%)	Water contact angle (°)
Cellulose, reference	3.5 ± 0.1	14.1 ± 0.4	12.9 ± 1.3	52 ± 1.8	46.9 ± 5.6
Cf_1	0.5 ± 0.1	13.3 ± 0.5	30.2 ± 1.2	60 ± 0.9	58.3 ± 3.8
Cf_2	1.0 ± 0.1	21.7 ± 1.3	35.7 ± 1.1	62 ± 1.8	62.7 ± 6.3
Cf_3	2.8 ± 0.1	25.1 ± 1.7	42.6 ± 2.0	75 ± 3.4	65.5 ± 5.9
Cf_4	3.6 ± 0.2	27.2 ± 1.5	61.8 ± 3.1	83 ± 4.9	73.4 ± 6.5
Cf_5	4.7 ± 0.1	27.4 ± 1.1	78.7 ± 3.5	97 ± 3.9	74.2 ± 7.3
Chitin, reference	3.3 ± 0.1	38.2 ± 2.6	96.4 ± 3.2	102 ± 1.8	75.1 ± 6.9

(78.7%) of the composite gel containing 20 wt% cellulose and 80 wt% chitin illustrated that cellulose is mainly reinforcing the composite material. In addition, compared to previously reports on the tensile strength (7.5–9.0 MPa) and elongation at break (3.7–11.0%) (Takegawa et al., 2010) for cellulose/chitin composites, our cellulose/chitin materials showed a lower strength, but increased elastic properties.

### 3.7. Water absorption capacity and contact angles

The results for water absorption and the measured contact angles are given in Table 4. All samples reached their absorption saturation of water within 24 h at room temperature. The water absorption capacity of the composite samples increased linearly with the chitin concentration. Especially, the composite sample with 80 wt% chitin exhibited a similar water absorbance capacity (i.e. 97 wt%) as the pure chitin gel (102 wt%). It should be noted that the cellulose/chitin material composites were still robust and flexible after soaking in water. The contact angle is defined by the angle between a water droplet and the sample interface, which describes the wetting behavior of materials (Shankar et al., 2015; Vogler, 1998). The contact angle of the pure cellulose film was 47°, which is considered quite hydrophilic. On the contrary, pure chitin films were more hydrophobic, resulting in higher contact angle of 75°. The water contact angles of the cellulose/chitin films increased

linearly with the chitin concentration, which were ranging from 58 to 74°. The results illustrated that chitin rendered the composite materials more hydrophobic.

## 4. Conclusion

Cellulose/chitin composite materials were successfully prepared by using a novel solvent system composed of only one single ionic liquid (BmimOAc) and a biosourced co-solvent GVL with different cellulose to chitin molar ratio. By adding GVL, the amount of environmentally arguable IL can be significantly reduced. Clear solutions could be obtained within 3 h, which is much faster compared to previously reported dissolutions time of 24 h. Analytical results indicated that chitin was not deacetylated into chitosan, which is critical for the use of intact chitin in composite materials. The XRD examination showed that the obtained composite materials exhibited the crystal patterns of  $\alpha$ -chitin and  $\beta$ -chitin, but with a relatively low crystallinity index CI and crystallite size. Furthermore, the mechanical properties of the cellulose/chitin composites were evaluated. Increasing the chitin content was beneficial for achieving elastic properties of the composite material. The water absorption capacity was also depended on the chitin concentration. It was additionally found that the wetting behavior of the cellulose/chitin composite materials can be tuned with the chitin concentration and chitin rendered the films more hydrophobic. The presented cellulose/chitin biopolymer composites could be applied in packaging, medical or textile applications replacing fossil resource based materials.

## Acknowledgements

This research was performed in the frame of the project ForCycle (BAF01SoFo-65212), financially supported by the Bavarian State Ministry of the Environment and Consumer Protection, Germany.

## Appendix A. Supplementary data

Supplementary data associated with this article can be found, in the online version, at <https://doi.org/10.1016/j.carbpol.2018.03.045>.

## References

- Alonso, D. M., Wettstein, S. G., & Dumesic, J. A. (2013). Gamma-valerolactone, a sustainable platform molecule derived from lignocellulosic biomass. *Green Chemistry*, 15(3), 584–595. <http://dx.doi.org/10.1039/C3GC37065H>.
- Ardizzone, S., Dioguardi, F., Mussini, T., Mussini, P., Rondinini, S., Vercelli, B., et al. (1999). Microcrystalline cellulose powders: Structure, surface features and water sorption capability. *Cellulose*, 6(1), 57–69.
- Cárdenas, G., Cabrera, G., Taboada, E., & Miranda, S. P. (2004). Chitin characterization by SEM, FTIR, XRD, and <sup>13</sup>C cross polarization/mass angle spinning NMR. *Journal of Applied Polymer Science*, 93(4), 1876–1885.
- Das, K., Ray, D., Bandyopadhyay, N., Ghosh, T., Mohanty, A. K., & Misra, M. (2009). A study of the mechanical, thermal and morphological properties of microcrystalline cellulose particles prepared from cotton slivers using different acid concentrations.

- Cellulose, 16(5), 783–793.
- Deguchi, S. (2017). *Comparative in situ microscopic observation of cellulose and chitin in hydrothermal conditions. Extreme biotronics*. Springer:119–133.
- El-Nesr, E., Raafat, A., Nasef, S. M., Soliman, E., & Hegazy, E. (2013). Chitin and chitosan extracted from irradiated and non-irradiated shrimp wastes (Comparative Analysis Study). *Arab Journal of Nuclear Science and Applications*, 46(1), 53–66.
- Focher, B., Beltrame, P., Naggi, A., & Torri, G. (1990). Alkaline N-deacetylation of chitin enhanced by flash treatments. Reaction kinetics and structure modifications. *Carbohydrate Polymers*, 12(4), 405–418.
- Gontard, N., Angellier-Coussy, H., Chalier, P., Gastaldi, E., Guillard, V., Guillaume, C., et al. (2011). *Food packaging applications of biopolymer-based films. Biopolymers – New materials for sustainable films and coatings*. John Wiley & Sons Ltd:211–232.
- Heinze, T., & Koschella, A. (2005). Solvents applied in the field of cellulose chemistry: A mini review. *Polímeros*, 15, 84–90.
- Herrera, N., Salaberria, A. M., Mathew, A. P., & Oksman, K. (2016). Plasticized polylactic acid nanocomposite films with cellulose and chitin nanocrystals prepared using extrusion and compression molding with two cooling rates: Effects on mechanical, thermal and optical properties. *Composites Part A: Applied Science and Manufacturing*, 83, 89–97.
- Houghton, J. I., & Quarmby, J. (1999). Biopolymers in wastewater treatment. *Current Opinion in Biotechnology*, 10(3), 259–262. [http://dx.doi.org/10.1016/S0958-1669\(99\)80045-7](http://dx.doi.org/10.1016/S0958-1669(99)80045-7).
- Jin, A. X., Ren, J. L., Peng, F., Xu, F., Zhou, G. Y., Sun, R. C., et al. (2009). *Comparative characterization of degraded and non-degraded hemicelluloses from barley straw and maize stems: Composition, structure, and thermal properties*, Vol. 78. Kidlington, United Kingdom: Elsevier.
- Kadokawa, J.-I., Hirohama, K., Mine, S., Kato, T., & Yamamoto, K. (2012). Facile preparation of chitin/cellulose composite films using ionic liquids. *Journal of Polymers and the Environment*, 20(1), 37–42. <http://dx.doi.org/10.1007/s10924-011-0331-3>.
- Kasaai, M. R. (2008). A review of several reported procedures to determine the degree of N-acetylation for chitin and chitosan using infrared spectroscopy. *Carbohydrate Polymers*, 71(4), 497–508. <http://dx.doi.org/10.1016/j.carbpol.2007.07.009>.
- Khalaf, M. N. (2016). *Green polymers and environmental pollution control*. CRC Press.
- Klemm, D., Heublein, B., Fink, H.-P., & Bohn, A. (2005). Cellulose: Fascinating biopolymer and sustainable raw material. *Angewandte Chemie International Edition*, 44(22), 3358–3393. <http://dx.doi.org/10.1002/anie.200460587>.
- Kurita, K. (2001). Controlled functionalization of the polysaccharide chitin. *Progress in Polymer Science*, 26(9), 1921–1971. [http://dx.doi.org/10.1016/S0079-6700\(01\)00007-7](http://dx.doi.org/10.1016/S0079-6700(01)00007-7).
- Nelson, M. L., & O'Connor, R. T. (1964a). Relation of certain infrared bands to cellulose crystallinity and crystal lattice type. Part II. A new infrared ratio for estimation of crystallinity in celluloses I and II. *Journal of Applied Polymer Science*, 8(3), 1325–1341.
- Nelson, M. L., & O'Connor, R. T. (1964b). Relation of certain infrared bands to cellulose crystallinity and crystal lattice type. Part I. Spectra of lattice types I, II, III and of amorphous cellulose. *Journal of Applied Polymer Science*, 8(3), 1311–1324. <http://dx.doi.org/10.1002/app.1964.070080322>.
- Pang, J.-H., Liu, X., Wu, M., Wu, Y.-Y., Zhang, X.-M., & Sun, R.-C. (2014). Fabrication and characterization of regenerated cellulose films using different ionic liquids. *Journal of Spectroscopy*, 2014, 8. <http://dx.doi.org/10.1155/2014/214057>.
- Park, B. K., & Kim, M.-M. (2010). Applications of chitin and its derivatives in biological medicine. *International Journal of Molecular Sciences*, 11(12), 5152–5164.
- Park, S., Baker, J. O., Himmel, M. E., Parilla, P. A., & Johnson, D. K. (2010). Cellulose crystallinity index: Measurement techniques and their impact on interpreting cellulase performance. *Biotechnology for Biofuels*, 3(1), 10.
- Pillai, C. K. S., Paul, W., & Sharma, C. P. (2009). Chitin and chitosan polymers: Chemistry, solubility and fiber formation. *Progress in Polymer Science*, 34(7), 641–678. <http://dx.doi.org/10.1016/j.progpolymsci.2009.04.001>.
- Qiu, Y., & Park, K. (2001). Environment-sensitive hydrogels for drug delivery. *Advanced Drug Delivery Reviews*, 53(3), 321–339. [http://dx.doi.org/10.1016/S0169-409X\(01\)00203-4](http://dx.doi.org/10.1016/S0169-409X(01)00203-4).
- Rinaudo, M. (2006). Chitin and chitosan: Properties and applications. *Progress in Polymer Science*, 31(7), 603–632. <http://dx.doi.org/10.1016/j.progpolymsci.2006.06.001>.
- Sajomsang, W., & Gonil, P. (2010). Preparation and characterization of  $\alpha$ -chitin from cicada sloughs. *Materials Science and Engineering C*, 30(3), 357–363. <http://dx.doi.org/10.1016/j.msec.2009.11.014>.
- Shankar, S., Reddy, J. P., Rhim, J.-W., & Kim, H.-Y. (2015). Preparation, characterization, and antimicrobial activity of chitin nanofibrils reinforced carrageenan nanocomposite films. *Carbohydrate Polymers*, 117, 468–475.
- Shen, X., Shamshina, J. L., Berton, P., Gurau, G., & Rogers, R. D. (2016). Hydrogels based on cellulose and chitin: Fabrication, properties, and applications. *Green Chemistry*, 18(1), 53–75. <http://dx.doi.org/10.1039/C5GC02396C>.
- Shigemasa, Y., Matsuura, H., Sashiwa, H., & Saimoto, H. (1996). Evaluation of different absorbance ratios from infrared spectroscopy for analyzing the degree of deacetylation in chitin. *International Journal of Biological Macromolecules*, 18(3), 237–242.
- Shokri, J., & Adibkia, K. (2013). *Application of cellulose and cellulose derivatives in pharmaceutical industries*.
- Stolte, S., Matzke, M., Arning, J., Bösch, A., Pitner, W.-R., Welz-Biermann, U., et al. (2007). Effects of different head groups and functionalised side chains on the aquatic toxicity of ionic liquids. *Green Chemistry*, 9(11), 1170–1179.
- Takegawa, A., Murakami, M.-A., Kaneko, Y., & Kadokawa, J.-I. (2010). Preparation of chitin/cellulose composite gels and films with ionic liquids. *Carbohydrate Polymers*, 79(1), 85–90. <http://dx.doi.org/10.1016/j.carbpol.2009.07.030>.
- Varshney, V., & Nalthani, S. (2011). *Chemical functionalization of cellulose derived from nonconventional sources. Cellulose fibers: Bio- and nano-polymer composites*. Springer:43–60.
- Vogler, E. A. (1998). Structure and reactivity of water at biomaterial surfaces. *Advances in Colloid and Interface Science*, 74(1), 69–117.
- Wood, N., & Stephens, G. (2010). Accelerating the discovery of biocompatible ionic liquids. *Physical Chemistry Chemical Physics*, 12(8), 1670–1674.
- Wu, Y., Sasaki, T., Irie, S., & Sakurai, K. (2008). A novel biomass-ionic liquid platform for the utilization of native chitin. *Polymer*, 49(9), 2321–2327.
- Wysokowski, M., Klapiszewski, Moszyński, D., Bartzak, P., Szatkowski, T., Majchrzak, I., et al. (2014). Modification of chitin with kraft lignin and development of new biosorbents for removal of cadmium(II) and nickel(II) ions. *Marine Drugs*, 12(4), 2245.
- Xu, J., McCarthy, S. P., Gross, R. A., & Kaplan, D. L. (1996). Chitosan film acylation and effects on biodegradability. *Macromolecules*, 29(10), 3436–3440.



Appendices. A: Supplementary materials

## Cellulose and Chitin Composite Materials from a Green Solvent

Yaqing Duan <sup>a</sup>, Auriane Freyburger <sup>b</sup>, Werner Kunz <sup>b</sup>, Cordt Zollfrank <sup>a,\*</sup>

<sup>a</sup> Chair of Biogenic Polymers, TUM Campus Straubing for Biotechnology and Sustainability, Technical University of Munich, Straubing, Germany.

E-Mail: [yaqing.duan@tum.de](mailto:yaqing.duan@tum.de); [cordt.zollfrank@tum.de](mailto:cordt.zollfrank@tum.de).

<sup>b</sup> Institute of Physical and Theoretical Chemistry, University of Regensburg, Regensburg, Germany.

E-Mail: [Auriane.Freyburger@chemie.uni-regensburg.de](mailto:Auriane.Freyburger@chemie.uni-regensburg.de); [Werner.Kunz@chemie.uni-regensburg.de](mailto:Werner.Kunz@chemie.uni-regensburg.de).

\* Corresponding author: E-Mail: [cordt.zollfrank@tum.de](mailto:cordt.zollfrank@tum.de);

Tel.: +49 (0) 9421 187-450.

Fax.: +49 (0) 9421 187-130

## 1. Degree of polymerization

The degree of polymerization of native cellulose and chitin powder were according to DIN 54 270. First, native cellulose and chitin powder were dissolved in Cuen and DMAc /LiCl (5%, w:w) solvent, respectively)(Table A1). The intrinsic viscosities  $[\eta]$  of the two polymer solutions were calculated by their efflux time in according to the Schulz-Blaschke equation. (A.1).

$$[\eta] = (\eta_{rel} - 1) / (1 + K_{\eta} \times (\eta_{rel} - 1)) \quad (A.1)$$

Where  $\eta_{rel}$  is the relative viscosity and  $K_{\eta}$  is a coefficient ( $K_{\eta} = 0.3$ )

The molecular mass (M) and DP of the two biopolymers were evaluated by the Kuhn-Mark-Houwin-Sakurada (KMHS) equation. (A.2).

$$[\eta] = K \times M^{\alpha} \quad (A.2)$$

Where K is a constant value ( $K = 7.6 \times 10^{-3}$ ) and  $\alpha$  is 0.95

*Table A1. Viscosimetric determinations of DP of native cellulose and chitin powders.*

Sample	Concentration	Solvent	Temperature(°C)	DP	Ref
Native cellulose powder	0.03 g/dL	cupriethylenediamine hydroxide solution (Cuen)	20	124	DIN54 270 (Biliuta, Fras, Harabagiu, & Coseri, 2011)
Native chitin powder	0.01 g/dL	N,N-dimethylacetamide (DMAc)/LiCl (5%, w:w)	30	1691	(Rinaudo, 2006)

## 2. Viscosity of solvents

The dynamic viscosity of the solvent was determined using a falling ball viscometer (Anton Paar, AMVn) in the temperature range from 25 to 110 ° C. The dynamic viscosity ( $\eta$ ) is determined by the equation. (A.3).

$$\eta = K (\rho_{ball} - \rho_{sample}) t \quad (A.3)$$

where  $K$  is a calibration constant that depends on temperature and tilt angle.  $\rho_{\text{ball}}$  is the density of the sphere and  $\rho_{\text{sample}}$  means the density of the sample, which is measured by a bending oscillator (DMA 5000M, Anton Paar);  $t$  is the measured roll time of the ball in the capillary.

Fig. A1 shows the viscosity curves of the two solvents as pure BmimOAc and a mixture of BmimOAc with GVL (8:1, mol:mol). It was clearly found that the high viscosity of BmimOAc was significantly reduced by adding GVL.

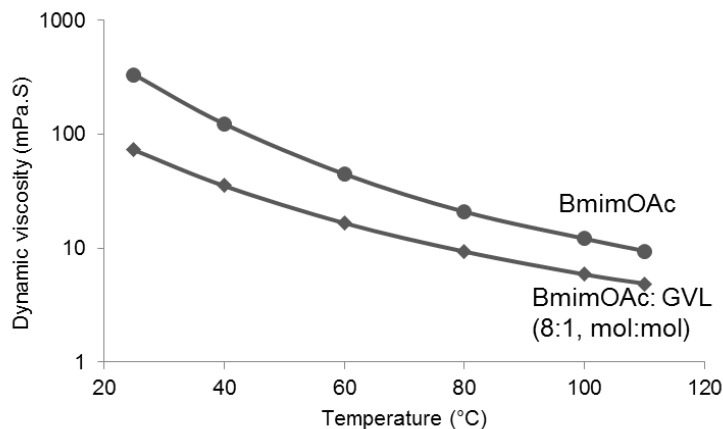


Fig. A1. Viscosity data of pure BmimOAc and the mixture of BmimOAc and GVL (8:1, mol:mol) from 25 °C to 110 °C. Lines correspond to correlations using the Vogel-Fulcher-Tammann equation.

### 3. SEM measurement of composite cellulose/chitin materials

The morphology of the prepared pure and composite materials were analyzed by digital scanning electron microscopy (DSM 940 A, Zeiss, Oberkochen, Germany) in secondary imaging mode at 10 kV and current at 3.20A (samples were sputtered with Au). As shown in Fig. A2, the composite sample showed the morphology of both cellulose and chitin, which indicated its homogeneous. Furthermore, it was observed that the morphology of the materials became rougher with the increasing content of chitin.

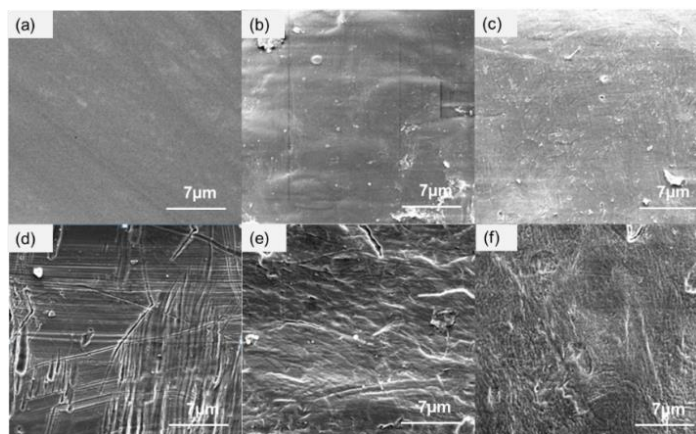


Fig. A2. SEM micrographs of the surface of films and gels ((a) cellulose film, (b) Cf\_3, (c) chitin film, (d) cellulose gel, (e) Cg\_3, (f) chitin gel).

#### 4. TGA measurement of composite cellulose/chitin materials

Thermal analysis were determined by using thermogravimetric analysis (TGA) and differential thermal analysis (DTA) on a simultaneous thermal analyzer (STA PT1600 TGA/DSC, Linseis) from room temperature to 600°C with a heating rate of 10 °C/min under inert atmosphere of Ar<sub>2</sub>. Fig. A3 illustrated that all the samples started with a considerable sharp weight loss between ca. 260 °C and 300 °C, due to the thermal hydrolysis of their polymer chains. Because of the high crystallinity of the native cellulose and chitin powders, they showed comparable higher onset decomposition temperatures than the regenerated gels. However, the latter exhibited higher decomposition temperatures at 50 wt% mass loss, which indicated an improved thermal stability. In addition, Cg\_5 with 80 wt% chitin content showed analogous behavior as pure chitin gel on thermal stability.

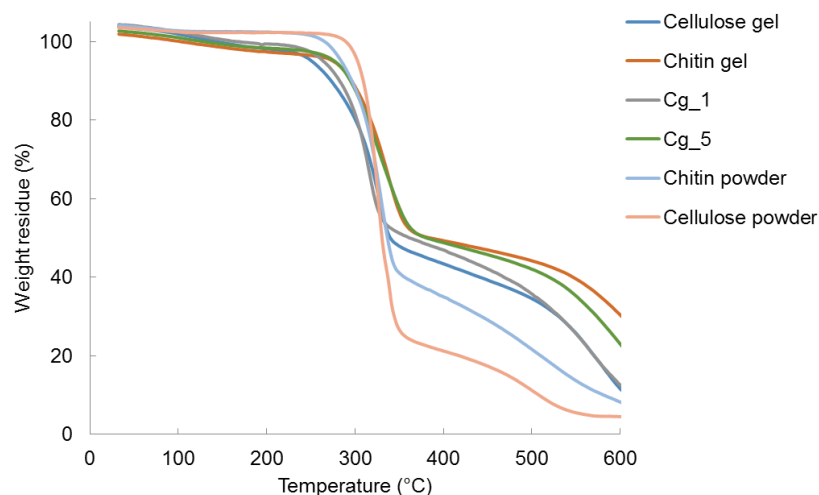


Fig. A3. TGA curves of native cellulose and chitin powders, regenerated cellulose and chitin gels and selected composite samples

#### 5. Mechanical testing of composite cellulose/chitin materials

Fig. A4 shows the strength and elastic properties of the Cg\_4 during the tensile testing, which supported the mechanical properties results described in the article.

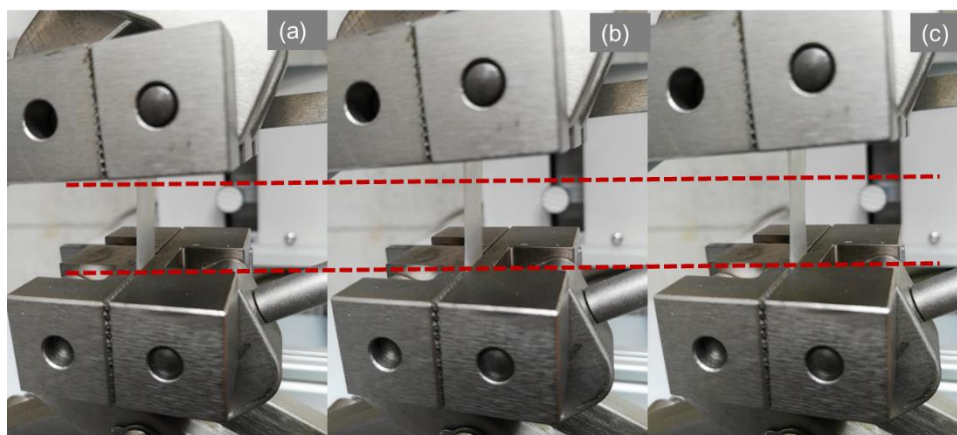


Fig. A4. Photograph of the selected sample (Cg\_4) during the tensile testing.

#### 6. Determination of the structures of the recycled green solvents

After the Soxhlet procedure, the ethanol-based coagulation solutions was first concentrated using a rotary evaporator (100 mbar) at 45°C until the ethanol was nearly evaporated. Then, the

residual solvent was dried with a high vacuum ( $10^{-6}$  mbar) at  $40^{\circ}\text{C}$  for 5 days. The chemical structures of the recycled solvents were identified using nuclear magnetic resonance (NMR, ECA400, Jeol Inc, USA) by dissolving them in dimethyl sulfoxide- $d_6$ . The  $^{13}\text{C}$ -NMR and  $^1\text{H}$ -NMR spectra of the recycled green solvents illustrated that the chemical structures of BmimOAc and GVL were not changed in the preparation process of composite materials (Fig. A5). The result confirmed that there was no reaction between the biopolymers and the solvents.

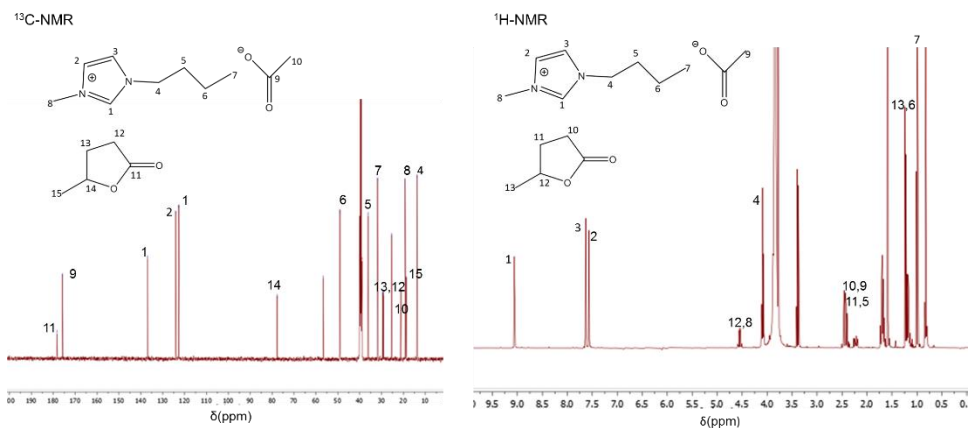


Fig. A5.  $^{13}\text{C}$ -NMR and  $^1\text{H}$ -NMR spectra from recycled BmimOAc and GVL

## **Publication #B**

### **Lignin/chitin films and their adsorption characteristics for heavy metal ions**

Yaqing Duan, Auriane Freyburger, Werner Kunz, Cordt Zollfrank

ACS Sustainable Chemistry & Engineering; <https://doi.org/10.1021/acssuschemeng.8b00805>

This study presents the fabrication of novel lignin/chitin films from a solvent system composed of the ionic liquid 1-butyl-3-methylimidazolium acetate and  $\gamma$ -valerolactone as a bio-sourced co-solvent. Scanning electron microscopy and attenuated total reflectance Fourier transform infrared spectroscopy confirmed the successful preparation of the lignin/chitin films.

This work also first studied the application of lignin/chitin film as an adsorbent for Fe(III) and Cu(II) cation uptake from aqueous solutions. It was observed that the maximum adsorption capacity for Fe(III) was 84 wt% and for Cu(II) was 22 wt% within 48 h. The adsorption kinetics of the lignin/chitin bio-adsorbent film is discussed. Moreover, the lignin/chitin films could be regenerated by desorption of the Fe(III) and Cu(II) ions. Up to 12 wt% and 46 wt%, respectively, could be released within 48 h by directly soaking the metal ion loaded film within water at room temperature. The lignin/chitin film can be considered as a stable and recyclable bio-adsorbent material with a high adsorption metal ion capacity for water purification.

The work was performed under the supervision of Prof. Dr. Cordt Zollfrank, Biogenic Polymers, TUM and Prof. Dr. Werner Kunz, Institute of Physical and Theoretical Chemistry, UR. The solvent for the dissolution of chitin was developed in collaboration with Dr. Auriane Freyburger (UR). The preparation, measurement and characterization the composite lignin/chitin samples as well as evaluation and kinetics study of their absorption properties were carried out by the author of this dissertation.



## 1 Lignin/Chitin Films and Their Adsorption Characteristics for Heavy 2 Metal Ions

3 Yaqing Duan,<sup>†</sup> Auriane Freyburger,<sup>‡</sup> Werner Kunz,<sup>‡</sup> and Cordt Zollfrank<sup>\*,†</sup>

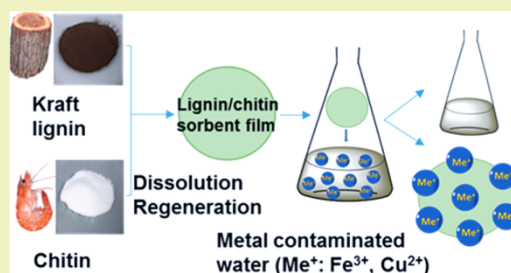
4 <sup>†</sup>Chair of Biogenic Polymers, TUM Campus Straubing for Biotechnology and Sustainability, Technical University of Munich,  
5 Schulgasse 16, 94315, Straubing, Germany

6 <sup>‡</sup>Institute of Physical and Theoretical Chemistry, University of Regensburg, Universitätsstraße 31, 93040, Regensburg, Germany

7 **S** Supporting Information

8 **ABSTRACT:** This study presents the fabrication of novel  
9 lignin/chitin films from a solvent system composed of the ionic  
10 liquid 1-butyl-3-methylimidazolium acetate and  $\gamma$ -valerolactone  
11 as a biosourced cosolvent. Scanning electron microscopy and  
12 attenuated total reflectance Fourier transform infrared spectroscopy  
13 confirmed the successful preparation of the lignin/  
14 chitin films. The application of lignin/chitin film as an adsorbent  
15 for Fe(III) and Cu(II) cation uptake from aqueous solutions is  
16 discussed. It was observed that the maximum adsorption  
17 capacity for Fe(III) was 84 wt % and for Cu(II) was 22 wt %  
18 within 48 h. The lignin/chitin films could be regenerated by  
19 desorption of the Fe(III) and Cu(II) ions. Up to 12 and 46 wt  
20 %, respectively, could be released within 48 h by directly soaking  
21 the metal ion loaded film within water at room temperature.  
22 The lignin/chitin film can be considered as a stable and recyclable  
23 bioadsorbent material with a high adsorption metal ion  
24 capacity for water purification.

**KEYWORDS:** lignin, chitin, biofilm sorbent, ionic liquids, heavy metal adsorption, desorption



### 24 ■ INTRODUCTION

25 Water pollution with toxic heavy metals is an increasing threat  
26 to the ecosystems of the earth.<sup>1</sup> Especially, the pollution with  
27 Fe (III) and Cu (II) from highly loaded industrial sewage water  
28 and other pollution sources is known to be the most common  
29 and toxic one, which is of major concern.<sup>2</sup> Hence, the removal  
30 of heavy metals from sewage is an important topic for the  
31 environmental issues. Numerous research work toward the  
32 development of various technologies for the removal of toxic  
33 metal ions from water have been reported such as ion exchange  
34 resins,<sup>3</sup> chemical precipitation<sup>4</sup> and coagulation-flocculation,<sup>4,5</sup>  
35 electrolytic reduction,<sup>6</sup> membrane technology,<sup>7</sup> and biosorb-  
36 ents.<sup>8</sup> Many alternatives with respect to fossil resource based  
37 solid-phase sorbents prepared from the renewable resources  
38 such as cellulose, lignin, and chitin have gained special  
39 attention.<sup>9–13</sup>

40 Lignin is one of the three essential components from  
41 wood<sup>12–14</sup> and also one of the most abundant biopolymers next  
42 to cellulose and chitin. The chemical structure of lignin is  
43 complex. It is referred to as a three-dimensional amorphous  
44 polymer consisting of phenylpropane units based on the three  
45 monolignols as coniferyl, sinapyl, and *p*-coumaryl alcohol.<sup>15,16</sup>  
46 The amount of total lignin biomass was estimated to be about  
47 300 billion tons in the year of 2012, and around 20 billion tons  
48 of lignin are formed every year. In 2010, 50 million tons of  
49 lignin were produced in the paper and pulp industry, of which  
50 only two percent were used in commercially applications.<sup>17</sup>

Lignin is also considered as a biomass resource with a high  
51 potential in various and value added productions. It was  
52 reported that Kraft lignin and lignin from other sources could  
53 be used as a metal ion adsorbent for treating wastewater.<sup>18</sup>

54 Another important and abundant natural biomass resource is  
55 the polysaccharide chitin, which occurs primarily as a  
56 characteristic component of cell walls of fungi, the exoskeletons  
57 of arthropods such as crustaceans (e.g., crabs, lobsters, and  
58 shrimps), and insects.<sup>19</sup> The chemical structure of chitin is an  
59 amino-polysaccharide, which consists of a glucose polymer  
60 linked through  $\beta$  (1  $\rightarrow$  4) glycosidic linkages bearing acetamido  
61 groups at the C-2 positions. The annual production of chitin is  
62 more than 10<sup>7</sup> tons<sup>20</sup> and most of them occur as a byproduct  
63 (secondary resource) from shrimp production.<sup>21</sup> Because of its  
64 chemical stability, high reactivity, and nontoxicity, chitin is  
65 considered to be an attractive biomaterial.<sup>22,23</sup> The common  
66 features of both lignin and chitin are their feasible accessibility,  
67 biocompatibility, and environmental beneficial properties.  
68 Furthermore, it was reported that both biopolymers showed a  
69 sorption affinity for heavy metal ions.<sup>19–29</sup> Hence, lignin and  
70 chitin composite materials could be applied as a replacement  
71 for products from fossil resources.<sup>11–13,26</sup>

Received: February 18, 2018

Revised: March 26, 2018

Published: April 10, 2018

**Table 1.** Preparation of the Composite Lignin/Chitin Thin Films and Their Dimensional Changes after Drying as well as the Element Compositions of the Films, Lignin, and Chitin Native Powders<sup>a</sup>

samples	lignin:chitin		dimensional change (%)	elemental composition (wt %)					
	mass ratio feed	mass ratio film		C	N	S	H	N/C	S/C
lignin				62.8	0.5	1.1	5.6	0.01	0.018
LC1	4:1	3.1:1	61.1	50.3	3.7	0.4	6.0	0.07	0.008
LC2	3:1	2.4:1	50.0	45.4	3.6	0.3	5.9	0.08	0.007
LC3	2:1	1.6:1	22.2	53.5	5.7	0.1	6.5	0.01	0.002
LC4	1:1	1:1.2	16.7	48.4	5.5	n. d.	6.6	0.11	n. d.
LC5	1:2	1:2.0	5.6	46.0	6.1	n. d.	6.7	0.13	n. d.
LC6	1:3	1:2.9	1.3	48.0	6.7	n. d.	6.9	0.14	n. d.
LC7	1:4	1:4.4	0	46.7	7.2	n. d.	6.6	0.15	n. d.
chitin				44.4	6.5	n. d.	7.0	0.15	n. d.

<sup>a</sup>n.d.: not detected.

Composites from lignin and chitin have been scarcely studied in the literature. There are only a few reports, where the combination of lignin and modified chitin leads to improvement in the adsorption of hydrophobic organic compounds.<sup>22</sup>

However, the chemical modification process could bring some drawbacks as high cost, leaching of unexpected organic compounds as well as difficulties in recycling operations.<sup>10</sup> Moreover, compared to biosorbent composite materials prepared by a powder processing route from lignin and chitin,<sup>12,13,22</sup> films from solution processing might have advantages such as a high capacity for metal binding, simplified absorption processes, stability, facile desorption, and recyclability.<sup>10</sup>

Solution processing is commonly used for the fabrication of novel biomaterials. However, there are limitations with respect to the dissolution of both biopolymers simultaneously in one solvent. Especially, chitin exhibits a lack of solubility in water and common organic solvents, as a result of its strong inter- and intramolecular hydrogen bonds.<sup>30</sup> Several solvents have been reported for the dissolution of the two polymers.<sup>30–33</sup> However, most of those solvents exhibit disadvantages such as toxicity, high energy loss, and high cost, and they often yield products with poor properties.<sup>31,33</sup> Additionally, chitin might deacetylate into chitosan in many solvents. In order to prepare lignin and chitin composite film, a solvent, which has the ability to dissolve both lignin and chitin without derivatization and without being altered itself is required. In recent years, the ionic liquid (IL) 1-butyl-3-methylimidazolium acetate (BmimOAc) was found to dissolve lignin and chitin from different origins and molecular weight.<sup>21</sup> Because BmimOAc is partly toxic and poorly biodegradable,<sup>34</sup> reducing its amount for the dissolution of the biopolymers would be desirable.  $\gamma$ -Valerolactone (GVL), a readily available biosourced solvent derived from lignocellulosic biomass,<sup>35</sup> is suggested as a cosolvent for improving solution processing.

We present a method for the preparation of the lignin/chitin films, with a high adsorption capacity for Fe (III) and Cu (II) from aqueous media. Film samples were prepared by dissolving lignin and chitin in a BmimOAc-GVL solvent system without any chemical modification and alteration of the two biopolymers. The obtained films were characterized by scanning electron microscopy (SEM), element analysis (EA), and attenuated total reflectance Fourier transform infrared spectroscopy (ATR-FTIR). Special attention was paid to the investigation of the adsorption/desorption capacity for Fe(III) and Cu(II) from aqueous media, using atomic absorption

spectroscopy (AAS). In addition, the adsorption capacity of the films as a function of lignin to chitin mass ratio was studied.

## EXPERIMENTAL SECTION

**Chemicals and Materials.** Kraft lignin powder (Includin AT) was purchased from MeadWestvaco (U.S.A.). Its number-average molecular weight ( $M_n$ ) and weight-average molecular weight ( $M_w$ ) is 600 g/mol and 4540 g/mol, respectively, as determined by gel permeation chromatography (GPC) (Supporting Information). Kraft lignin powder was first washed with ethanol by Soxhlet extraction at 90 °C for 48 h. The solid residue was subsequently collected and dried at 80 °C for 1 day. Chitin powder ( $\alpha$ -chitin) extracted from shrimp shells was purchased from Sigma-Aldrich (Germany) and dried at 90 °C for 1 day prior to use. The degree of polymerization (DP) of chitin was 1691 as evaluated by solution viscosimetry (Supporting Information). 1-Butyl-3-methylimidazolium acetate (BmimOAc, purity  $\geq 98\%$ ), purchased from Sigma-Aldrich (Germany), was dried with a high vacuum setup at  $10^{-7}$  mbar for 5 days.  $\gamma$ -Valerolactone (GVL, Reagent Plus, purity  $\geq 99\%$ ) was obtained from Sigma-Aldrich (Germany) and dried with 3 Å molecular sieves. All biopolymers and solvents were stored in a desiccator over silica gel after drying. Fe(III) and Cu(II) cations in diluted nitric acid HNO<sub>3</sub> with a concentration of 0.2 and 0.02 mol/L, respectively, (RoTi STAR, purity  $\geq 99\%$ ) were purchased from Sigma-Aldrich (Germany). All materials were used without further modification.

**Dissolution of Kraft Lignin and Chitin in the BmimOAc-GVL Solvent System.** The solvent system was obtained by mixing BmimOAc and GVL at a mass ratio of 4:1 in a glass vial at room temperature. They were immediately stirred to obtain a clear and homogeneous solution (Supporting Information).

Solutions of 20 wt % lignin and 2 wt % chitin were obtained by dissolving the two biopolymer powders in the BmimOAc-GVL solvent system, respectively, at 90 °C with magnetic stirring for 3 h (Supporting Information). The composite samples were prepared by mixing the two solutions according to the desired mass ratio of lignin to chitin as shown in Table 1.

**Preparation of Lignin/Chitin Films with BmimOAc-GVL.** The lignin/chitin films were prepared as follows: First, 2 g of the hot mixture solution was poured into a Petri dish ( $d = 4$  cm) with a syringe and subsequently casted by immediately shaking the Petri dish to obtain a 0.2 mm thick film. Then, the films were stored at room temperature until they cooled down. The casted solution was covered with ethanol for 12 h until the gel-like material could be easily removed from the Petri dish. The obtained gels were continuously washed with ethanol for 48 h in order to remove residual BmimOAc-GVL solution. The lignin/chitin thin films were obtained by drying the gel-like materials between two Teflon plates under ambient conditions for 1 day. Because some lignin was released from the composite samples into ethanol during the coagulation process (Supporting Information), the mass ratio of lignin to chitin in the films were

168 calculated from the dissolved amounts of lignin for each sample. The  
169 compositions of the lignin/chitin films are summarized in Table 1.

170 **Shrinkage.** The linear dimensional change of the lignin/chitin  
171 films after drying was evaluated by the following eq 1:

$$172 \quad D = (A_0 - A_1)/A_0 \times 100 \quad (1)$$

173 where  $D$  is the dimensional change (%),  $A_0$  is the initial area of the  
174 films before drying ( $\text{cm}^2$ ), and  $A_1$  is the final area of the film samples  
175 after drying ( $\text{cm}^2$ ).

176 **Elemental Analysis.** The elemental compositions of the lignin/  
177 chitin films were investigated in an element analyzer Euro EA  
178 (HEKAtech GmbH Germany). After oxidation at  $1000^\circ\text{C}$ , the  
179 gaseous products were separated by gas chromatography and detected  
180 with a thermal conductivity detector. Carbon (C), hydrogen (H),  
181 nitrogen (N), and sulfur (S) relative contents were determined using  
182 tin capsules, containing 1–3 mg of sample.

183 **Scanning Electron Microscopy.** The surface morphology of the  
184 lignin/chitin films were analyzed by scanning electron microscopy  
185 (SEM) in secondary imaging mode at 10 kV and current of  $3.20 \mu\text{A}$   
186 with a working distance of 7 to 9 mm (DSM 940 A, Zeiss,  
187 Oberkochen, Germany). The samples were sputter-coated with Au.

188 **Fourier Transform Infrared Spectroscopy (FTIR).** Infrared  
189 spectra was obtained by attenuated total reflectance (ATR) in a  
190 Nicolet 380 FT-IR (Thermo Fisher Scientific, U.S.A.) equipped with a  
191 diamond crystal. The measurements were conducted on films and  
192 measured in the wavenumber region of  $4000\text{--}500 \text{ cm}^{-1}$ .

193 **Atomic Absorption Spectrometry (AAS).** Ion analysis was  
194 performed using an atomic absorption spectrometer (AAS, ZENit,  
195 analytic Jena, Germany) equipped with a hollow cathode lamp ( $I = 6$   
196 mA and  $\lambda = 248.3 \text{ nm}$ ), and a thermospray apparatus (50 mm in  
197 length and 9 mm in height) at a rate of 5 mL/min was used for Fe. For  
198 the determination of Cu, a hollow cathode lamp ( $I = 4 \text{ mA}$  and  $\lambda =$   
199  $324.8 \text{ nm}$ ) and a thermospray apparatus (about 50 mm in length and 7  
200 mm in height) was used. Acetylene and air at a flow rate of 50 L/h  
201 were used for the flame, respectively. The flow system was operated  
202 with a Teflon tube (diameter = 1 mm, Analytik Jena, Germany).

203 **Ion Adsorption Experiments.** The adsorption experiments were  
204 performed by soaking the films with different lignin to chitin mass  
205 ratios in aqueous Fe (III) or Cu (II) ion solutions of 3 mg/L at room  
206 temperature for various times (2, 5, 8, 24, and 48 h). As a reference  
207 sample, a pure chitin film was also measured under identical  
208 conditions. Evaluation of adsorption experiments were carried out  
209 by analyzing the cation concentration of the diluted aqueous ion  
210 solutions by AAS. Four specimens from each sample were measured.  
211 Additionally, the pH values of the corresponding aqueous ion  
212 solutions were measured using a digital pH meter (HI83141,  
213 HANNA, USA), at room temperature. The adsorption capacity of  
214 each sample for each tested time was calculated by eq 2.

$$215 \quad A = ((C_0 - C_t) \times V)/M \times 100\% \quad (2)$$

216 where  $A$  is the adsorption capacity of metal ions on the samples (%),  
217  $C_0$  is the initial concentration (mg/L) of Fe(III) and Cu(II) ions  
218 measured from AAS,  $C_t$  is the metal ion concentration of the solutions  
219 (mg/L) after adsorbed by AAS analysis in the tested time,  $V$  is the  
220 volume of tested solution (15 mL), and  $M$  is the initial weight of the  
221 respective film samples (mg).

222 **Kinetics Study.** The investigation of the kinetics of the adsorption  
223 process were carried out by soaking the film LC3 (Table 1) in aqueous  
224 Fe(III) or Cu(II) ion solutions with different concentrations: 1, 2, 3,  
225 and 4 mg/L. The tests were performed at room temperature for  
226 various times (2, 5, 8, 24, and 48 h). The adsorbed amount of metal  
227 ions ( $q_t$ , mg/g) on the samples for each time was calculated by eq 3.

$$228 \quad q_t = ((C_0 - C_t) \times V)/M \quad (3)$$

229 where  $C_0$  is the initial concentration (mg/L) of Fe(III) and Cu(II)  
230 ions,  $C_t$  is the metal ion concentration of the solutions (mg/L) by AAS  
231 analysis after the respective adsorption time,  $V$  is the volume of tested  
232 solution (15 mL), and  $M$  is the initial weight of the film samples (mg).

To investigate the type of adsorption mechanism for Fe(III) and  
Cu(II) of the lignin/chitin films, two kinetic models (pseudo-first-  
order and pseudo-second-order) were evaluated.<sup>11,13,36</sup>

Pseudo-first-order model: 236

$$\log(q_e - q_t) = \log q_e - K_1/2.303t \quad (4) \quad 237$$

Pseudo-second-order model: 238

$$t/q_t = 1/(k_2 \times q_e^2) + 1/q_e \times t \quad (5) \quad 239$$

where  $k_1$  is the rate constant of the adsorption process in the pseudo-  
first-order model ( $\text{h}^{-1}$ ), and  $k_2$  is the rate constant of the adsorption  
process in the pseudo-second-order model ( $\text{g/mg h}$ ).

**Equilibrium Study.** The amount of metal ions adsorbed by the  
lignin/chitin film (LC3) at equilibrium ( $q_e$ , mg/g) was calculated by  
eq 6

$$q_e = ((C_0 - C_e) \times V)/M \quad (6) \quad 246$$

where  $C_e$  is the equilibrium metal ion concentration (mg/L) of Fe(III)  
and Cu(II) ions. Freundlich and Langmuir models were used for the  
determination of the adsorption isotherms.<sup>36</sup>

Freundlich isotherms 249

$$\log(q_e) = \log K_F + 1/n \times \log C_e \quad (7) \quad 251$$

where  $K_F$  (mg/g) and  $n$  are the Freundlich constants. 252

Langmuir isotherms 253

$$q_e/C_e = K_L \times q_m - K_L \times q_e \quad (8) \quad 254$$

where  $K_L$  (L/mg) and  $q_m$  (mg/g) are Langmuir constants, 255  
representing the maximum adsorption capacity of the sorbent. 256

**Ion Desorption Experiments.** In order to investigate the  
recycling capability of the lignin/chitin films, the desorption processes  
were carried out by soaking the dried metal ion loaded films in water at  
room temperature ( $22^\circ\text{C}$ ) for 24 and 48 h, respectively. Desorption  
was evaluated by determining the concentrations of the released Fe  
(III) and Cu (II) ions from the loaded films in water using AAS. Four  
replicates from each sample were measured. The percentage of  
desorbed Fe (III) and Cu (II) from each films was calculated by the  
following eq 9:

$$D = ((C_1 \times V)/M)/A \times 100\% \quad (9) \quad 266$$

where  $D$  (%) is the percentage of the desorbed mass related to their  
initial mass after 24 and 48 h, respectively,  $A$  is the adsorbed amounts  
of metal ions on the film samples within 48 h (mg/mg),  $C_1$  is the  
metal ion concentration (mg/mL),  $V$  is the volume of solution (15  
mL), and  $M$  is the weight of the film sample (mg). 271

**Ion Readsorption Experiments.** In order to evaluate the  
reusability of the lignin/chitin films, they were collected after the  
desorption experiment and dried. Then they were soaked in aqueous  
Fe (III) or Cu (II) ion solutions of 3 mg/L at room temperature. The  
readsorption process and evaluation were performed in the same way  
as for the adsorption batch experiments. The readsorption capacity of  
each sample for each tested time was calculated by eq 10. 278

$$A_{re} = ((C_1 - C'_t) \times V)/M \times 100\% \quad (10) \quad 279$$

where  $A_{re}$  is the readsorption capacity of metal ions on the samples  
(%),  $C_0$  is the initial concentration (mg/L) of Fe(III) and Cu(II) ions  
measured from AAS,  $C'_t$  is the metal ion concentration of the solutions  
(mg/L) after adsorption by AAS analysis in the tested time,  $V$  is the  
volume of tested solution (15 mL), and  $M$  is the initial weight of the  
respective film samples (mg). 285

## RESULTS AND DISCUSSION 286

**Preparation of Lignin/Chitin Films.** The obtained lignin/  
chitin films were flexible gels with a brown color, which  
appeared darker with increasing content of Kraft lignin. After  
the samples were dried, the dimensional changes of the films  
were inversely proportional to the content of chitin (Figure 1). 291

C

DOI: 10.1021/acssuschemeng.8b00805  
ACS Sustainable Chem. Eng. XXXX, XXX, XXX–XXX

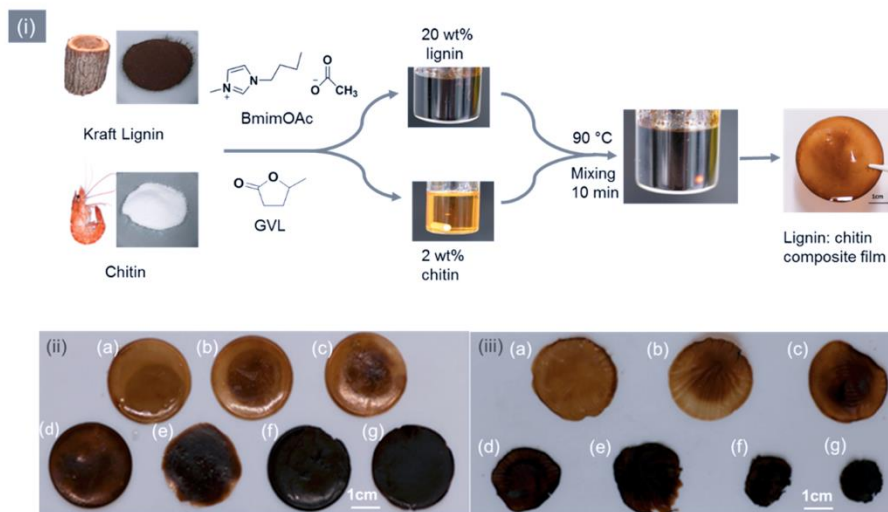


**Figure 1.** (i) Preparation procedure of the lignin/chitin films from BmimOAc-GVL solution; (ii) lignin/chitin films in wet state; (iii) lignin/chitin films in dry state ((a) LC7, (b) LC6, (c) LC5, (d) LC4, (e) LC3, (f) LC2, (g) LC1).

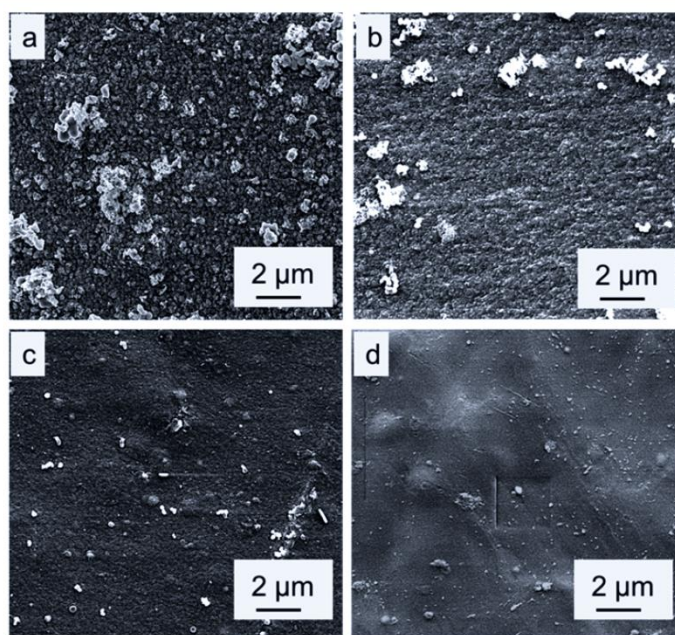


**Figure 2.** SEM micrographs of the surface of the selected lignin/chitin films ((a) LC1, (b) LC4, (c) LC7), and (d) chitin).

292 All samples were relatively robust materials both in wet and dry  
 293 state, except for the pure lignin sample. Although lignin was  
 294 released in minor fraction from the composites during  
 295 regeneration, the mass ratio of lignin to chitin in the obtained  
 296 films was almost the same for each sample (Table 1). The  
 297 obtained lignin/chitin films exhibited linear dimensional  
 298 changes after drying, which decreased with the increasing  
 299 concentration of chitin (Table 1). The sample LC7, which had  
 300 the highest chitin content, showed no dimensional change after  
 301 drying.

#### Elemental Analysis (EA) of the Lignin/Chitin Films.

302 Table 1 shows the result of elemental analysis of the samples.  
 303 Carbon (62.8 wt %), nitrogen (0.5 wt %), hydrogen (5.6 wt %),  
 304 and sulfur (1.1 wt %) were found for the Kraft lignin powder.  
 305 The EA result of chitin powder (carbon (44.4 wt %), nitrogen  
 306 (6.5 wt %), and hydrogen (7.0 wt %)) indicated a degree of N-  
 307 acetylation of 89%. The results of the lignin/chitin film samples  
 308 from EA confirmed the successful preparation. It was shown  
 309 that with the decreasing mass ratio of lignin in the prepared  
 310 films, the mass ratio of sulfur/carbon was also linearly reduced.  
 311 Because of the low content of lignin present in the film samples  
 312

D

DOI: 10.1021/acssuschemeng.8b00805  
 ACS Sustainable Chem. Eng. XXXX, XXX, XXX–XXX

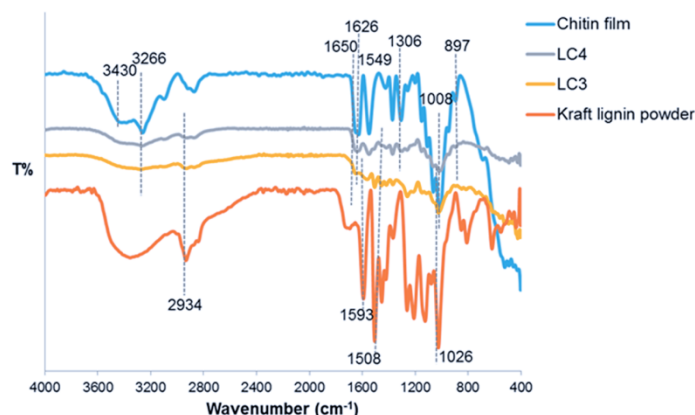


Figure 3. ATR- FTIR spectra of the selected lignin/chitin films (LC3 and LC4), Kraft lignin, and chitin.

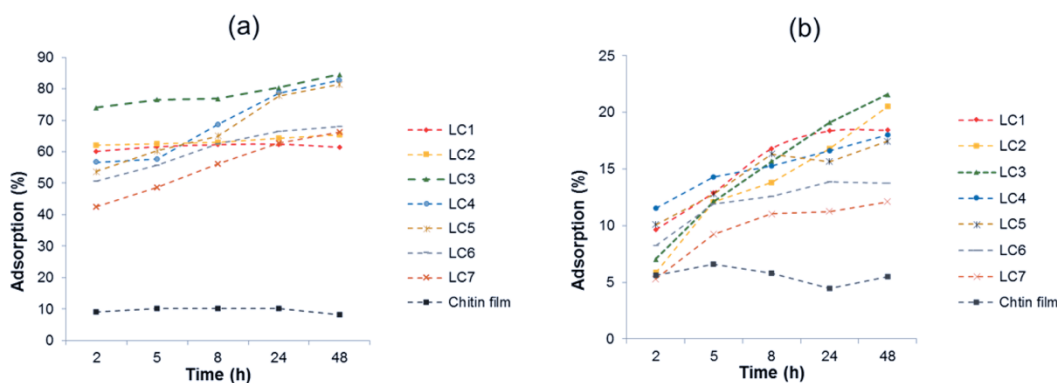


Figure 4. Adsorption curves of lignin/chitin films and pure chitin film for (a) Fe(III) and (b) Cu(II) within different contact times maximum standard deviation for the adsorption values of Fe(III) was  $\pm 6.13$  and of Cu(II) was  $\pm 2.24$ .

313 (LC4, LC5, LC6, and LC7), the sulfur could not be detected.  
 314 Additionally, the samples with increasing chitin content showed  
 315 a gradually increasing mass ratio of nitrogen/carbon (N/C).  
 316 This result confirmed that chitin was not deacetylated into  
 317 chitosan during its dissolution in BmimOAc-GVL.

318 **SEM Measurement of Lignin/Chitin Films.** It was  
 319 observed by SEM that the surface of sample LC1 with the  
 320 highest lignin content showed a rough morphology with many  
 321 small individual and irregular distributed lignin particles (Figure  
 322 2a). This appearance changed to a smoother surface with  
 323 increasing chitin content (Figure 2b,c). The pure chitin film  
 324 exhibited a dense, homogeneous, and firm surface morphology  
 325 (Figure 2d).

326 **ATR-FTIR Measurement of Lignin/Chitin Films.** Figure  
 327 3 shows the ATR-FTIR spectra of Kraft lignin in comparison to  
 328 chitin as well as selected samples LC3 and LC4. The spectrum  
 329 of Kraft lignin exhibits the following bands: The stretching  
 330 vibration bands of O–H group at  $3600\text{--}3200\text{ cm}^{-1}$  and C–H  
 331 at  $2934\text{ cm}^{-1}$ . The bands at  $1593$  and  $1508\text{ cm}^{-1}$  are associated  
 332 with the stretching of C–C vibration of the aromatic skeleton.  
 333 The bands at  $1200\text{--}1350$  and  $1026\text{ cm}^{-1}$  are attributed to the  
 334 stretching vibration of C–O, C–O (H), C–O (Ar), and C–  
 335 O–C etheric bond of the phenolic groups.<sup>22,37</sup> The character-  
 336 istic bands of chitin are the amide-I doublet bands located at  
 337  $1650$  and  $1626\text{ cm}^{-1}$ , amide-II band at  $1549\text{ cm}^{-1}$ , and the

338 amide-III band at  $1306\text{ cm}^{-1}$ . This confirms that chitin was not  
 339 degraded during the dissolution in BmimOAc-GVL (Support-  
 340 ing Information), which is in good agreement with the results  
 341 from element analysis. The bands located at  $3430$  and  $3266$   
 342  $\text{ cm}^{-1}$  are ascribed to the stretching vibration of O–H and N–H  
 343 groups. The intense peaks at  $1154\text{--}1010\text{ cm}^{-1}$  correspond to  
 344 the stretching vibration of C–O–C and C–O bonds, and the  
 345 peak at  $897\text{ cm}^{-1}$  confirms the presence of  $\beta$ -1,4-glycosidic  
 346 linkages.<sup>22</sup> The selected film samples LC3 and LC4, with a  
 347 lignin to chitin mass ratio of 1.6:1 and 1.2:1, showed the  
 348 characteristic spectra from both biopolymers, respectively. New  
 349 absorption peaks resulting from possible degradation products  
 350 were not observed (Supporting Information). Furthermore,  
 351 absorption peaks derived from the solvents are absent in the  
 352 spectra of all composite samples, indicating that BmimOAc and  
 353 GVL were completely removed from the films during  
 354 regeneration process.

355 **Adsorption Capacity of Lignin/Chitin Films for Fe(III)  
 356 and Cu(II).** The lignin/chitin films showed a considerable  
 357 adsorption for Fe(III) and Cu(II) from aqueous solutions, in  
 358 contrast to pure chitin films, where ion adsorption was quite  
 359 low. It was found that the adsorption amounts of all the  
 360 samples for both Fe(III) and Cu(II) increased with increasing  
 361 adsorption time (except for LC1, Figure 4). It is noticed that  
 362 the lignin/chitin films exhibited a higher affinity for Fe(III)

E

DOI: 10.1021/acssuschemeng.8b00805  
ACS Sustainable Chem. Eng. XXXX, XXX, XXX–XXX

**Table 2.** pH Values of the Fe(III) and Cu(II) Aqueous Solutions (3 mg/L) within the Lignin/Chitin Films and Pure Chitin Film after 2, 5, 8, 24, and 48 h, Respectively; Maximum Standard Deviation for the Experiments of Fe(III) was  $\pm 0.25$  and of Cu(II) was  $\pm 0.33$

samples	Fe(III) pH (initial) = 3.67; T = 22 °C pH					Cu(II) pH (initial) = 3.48; T = 22 °C pH				
	2 h	5 h	8 h	24 h	48 h	2 h	5 h	8 h	24 h	48 h
LC1	3.90	4.54	4.83	5.34	6.03	3.51	3.65	3.69	3.73	3.76
LC2	3.83	4.57	4.79	5.32	5.58	3.49	3.64	3.69	3.73	3.75
LC3	3.74	4.47	4.54	4.66	4.49	3.50	3.57	3.59	3.57	3.58
LC4	3.74	4.25	4.24	4.26	3.89	3.49	3.54	3.56	3.55	3.57
LC5	3.76	4.25	4.29	4.32	3.92	3.49	3.53	3.55	3.55	3.56
LC6	3.80	4.34	4.36	4.34	3.98	3.48	3.58	3.58	3.60	3.57
LC7	3.87	4.22	4.33	4.33	3.95	3.51	3.58	3.57	3.56	3.56
chitin film	3.70	4.06	4.08	4.16	3.81	3.48	3.53	3.58	3.59	3.56

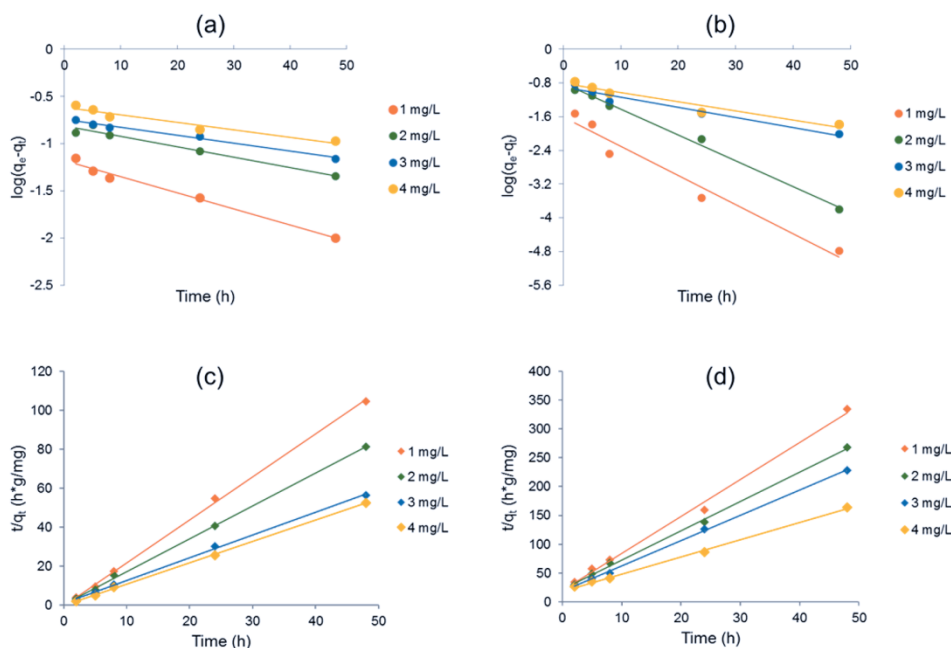


**Figure 5.** Pseudo-first-order kinetic model for adsorption for (a) Fe(III) and (b) Cu(II); pseudo-second-order kinetic model for adsorption for (c) Fe(III) and (d) Cu(II).

(adsorption capacity of 61%–84%) than for Cu(II) (adsorption capacity of 12%–22%) after 48 h. The highest adsorption capacity for Fe(III) and Cu(II) is found for LC3 with a lignin to chitin mass ratio of 1.6:1. The adsorption capacity of Fe(III) for the samples LC4 and LC5 showed only slight variations (83% and 81%). The second highest adsorption capacity of Cu(II) (i.e., 21%) was achieved by LC2 in 48 h. However, no significant correlation between the adsorption amounts of metal ions and the mass ratio of lignin could be observed (Figure 4). It should be noted that the adsorption capacity for sample LC1 with the highest lignin content slightly decreased for both Fe(III) and Cu(II) ions after 24 h. This phenomenon could be due to a slight partial disintegration of LC1 in the aqueous solutions, which leads to an increased ion release.

It should be noted that our lignin/chitin film sorbent show a lower sorption capacity and longer absorption time compared with previously reported results for lignin/chitin and lignin/chitosan biosorbents.<sup>10,13,22,40</sup> However, the efficient absorption

ability for the described materials might result from their higher specific surface area. However, the maximum capacity of our films for Fe(III) (i.e., 84%) and Cu(II) (i.e., 22%) after 48 h adsorption time at ambient condition suggests that they can be used as effective biosorbents.

Table 2 shows that the pH values of both Fe(III) and Cu(II) aqueous solutions increased with increasing time for LC1 and LC2. All other composite samples displayed a similar behavior concerning the pH values. The result indicates that the lignin/chitin films were relatively stable under experimental conditions. Due to the slight change of the pH values of the metal ion solutions from 2 to 24 h, it can be concluded that the predominant mechanism of the lignin/chitin films in this period is primarily adsorption.<sup>10</sup> The decreased pH values of the Fe(III) solutions from 24 to 48 h indicate an increased concentration of protons, which could result from the exchange process with Fe(III) from the film samples. Therefore, another possible mechanism such as ion-exchange can be also involved

F

DOI: 10.1021/acssuschemeng.8b00805  
ACS Sustainable Chem. Eng. XXXX, XXX, XXX–XXX

**Table 3.** Experimental and Calculated Data for the Pseudo-First-Order and Pseudo-Second-Order Kinetic Models According to the Freundlich and Langmuir Isotherms for Adsorption of Fe(III) and Cu(II) on Lignin/Chitin Film

model	unit	Fe(III)				Cu(II)				
		1 mg/L	2 mg/L	3 mg/L	4 mg/L	1 mg/L	2 mg/L	3 mg/L	4 mg/L	
pseudo-first-order	$K_1$	h <sup>-1</sup>	0.83	0.65	0.76	0.72	0.38	0.15	0.15	0.11
	$R^2$	-	0.9842	0.9636	0.9890	0.9434	0.9637	0.9952	0.9566	0.9437
pseudo-second-order	$K_2$	g/mg h	1.54	1.43	1.24	1.13	2.35	1.78	1.09	0.79
	$R^2$	-	0.9991	0.9992	0.9991	0.9995	0.9953	0.9984	0.9992	0.9975
Freundlich	$K_F$	mg/g			0.79				0.35	
	$n$	-			1.31				2.08	
	$R^2$	-			0.9387				0.989	
Langmuir	$K_L$	L/mg			52.1				1.5	
	$q_m$	mg/g			1.21				0.28	
	$R^2$	-			0.9736				0.9803	

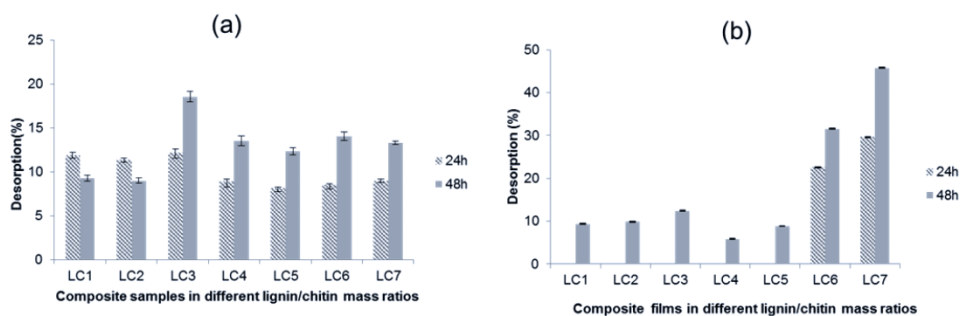


**Figure 6.** Desorption capacity of the metal ion loaded composites in water within 24 and 48 h: (a) Fe (III) and (b) Cu (II). The maximum standard deviation for the desorption of Fe (III) was  $\pm 0.46$  at 24 h and was  $\pm 0.59$  at 48 h as well as of Cu(II) was  $\pm 0.065$  at 24 h and was  $\pm 0.056$  at 48 h.

399 in the Fe(III) binding process during this time.<sup>10</sup> Overall, the  
400 results illustrate that the film LC3 with 1.6:1 lignin to chitin  
401 mass ratio, exhibited the highest adsorption capacity for Fe(III)  
402 and Cu(II) ions and a good stability in the metal ion solutions.

403 **Adsorption Kinetics.** The kinetic parameters of the lignin/  
404 chitin film (LC3) for adsorption of Fe(III) and Cu(II) were  
405 calculated according to the pseudo-first-order model (Figure  
406 5a,b) and pseudo-first-order model (Figure 5c,d). The  
407 correlation coefficient  $R^2$  (Table 3) obtained from the  
408 pseudo-first-order model range from 0.9434 to 0.9890 for the  
409 adsorption of Fe(III) ions and from 0.9437 to 0.9952 for  
410 Cu(II). The pseudo-second-order model exhibits high  
411 correlation coefficients ( $R^2$ ) close to 1.0 for all analyzed  
412 concentrations of Fe(III) and Cu(II)), which confirms an  
413 almost perfect match with the experimental data. The results  
414 corroborate previous literature reports, which showed that the  
415 adsorption for various metal ions on the lignin/chitin  
416 composites biosorbents followed a pseudo-second-order  
417 model.<sup>11,13</sup> Additionally, the fit for the pseudo-second-order  
418 model confirms that the adsorption of lignin/chitin film for  
419 Fe(III) and Cu(II) is a cooperative process from adsorption  
420 and ion exchange,<sup>11,36,38,39</sup> which is consistent with the  
421 proposed mechanism mentioned above. It should be noted  
422 that the rate constant ( $K_2$ ) decreased with increasing  
423 concentrations of both Fe(III) and Cu(II) ions, which might  
424 result from the competition between the increased amounts of  
425 ions and the active areas on the film.<sup>11</sup>

426 **Adsorption Isotherms.** Table 3 shows the parameters  
427 obtained from the Freundlich and Langmuir isotherm models.  
428 The coefficient of heterogeneity ( $n$ ) calculated according to the  
429 Freundlich model was 1.31 for Fe(III) and 2.08 for Cu(II) ( $1 <$

$n < 10$ ), indicating a physical interaction between the  
430 biosorbent film and the metal ions under favorable adsorption  
431 process condition.<sup>11,13,36</sup> However, due to the lower correlation  
432 coefficient ( $R^2$ ), the Freundlich model only fits poorly to the  
433 adsorption data for Cu(II). The calculated saturation capacity  
434 ( $q_m$ ) according to the Langmuir model was 1.21 mg/g for  
435 Fe(III) and 0.28 mg/g for Cu(II), respectively. The results  
436 show a significantly higher adsorption capacity of the lignin/  
437 chitin films for Fe(III) compared to Cu(II). The correlation  
438 coefficient  $R^2$  obtained from the Langmuir model was 0.9736  
439 for Fe(III) and 0.9803 for Cu(II), respectively, indicated an  
440 effective fit for the adsorption data. Additionally, the similar  $R^2$   
441 values calculated for the two isotherms models indicate that  
442 both of them could be used to describe the adsorption process  
443 of Fe(III) onto lignin/chitin film.<sup>13</sup>

444 **Desorption Characteristic of Lignin/Chitin Films.** The  
445 desorption results show that most of the lignin/chitin films  
446 exhibit an increased amount of the released metal ions with  
447 increasing desorption time, except for LC1 and LC2. For these  
448 samples more Fe(III) was released after 24 h than after 48 h  
449 (Figure 6). Similar to the results from adsorption, LC3 also  
450 showed the highest desorption values for Fe(III) ions (12.1%  
451 and 18.5%, after 24 and 48 h). The samples (except LC6 and  
452 LC7), which had lower adsorption capacities, also showed  
453 lower desorption rates of Cu(II) than of Fe(III). Because of the  
454 small absorbed amounts of Cu(II) on LC6 and LC7, their  
455 comparably higher desorption values could result from their  
456 weak adsorption interaction for Cu(II) ions.  
457

458 **Readsorption Characteristic of Lignin/Chitin Films.** It  
459 was found that after initial loading and desorption, the lignin/  
460 chitin films still showed a certain resorption amount for Fe(III)

461 ranging from 14% to 26% after 48 h (Supporting Information).  
 462 However, their readsorption capacity for Cu(II) was only  
 463 limited, which confirmed a better affinity of the lignin/chitin  
 464 film biosorbent for Fe(III). Furthermore, the pH values of  
 465 Fe(III) aqueous solutions slightly decreased with increasing  
 466 readsorption time whereas the pH of Cu(II) aqueous solutions  
 467 showed no changes (Supporting Information). Therefore, the  
 468 readsorption of the films for Cu(II) might be achieved by  
 469 further extending desorption-adsorption cycles. The results  
 470 show the stability and reusability of the biofilm sorbent.

## 471 ■ CONCLUSIONS

472 Lignin/chitin films were successfully prepared from a  
 473 BmimOAc-GVL mixture (4:1, w:w). From lignin alone, it was  
 474 not possible to obtain composite films from the solution  
 475 process. The flexibility of the composite films could be  
 476 attributed to the presence of chitin. The investigation of  
 477 lignin/chitin film as biosorbent was performed for Fe(III) and  
 478 Cu(II) aqueous solutions at room temperature. As the results  
 479 indicated, the film with a 1.6:1 lignin-to-chitin mass ratio  
 480 showed an optimum performance with respect to its high  
 481 adsorption/desorption capacity for Fe(III) and Cu(II) cations  
 482 and higher affinity for Fe(III). The adsorption process followed  
 483 a pseudo-second-order kinetic model indicating that two  
 484 mechanisms such as adsorption and ion-exchange were  
 485 responsible for uptake of metal ions in the lignin/chitin films.  
 486 The adsorption isotherms for both Fe(III) and Cu(II) can be  
 487 described according to the Langmuir model. This is the first  
 488 study using the two biopolymers lignin and chitin to obtain  
 489 heavy metal film biosorbent. The lignin/chitin film biosorbents  
 490 show advantages such as high adsorption capacity for metal  
 491 ions especially at low concentration, stability in aqueous  
 492 solution, easy to use, facile desorption as well as reusability,  
 493 which are all requirements for their application in water  
 494 purification.

## 495 ■ ASSOCIATED CONTENT

### 496 ■ Supporting Information

497 The Supporting Information is available free of charge on the  
 498 ACS Publications website at DOI: 10.1021/acssuschemeng.8b00805.

500 Determination the degree of polymerization of kraft  
 501 lignin and chitin as well as the degree of acetylation (DA)  
 502 of chitin, investigation the dissolution of kraft lignin and  
 503 chitin in BmimOAc-GVL (4:1, w:w), ATR-FTIR  
 504 measurement of the solvent system, TGA measurement  
 505 of lignin/chitin films, adsorption and readsorption  
 506 experiments of the lignin/chitin films for Fe(III) and  
 507 Cu(II) (PDF)

## 508 ■ AUTHOR INFORMATION

### 509 Corresponding Author

510 \*E-mail: cordt.zollfrank@tum.de. Tel.: +49 (0) 9421 187-450.  
 511 Fax: +49 (0) 9421 187-130.

### 512 ORCID

513 Cordt Zollfrank: 0000-0002-2717-4161

### 514 Notes

515 The authors declare no competing financial interest.

## ■ ACKNOWLEDGMENTS

This research was conducted in the frame of the project  
 “ForCycle” (BAF01SoFo-65212), supported by the Bavarian  
 State Ministry of the Environment and Consumer Protection.  
 The authors would like to thank Christina Sagmeister (TUM  
 Campus Straubing for Biotechnology and Sustainability,  
 Technical University of Munich) for technical assistance of  
 this work.

## ■ REFERENCES

- (1) Guo, J. Characteristics and mechanisms of Cu(II) sorption from aqueous solution by using bioflocculant MBFR10543. *Appl. Microbiol. Biotechnol.* **2015**, *99* (1), 229–240.
- (2) Figueroa-Torres, G. M.; Certucha-Barragán, M. T.; Acedo-Félix, E.; Monge-Amaya, O.; Almendariz-Tapia, F. J.; Gasca-Estefanía, L. A. Kinetic studies of heavy metals biosorption by acidogenic biomass immobilized in clinoptilolite. *J. Taiwan Inst. Chem. Eng.* **2016**, *61*, 241–246.
- (3) Vaaramaa, K.; Lehto, J. Removal of metals and anions from drinking water by ion exchange. *Desalination* **2003**, *155* (2), 157–170.
- (4) Lim, A. P.; Aris, A. Z. A review on economically adsorbents on heavy metals removal in water and wastewater. *Rev. Environ. Sci. Bio/Technol.* **2014**, *13* (2), 163–181.
- (5) Fu, F.; Wang, Q. Removal of heavy metal ions from wastewaters: a review. *J. Environ. Manage.* **2011**, *92* (3), 407–418.
- (6) Dermentzis, K.; Christoforidis, A.; Valsamidou, E. Removal of nickel, copper, zinc and chromium from synthetic and industrial wastewater by electrocoagulation. *Int. J. Environ. Sci.* **2011**, *1* (5), 697.
- (7) Kurniawan, T. A.; Chan, G. Y.; Lo, W.-H.; Babel, S. Physico-chemical treatment techniques for wastewater laden with heavy metals. *Chem. Eng. J.* **2006**, *118* (1), 83–98.
- (8) Turhanen, P. A.; Vepsäläinen, J. J.; Peräniemi, S. Advanced material and approach for metal ions removal from aqueous solutions. *Sci. Rep.* **2015**, *5*, 8992.
- (9) Wang, J.; Chen, C. Chitosan-based biosorbents: Modification and application for biosorption of heavy metals and radionuclides. *Bioresour. Technol.* **2014**, *160*, 129–141.
- (10) Salman, M.; Athar, M.; Farooq, U. Biosorption of heavy metals from aqueous solutions using indigenous and modified lignocellulosic materials. *Rev. Environ. Sci. Bio/Technol.* **2015**, *14* (2), 211–228.
- (11) Wysokowski, M.; Bartczak, P.; Żółtowska-Aksamitowska, S.; Chudzińska, A.; Piasecki, A.; Langer, E.; Bazhenov, V. V.; Petrenko, I.; Noga, T.; Stelling, A. L. Adhesive Stalks of Diatom *Didymosphenia geminata* as a Novel Biological Adsorbent for Hazardous Metals Removal. *Clean: Soil, Air, Water* **2017**, *45* (11), 1600678.
- (12) Klapiszewski, Ł.; Wysokowski, M.; Majchrzak, I.; Szatkowski, T.; Nowacka, M.; Siwińska-Stefańska, K.; Szwarc-Rzepka, K.; Bartczak, P.; Ehrlich, H.; Jesionowski, T. Preparation and characterization of multifunctional chitin/lignin materials. *J. Nanomater.* **2013**, *2013*, 12.
- (13) Bartczak, P.; Klapiszewski, Ł.; Wysokowski, M.; Majchrzak, I.; Czernicka, W.; Piasecki, A.; Ehrlich, H.; Jesionowski, T. Treatment of model solutions and wastewater containing selected hazardous metal ions using a chitin/lignin hybrid material as an effective sorbent. *J. Environ. Manage.* **2017**, *204*, 300–310.
- (14) Chakar, F. S.; Ragauskas, A. J. Review of current and future softwood kraft lignin process chemistry. *Ind. Crops Prod.* **2004**, *20* (2), 131–141.
- (15) Sarkanen, K. V.; Ludwig, C. H. *Lignins. Occurrence, formation, structure, and reactions*; Wiley-Interscience: New York, 1971.
- (16) Lewis, N. G. A 20th century roller coaster ride: a short account of lignification. *Curr. Opin. Plant Biol.* **1999**, *2* (2), 153–162.
- (17) Gosselink, R. J. A.; de Jong, E.; Guran, B.; Abächerli, A. Co-ordination network for lignin—standardisation, production and applications adapted to market requirements (EUROLIGNIN). *Ind. Crops Prod.* **2004**, *20* (2), 121–129.
- (18) Mohan, D.; Pittman, C. U., Jr; Steele, P. H. Single, binary and multi-component adsorption of copper and cadmium from aqueous

- solutions on Kraft lignin—a biosorbent. *J. Colloid Interface Sci.* **2006**, 583 297 (2), 489–504.
- (19) Kurita, K. Controlled functionalization of the polysaccharide chitin. *Prog. Polym. Sci.* **2001**, 26 (9), 1921–1971.
- (20) Park, B. K.; Kim, M.-M. Applications of chitin and its derivatives in biological medicine. *Int. J. Mol. Sci.* **2010**, 11 (12), 5152–5164.
- (21) Wu, Y.; Sasaki, T.; Irie, S.; Sakurai, K. A novel biomass-ionic liquid platform for the utilization of native chitin. *Polymer* **2008**, 49 (9), 2321–2327.
- (22) Wysokowski, M.; Klapiszewski, L.; Moszyński, D.; Bartzak, P.; Szatkowski, T.; Majchrzak, L.; Siwińska-Stefańska, K.; Bazhenov, V.; Jesionowski, T. Modification of Chitin with Kraft Lignin and Development of New Biosorbents for Removal of Cadmium(II) and Nickel(II) Ions. *Mar. Drugs* **2014**, 12 (4), 2245.
- (23) Herrera, N.; Salaberria, A. M.; Mathew, A. P.; Oksman, K. Plasticized polylactic acid nanocomposite films with cellulose and chitin nanocrystals prepared using extrusion and compression molding with two cooling rates: Effects on mechanical, thermal and optical properties. *Composites, Part A* **2016**, 83, 89–97.
- (24) Schleuter, D.; Günther, A.; Paasch, S.; Ehrlich, H.; Kljajić, Z.; Hanke, T.; Bernhard, G.; Brunner, E. Chitin-based renewable materials from marine sponges for uranium adsorption. *Carbohydr. Polym.* **2013**, 92 (1), 712–718.
- (25) Petrenko, I.; Bazhenov, V. V.; Galli, R.; Wysokowski, M.; Fromont, J.; Schupp, P. J.; Stelling, A. L.; Niederschlag, E.; Stöker, H.; Kutsova, V. Z.; et al. Chitin of poriferan origin and the bioelectrometallurgy of copper/copper oxide. *Int. J. Biol. Macromol.* **2017**, 104, 1626–1632.
- (26) Wysokowski, M.; Petrenko, I.; Stelling, A. L.; Stawski, D.; Jesionowski, T.; Ehrlich, H. Poriferan chitin as a versatile template for extreme biomimetics. *Polymers* **2015**, 7 (2), 235–265.
- (27) González, J. A.; Villanueva, M. E.; Piehl, L. L.; Copello, G. J. Development of a chitin/graphene oxide hybrid composite for the removal of pollutant dyes: Adsorption and desorption study. *Chem. Eng. J.* **2015**, 280, 41–48.
- (28) Tang, H.; Zhou, W.; Zhang, L. Adsorption isotherms and kinetics studies of malachite green on chitin hydrogels. *J. Hazard. Mater.* **2012**, 209, 218–225.
- (29) Wang, X.; Xing, B. Importance of Structural Makeup of Biopolymers for Organic Contaminant Sorption. *Environ. Sci. Technol.* **2007**, 41 (10), 3559–3565.
- (30) Takegawa, A.; Murakami, M.-a.; Kaneko, Y.; Kadokawa, J.-i. Preparation of chitin/cellulose composite gels and films with ionic liquids. *Carbohydr. Polym.* **2010**, 79 (1), 85–90.
- (31) Pillai, C. K. S.; Paul, W.; Sharma, C. P. Chitin and chitosan polymers: Chemistry, solubility and fiber formation. *Prog. Polym. Sci.* **2009**, 34 (7), 641–678.
- (32) Barber, P. S.; Griggs, C. S.; Gurau, G.; Liu, Z.; Li, S.; Li, Z.; Lu, X.; Zhang, S.; Rogers, R. D. Coagulation of Chitin and Cellulose from 1-Ethyl-3-methylimidazolium Acetate Ionic-Liquid Solutions Using Carbon Dioxide. *Angew. Chem.* **2013**, 125 (47), 12576–12579.
- (33) Pu, Y.; Jiang, N.; Ragauskas, A. J. Ionic liquid as a green solvent for lignin. *J. Wood Chem. Technol.* **2007**, 27 (1), 23–33.
- (34) Wood, N.; Stephens, G. Accelerating the discovery of biocompatible ionic liquids. *Phys. Chem. Chem. Phys.* **2010**, 12 (8), 1670–1674.
- (35) Alonso, D. M.; Wettstein, S. G.; Dumesic, J. A. Gamma-valerolactone, a sustainable platform molecule derived from lignocellulosic biomass. *Green Chem.* **2013**, 15 (3), 584–595.
- (36) Febrianto, J.; Kosasih, A. N.; Sunarso, J.; Ju, Y.-H.; Indraswati, N.; Ismadji, S. Equilibrium and kinetic studies in adsorption of heavy metals using biosorbent: a summary of recent studies. *J. Hazard. Mater.* **2009**, 162 (2–3), 616–645.
- (37) Klapiszewski, L.; Nowacka, M.; Milczarek, G.; Jesionowski, T. Physicochemical and electrokinetic properties of silica/lignin bio-composites. *Carbohydr. Polym.* **2013**, 94 (1), 345–355.
- (38) Żółtowska-Aksamitowska, S.; Bartzak, P.; Zembrzaska, J.; Jesionowski, T. Removal of hazardous non-steroidal anti-inflammatory drugs from aqueous solutions by biosorbent based on chitin and lignin. *Sci. Total Environ.* **2018**, 612, 1223–1233.
- (39) Kadous, A.; Didi, M. A.; Villemin, D. A new sorbent for uranium extraction: ethylenediamino tris (methylene phosphonic) acid grafted on polystyrene resin. *J. Radioanal. Nucl. Chem.* **2010**, 284 (2), 431–438.
- (40) Mishra, S. B.; Mishra, A. K. *Bio-and Nanosorbents from Natural Resources*; Springer: Berlin, 2017.



## Supporting Information

### Lignin/chitin films

#### and their adsorption characteristics for heavy metal ions

Yaqing Duan<sup>a</sup>, Auriane Freyburger<sup>b</sup>, Werner Kunz<sup>b</sup>, Cordt Zollfrank<sup>a,\*</sup>

<sup>a</sup> Chair of Biogenic Polymers, TUM Campus Straubing for Biotechnology and Sustainability, Technical University of Munich, Schulgasse 16, 94315, Straubing, Germany;

<sup>b</sup> Institute of Physical and Theoretical Chemistry, University of Regensburg, Universitätsstraße 31, 93040, Regensburg, Germany

\*corresponding author:

email: cordt.zollfrank@tum.de

Tel.: +49 (0) 9421 187-450.

Fax.: +49 (0) 9421 187-130

## 1. Degree of polymerization

The molecular weight of native Kraft lignin powder was determined by gel permeation chromatography (Polymer Win GPC Unichrom; Polymer Standard Service, PSS, Mainz, Germany) at 50 °C in a DMSO/0.075 LiNO<sub>3</sub> solution as eluent at a flow rate of 0.4 mL/min and a refractive index (RI) detector. Columns of PSS Gram 30A, PSS Gram 1000A and DMSO-Phil-P-300 (30 cm long with diameter of 0.8 cm) were used. Molecular weight of Kraft lignin was calculated using pullulan as calibrator.

The DP of native chitin powder was measured as follows: First, chitin was dissolved in DMAc /LiCl (5% W/V) solvent<sup>1</sup> at 30 °C. Then, the intrinsic viscosity  $[\eta]$  of the solution with a chitin concentration of 0.01 g/dL was calculated by its efflux time in according to the Schulz-Blaschke equation (eq.S1).

$$[\eta] = (\eta_{rel} - 1) / (1 + K\eta \times (\eta_{rel} - 1)) \quad (S1)$$

Where  $\eta_{rel}$  is the relative viscosity and  $K\eta$  is a coefficient ( $K\eta = 0.3$ )

Then, the DP of chitin was evaluated by the calculated molecular mass (M) from the Kuhn-Mark-Houwin-Sakurada (KMHS) equation (eq.S2).

$$[\eta] = K \times M^\alpha \quad (S2)$$

Where K is a constant value ( $K = 7.6 \times 10^{-3}$ ) and  $\alpha$  is 0.95

*Table S1. Molecular weights of native Kraft lignin and chitin powders determined by GPC and viscosimetric. (Mn: number average molecular weight; Mw: weight average molecular weight.)*

Sample	Mn (g/mol)	Mw (g/mol)	DP
Kraft lignin	600	4540	-
chitin	-	-	1691

## 2. Dissolution of Kraft lignin and chitin in BmimOAc-GVL

Complete dissolution of 2 wt% chitin was obtained only with BmimOAc and GVL at an optimum mass ratio of 4:1 at 90 °C for 3 h (Fig. S1 (i a) (ii c)) observed under microscopy.

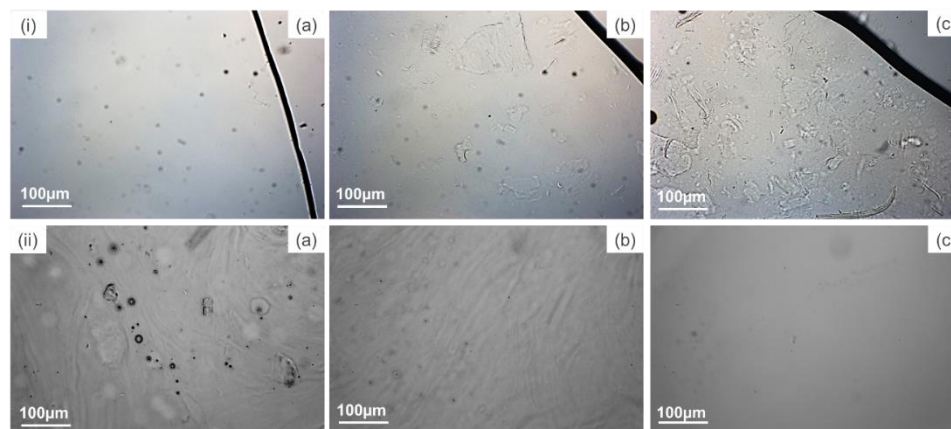


Fig. S1. Optical microscopy images of (i) the dissolution of 2 wt% chitin in the solvent system composed with different mass ratio of BmimOAc to GVL (a)4:1, (b) 2:1 (c)1:1; (ii) of the dissolution of 2 wt% chitin in BmimOAc-GVL (4:1, w:w) within (a) 1h, (b) 2h, (c) 3h.

The dynamic viscosities of the solvents as pure BmimOAc and BmimOAc-GVL (4:1, w:w) were determined using a falling ball viscometer (Anton Paar, AMVn) at the temperature range from 25 to 110 ° C. Their dynamic viscosity ( $\eta$ ) are determined by the equation (eq. S3).

$$\eta = K \times (\rho_0 - \rho_1) \times t \quad (\text{S3})$$

where K is a calibration constant that depends on temperature and tilt angle.  $\rho_0$  is the density of the sphere and  $\rho_1$  means the density of the sample, which is measured by a bending oscillator (DMA 5000M, Anton Paar); t is the measured roll time of the ball in the capillary.

Fig. S2 shows the viscosity curves of the two solvents as pure BmimOAc and a mixture of BmimOAc with GVL (4:1, w:w). It was clearly found that the high viscosity of BmimOAc was significantly reduced by adding GVL.

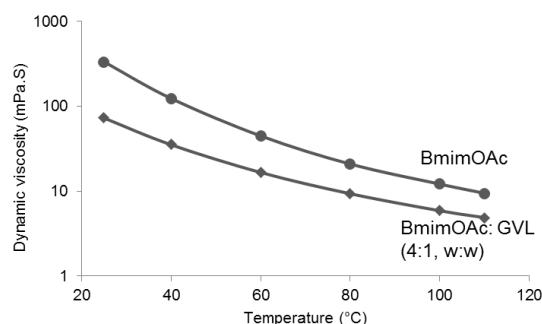


Fig.S2. Viscosity data of pure BmimOAc and the mixture of BmimOAc and GVL (4:1, w:w) from 25 °C to 110 °C. Lines correspond to correlations using the Vogel-Fulcher-Tammann equation.

The dissolution of 20 wt% Kraft lignin, 2 wt% chitin and lignin/chitin mixture (1:1, wt:wt), which composed with 2 wt% lignin and 2 wt% chitin, in BmimOAc-GVL (4:1, w:w) were estimated by visual and optical microscopy. Fig. S3 shows that all the samples formed clear and homogeneous solutions, which indicated a complete dissolution of the biopolymers in the solvent system of BmimOAc-GVL (4:1, w:w) under the experimental conditions. The results proved that the improved dissolution process by adding GVL as co-solvent.

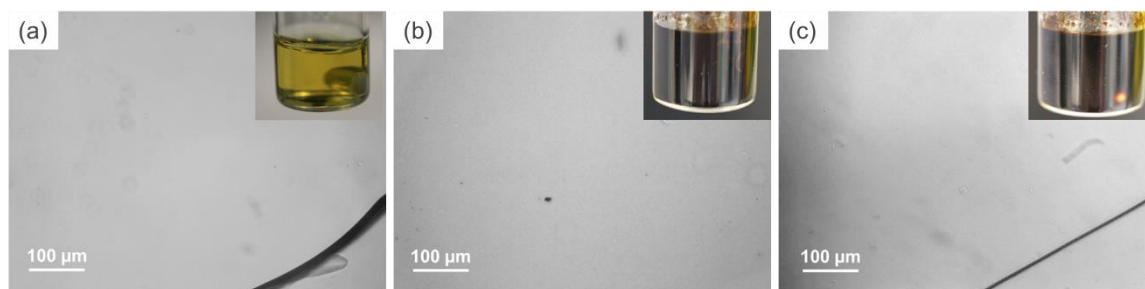


Fig. S3. Visual appearances and optical microscopy images of the prepared resulting mixtures with BmimOAc-GVL ((a) 2wt% chitin, (b) 20wt% lignin, (c) lignin: chitin, 1:1, w:w).

Fig. S4 shows the visual appearances of the selected lignin/chitin films. Pure lignin is not able to make film in the ethanol coagulation bath. The required flexibility of the lignin/chitin film is brought in by a certain amount of chitin and the more content of chitin, the more strength and easy-to-handle of the film.

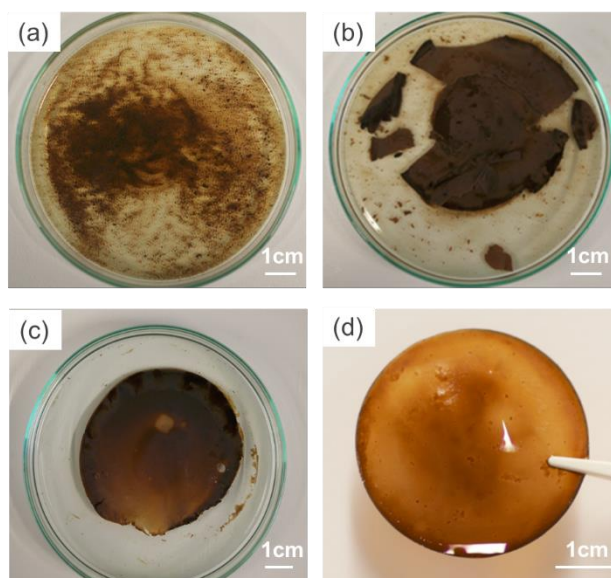


Fig. S4. Visual appearances of the prepared lignin/chitin films ((a) pure lignin, (b) lignin:chitin,, 7:1, w:w, (c) LC1, (d) LC4).

### 3. Degree of acetylation (DA) determination of native chitin powder

The DA of chitin (%) was determined using the element composition of the samples from EA analysis and was calculated with the following equation (S4).

$$DA = (C/N - 5.14) / 1.72 \times 100 \quad (S4)$$

where C/N is the mass ratio (w/w) of carbon to nitrogen.

### 4. ATR-FTIR measurement of the solvent system

The completely removed solvent system from the lignin/chitin films was examined by ATR-FTIR (Fig. S4). It was found that no absorption peaks derived from the two solvents were observed in any spectra of the composite samples. The results indicated that the successful preparation of lignin/chitin films using BmimOAc-GVL.

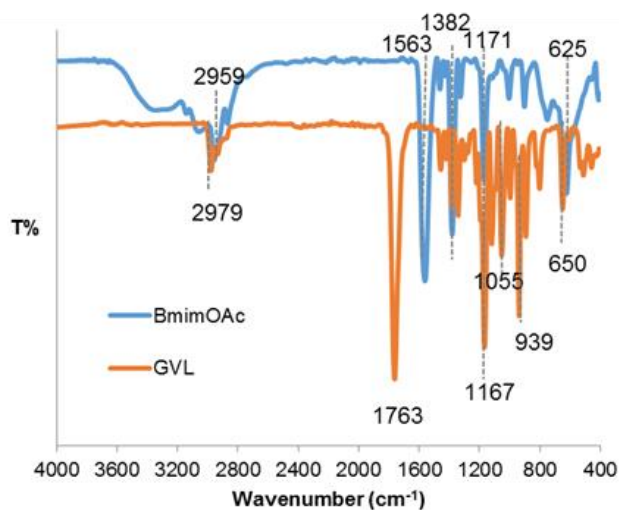


Fig. S5. ATR-FTIR curves of the solvents BmimOAc and GVL.

### 5. TGA measurement of lignin/chitin films

The thermal properties of selected lignin/chitin films were determined by thermogravimetric analysis (TGA) with a simultaneous thermal analyzer (STA PT1600 TGA/DSC, Linseis)) with a

heating rate of 10 °C /min under inert atmosphere of air. 12-20 mg of the samples were heated from room temperature to 600 °C.

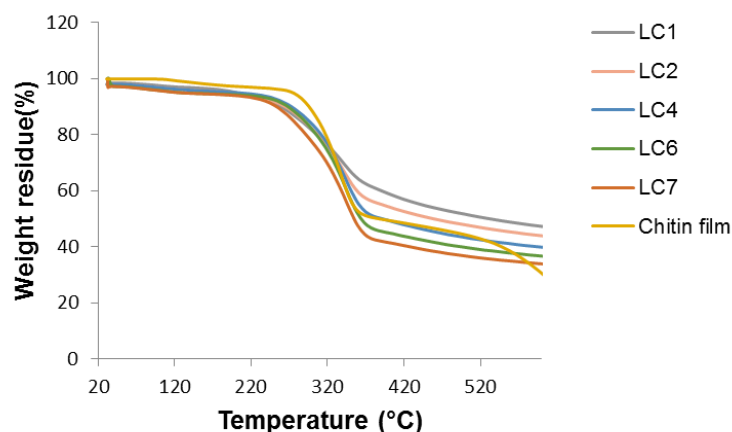


Fig. S6. TGA curves of the selected composite lignin/chitin thin films prepared in different lignin to chitin mass ratios as well as of the chitin films.

## 6. Adsorption experiments

Fig. S7 shows the visual appearances of the composite lignin/chitin films after the adsorption experiments and two groups of Fe (III) aqueous solution (3 mg/L) adsorbed with LC3 and pure chitin film, respectively, under identical conditions. The images below supported the adsorption capacity of the lignin/chitin film for Fe (III) cations.

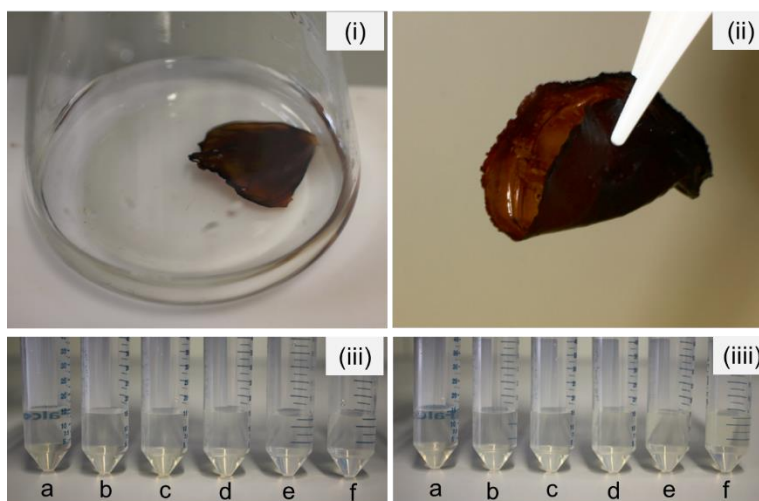


Fig. S7. (i) Photographs of LC2 in the Fe (III) aqueous solution, (ii) of LC2 removed from the Fe (III) aqueous solution; (iii) of the Fe(III) aqueous solution(3mg/L) adsorbed with (LC3) and (iii) pure chitin film on the tested time: (a) 0 h, (b) 2 h, (c) 5 h, (d) 8 h, (e) 24 h (f) 48 h.

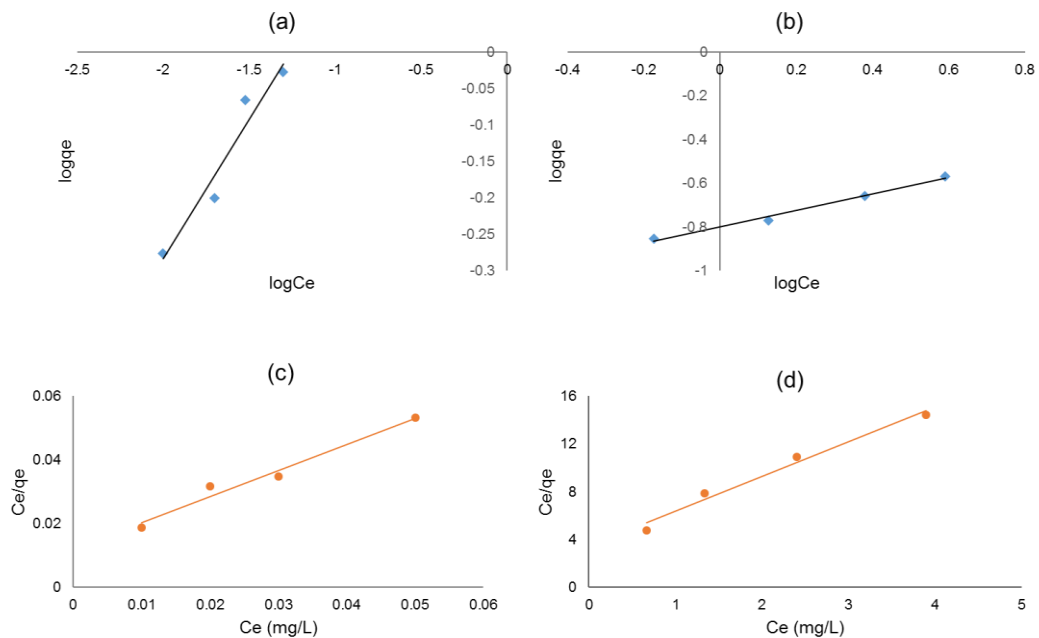


Fig. S8. Linear forms of Freundlich isotherm model for adsorption of Fe(III) (a) and Cu(II) (b) and Langmuir isotherm model for adsorption of Fe(III) (c) and Cu(II) (d) on lignin/chitin film.

### 7. Readsorption experiments

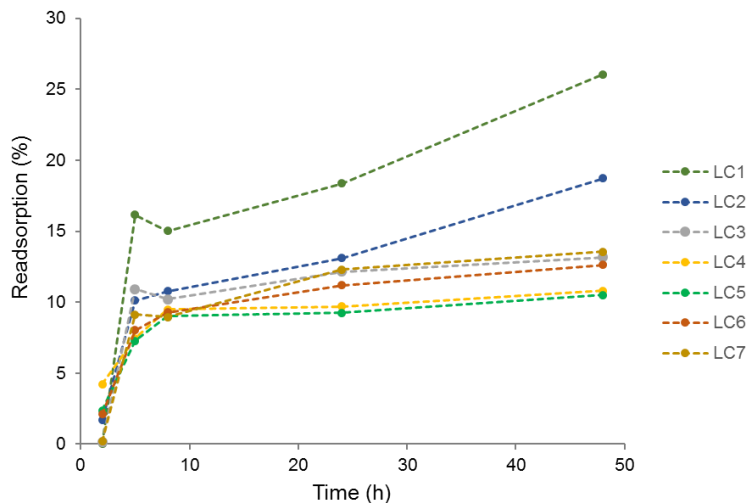


Fig. S9. Readsorption curves of lignin/chitin films for Fe (III) within different contact times; maximum standard deviation for the readsorption values of Fe (III) was  $\pm 3.39$ .

Table S2. pH values of the Fe (III) aqueous solutions (3 mg/L) within the lignin/chitin films for the readsorption experiment after 2 h, 5 h, 8 h, 24 h and 48 h respectively; maximum standard deviation for Fe (III) was  $\pm 0.18$ .

Samples	Fe(III) pH (initial) =4.49; T=19.9 °C				
	PH				
	2 h	5 h	8 h	24 h	48 h
LC1	3.66	3.64	3.64	3.68	3.72
LC2	3.77	3.65	3.63	3.70	3.78
LC3	3.88	3.59	3.58	3.58	3.64
LC4	4.01	3.62	3.59	3.61	3.60
LC5	4.02	3.62	3.61	3.62	3.61
LC6	4.09	3.65	3.64	3.65	3.64
LC7	4.23	3.68	3.65	3.67	3.66

## **Publication #C**

### **Chitin coated cellulosic textiles as natural barrier materials**

Auriane Freyburger, Yaqing Duan, Cordt Zollfrank, Werner Kunz

Lenzinger Berichte 94/2018; [www.lenzinger-berichte.com](http://www.lenzinger-berichte.com)

In this work, investigations were carried on the chitin coated cellulosic textiles produced from TENCEL®, Lenzing Viscose®, Lenzing Modal® and cotton fibers were coated by regenerating chitin from a mixture of an ionic liquid (1-butyl-3-methylimidazolium acetate) and a bio-sourced co-solvent ( $\gamma$ -valerolactone). The coat was applied only on one side of the textiles. Structural and morphological analysis demonstrated that a uniform and non-modified chitin film of 10  $\mu\text{m}$  was successfully coated on all type of textiles without damaging their network. These new composite materials exhibited the unique properties of chitin on one side without degrading cellulose properties on the other side. The influence of the chitin coat on the textiles properties was characterized by water contact angles, and gas/water permeability comparative studies of the conventional and coated textiles. The results demonstrated that the presence of chitin decreased the water wettability of the textiles solely on the coated site. Moreover, the chitin layer acted as a promising water and oxygen barrier independently of the nature of the textiles. Further optimization, as for instance the increase of the thickness of the coat, could improve the barrier properties of these new materials, making them potential candidates for various applications as impermeable textiles for hygiene products. Finally, a procedure to recover the ionic liquid during the process was proposed for sustainable concerns.

The work was accomplished under the supervision of Prof. Dr. Werner Kunz, Institute of Physical and Theoretical Chemistry, UR and Prof. Dr. Cordt Zollfrank, Biogenic Polymers, TUM. The preparation and evaluation of the samples were mainly carried out by Dr. Auriane Freyburger, UR. Characterization and measurement were performed in collaboration with the author of this dissertation.



# Chitin Coated Cellulosic Textiles as Natural Barrier Materials

Auriane Freyburger<sup>1</sup>, Yaqing Duan<sup>2</sup>, Cordt Zollfrank<sup>2</sup>, Thomas Röder<sup>3</sup>,  
and Werner Kunz<sup>1\*</sup>

<sup>1</sup> Institute of Physical and Theoretical Chemistry, University of Regensburg, Regensburg, Germany

<sup>2</sup> Biogenic Polymers, Technical University of Munich and Straubing Center of Science for Renewable Resources, Straubing, Germany

<sup>3</sup> Lenzing AG, Werkstraße 2, 4860 Lenzing, Austria

\* Contact: werner.kunz@chemie.uni-regensburg.de

## Abstract

The two most abundant biopolymers chitin and cellulose have unique properties suitable for designing renewable materials. Cellulose already plays a significant role in the production of daily materials such as textile fibers while chitin still remains widely less utilized. In this work, new cellulose/chitin composite materials were prepared to study the advantages of a chitin coat on the properties of cellulose-based textiles. Textiles produced from TENCEL<sup>®</sup>, Lenzing Viscose<sup>®</sup>, Lenzing Modal<sup>®</sup> and cotton fibers were coated by regenerating chitin from a mixture of an ionic liquid (1-butyl-3-methylimidazolium acetate) and a bio-sourced co-solvent ( $\gamma$ -valerolactone). The coat was applied only on one side of the textiles. Structural and morphological analysis demonstrated that a uniform and non-modified chitin film of 10  $\mu\text{m}$  was successfully coated on all type of textiles without damaging their network. The degree of acetylation of the used chitin and the fabricated chitin coating determined by elemental analysis was 95.8% and 91.9%, respectively. The influence of the chitin coat on the textiles properties was characterized by wetting, and gas/water permeability comparative studies of the conventional and coated textiles. The results demonstrated that the presence of chitin decreased the water wettability of the textiles solely on the coated site. Moreover, the chitin layer acted as a promising water and oxygen barrier independently of the nature of the textiles.

**Keywords:** Chitin coating, water and oxygen barrier, TENCEL<sup>®</sup>, Lenzing Viscose<sup>®</sup>, Lenzing Modal<sup>®</sup>, cotton, textile fibers.

## Introduction

Currently, most polymeric materials are manufactured from petrochemical (fossil) resources. In order to reduce the dependence on petrochemical feedstocks and their environmental impacts, the development and the use of polymers from biomass as renewable materials is important to our society [1]. In biomass, the natural polysaccharides cellulose (poly  $\beta$ -(1,4)-D-glucopyranose) and chitin (poly  $\beta$ -(1,4)-2-acetamido-2-desoxy-D-glucopyranose) are the most abundant biopolymer resources. With cellulose being the principal structural component in higher plants, it has an estimated annual production of  $10^{12}$  tons, while chitin is mainly contained in crustacean shells up to 75 000 tons per year [2,3]. In addition to their abundance and bio-

degradability, they have good chemical and mechanical properties suitable for various applications as filtration process, textile, hygienic, packaging and biomedical utilization [2,4,5]. However, being not meltable below their degradation temperature and having rigid bulk structures, the processing of these biopolymers is a real challenge and research on it has been increasing exponentially [2,6].

Cellulose processing has been successfully performed by more or less complex and polluting methods and is mainly industrially used in the production of fibers for textile and nonwoven applications. Among the most prominent man-made cellulose fiber generations one finds viscose, the Modal and Tencel<sup>®</sup> fibers. The first

generation of cellulosic fibers, viscose, is manufactured by derivatization of cellulose pulp with sodium hydroxide and carbon disulfide to cellulose xanthate and subsequent regeneration of the cellulose by solution spinning. Modal is the second generation of regenerated cellulose fibers and produced by a modified viscose process, *inter alia*, by using a pulp with a higher degree of polymerization. The third generation named Tencel® is manufactured by the Lyocell process, an environmentally friendlier way to produce fibers from cellulose solutions in N-methylmorpholine-N-oxide in presence of water. Besides these man-made fibers, the natural cellulosic fibers from cotton are still the most widely applied raw materials used to produce textiles. [7]

Chitin has not achieved the same commercial value as has cellulose and a large majority of its production (60-70%) is used to produce its de-acetylated derivative chitosan [8]. Chitin is structurally similar to cellulose, but bears an acetamido group at the C<sub>2</sub> position of the glucose units instead of an hydroxyl group. This particularity confers it advantages over cellulose such as excellent antibacterial properties, a less hydrophilic character and water retention/chelate metal ions capacity [4,9]. However, it induces also a more complex inter- and intramolecular hydrogen bonding network, causing a decreased solubility [10]. To date, the only promising environmentally friendly and direct solvents for chitin are ionic liquids (ILs). ILs are salts with a melting point below 100 °C. Imidazolium-based ILs, for instance 1-butyl-3-methylimidazolium acetate (BmimOAc), were described as the most effective solvents without changing drastically the properties of chitin [10-12]. I.e. the chitin can be recovered without deacetylation, which is a prerequisite for maintaining the chitin properties.

The aim of this study is to give new functional properties to four different cellulosic fibers (cotton, viscose, modal and lyocell textiles) applying chitin coatings. For this purpose, 1-butyl-3-methylimidazolium acetate has been used to dissolve chitin in presence of the co-solvent,  $\gamma$ -valerolactone (GVL) obtainable from renewable resources, for facilitating the polymer solution processing. By coating the chitin dope on the textiles, composite materials could be prepared having distinguished properties of each polymer, i.e. cellulose and chitin, on each face. The effect of the regenerated chitin film on the structure and the properties of the textiles were characterized by scanning electron microscopy, infrared spectroscopy, water contact angle measurements and water/gas permeability studies. Furthermore, a method was also used to recycle and reuse the costly ionic liquid at the end of the coating route.

## Materials and Methods

### Materials

Textiles used in this work were obtained from Lenzing AG (Austria) and produced from four different cellulosic fibers: TENCEL®, cotton, Lenzing Viscose®, and Lenzing Modal®. All textiles were washed and desized by Lenzing AG and dried at 70 °C for 5 days in an oven prior to use.

Chitin solutions were prepared with dried  $\alpha$ -chitin powder from shrimp shells purchased from Sigma Aldrich (Germany). Its degree of polymerization and of acetylation were measured to be 1690 and 95.8%, respectively. The solvent system used to dissolve chitin was composed of  $\gamma$ -valerolactone (Reagent Plus®, purity  $\geq 99\%$ ) from Sigma Aldrich (Germany) and 1-butyl-3-methylimidazolium acetate (BmimOAc, purity  $\geq 98\%$ ) from IoLiTec (Germany). The latter was dried using a high vacuum setup (at  $10^{-6}$  mbar) for 5 days, prior to dissolution of the chitin. All other chemicals were used without further purification.

### Methods

Chitin solutions were prepared by dissolving  $\alpha$ -chitin (2 wt%) in BmimOAc (88 wt%) and GVL (10 wt%) under nitrogen atmosphere at 110 °C. After total dissolution of chitin, a small amount of GVL was added to dilute the highly viscous gel and to facilitate the coating. The final solution was composed of 1.6 wt% chitin, 30 wt% GVL and 68.4 wt% BmimOAc.

Chitin coating was performed by putting one face of the textiles in contact with the chitin solution at 100 °C. Textiles were then moved on the chitin solution surface by a pair of tweezers for 5 minutes to provide a homogeneous chitin layer. Chitin covered textiles were left at room temperature for 2 hours to allow a slow gelation of the chitin. Each material was subsequently soaked in ethanol for 2 days and in deionized water for 2 days in order to remove the solvent residues, i.e. BmimOAc and GVL, and to induce coagulation of the chitin layer. The produced materials were dried between 2 glass plates at room temperature for several days.

Recovery of the ionic liquid BmimOAc was accomplished after the coating procedure using the following method. The ethanol-based coagulation solutions were first filtrated with a 0.2  $\mu$ m polytetrafluorethylene (PTFE) membrane filter to remove any possible polymer residues. The obtained liquids were dried for two hours under reduced pressure (100 mbar) at 40 °C using a rotary evaporator. Further drying was carried out with a high vacuum setup ( $10^{-6}$  mbar) at 40 °C for 5 days. The purity of the recycled BmimOAc was

analyzed by  $^1\text{H}$ - and  $^{13}\text{C}$ -NMR measurements in dimethyl sulfoxide- $d_6$  recorded with a Bruker Avance 300 spectrometer (Germany) at 300 MHz.

To characterize the composition of the materials, infrared spectra were measured with a Fourier transform infrared spectroscopy (FTIR) instrument equipped with an attenuated total reflectance (ATR) sampler by pressing the samples against a Smart Diamond ATR sensor (Nicolet 380, Thermo Fisher Scientific, USA). Spectra were recorded in the range from 400 to 4000  $\text{cm}^{-1}$ .

Films morphologies were studied by scanning electron microscopy (SEM). Dried samples were placed on carbon tape and coated with Au/Pd. SEM images were obtained with a digital scanning electron microscope (DSM 940 A, Zeiss, Germany) in secondary imaging mode at an acceleration voltage of 10 kV.

The wetting properties of the films were characterized by water contact angle measurements using a goniometer type P1 equipped with a microscope and a back light (Erna Inc., Japan). Measurements were performed at room temperature on both surfaces of the coated films, i.e. on the chitin layer and the untreated textile layer. A 2  $\mu\text{L}$  drop of deionized and sterile filtered water was formed by an automated micrometer pipette (Hamilton Company, USA) and placed on the sample surface. The angle of the tangent formed at the water drop base was recorded as well as the liquid drop absorption time on each material. Overall five drops were placed on various surface locations for each sample.

The ability of water and oxygen to pass the materials was investigated with permeability tests at a constant temperature of  $20 \pm 1$   $^\circ\text{C}$ . Water permeability measurements were performed using a setup with two cells allowing the film to be in contact with 8 mL of two different solvents, deionized water and ethyl lactate (EL), through a hole of 3 mm in diameter. For the coated materials, the chitin coat was in contact with the water cell. Both solutions were stirred at 200 rpm for 7 h and 150  $\mu\text{L}$  were collected with an Eppendorf pipette from each cell at the same time at defined time intervals. The water concentration in each cell in function of time was measured by volumetric Karl-Fischer-Titration (870 KF Titrino plus, Metrohm, Switzerland). The water permeability coefficient,  $P_{\text{H}_2\text{O}}$  was used to characterize the water barrier property of the films and was determined using Fick's first law as [13]:

$$J_{\text{H}_2\text{O}} = P_{\text{H}_2\text{O}} \times \Delta c_{\text{H}_2\text{O}} \quad (1)$$

where  $J_{\text{H}_2\text{O}}$  represents the flow of water per unit area,  $\Delta c_{\text{H}_2\text{O}}$  the difference in water concentration between

the ethyl lactate and the water filled cell. The flux  $J_{\text{H}_2\text{O}}$  can be also expressed by Equation 2:

$$J_{\text{H}_2\text{O}} = \frac{1}{A} \times \frac{dc_{\text{H}_2\text{O in EL cell}}}{dt} \times V \quad (2)$$

with the permeation area  $A$ , the water concentration in the ethyl lactate cell  $c_{\text{H}_2\text{O}}$  in EL cell), the volume related to the water concentration  $V$ , and the time  $t$ . Thus, the water permeability coefficient can be calculated from Equations 1 and 2 by:

$$|P_{\text{H}_2\text{O}}| = \frac{V}{A \times |\Delta c_{\text{H}_2\text{O}}|} \times \frac{dc_{\text{H}_2\text{O in EL cell}}}{dt} \quad (3)$$

Water permeability coefficients were calculated considering only the average of the values between 120 and 420 min. Before 120 min, the difference in water concentration between the two cells could not be precisely determined due to the uncertainty of the water concentration measurements in the pure water cell carried out by Karl-Fischer-Titration.

Oxygen permeation under dry condition was evaluated with an optical measurement conducted by a chemical optical sensor (type PSt6 from PreSens, Germany). The experimental setup consists of a self-developed measurement cell comprising the chemical optical sensor spot inside, read out via a polymer optical fiber (POF-2SMA from PreSens, Germany) connected to a fiber optic oxygen transmitter (Fibox 4 trace from PreSens, Germany). The film was fixed on the top of the permeation cell with a constant volume of 49.38  $\text{cm}^3$  and was in contact with the ambient air through a hole of 5 mm diameter. After flushing the chamber three times with nitrogen, the increase of the oxygen partial pressure over time in the chamber was recorded three times for each sample. The time range was selected from 0 to 13 min, which is the period of time where accurate oxygen partial pressures (from 0 to 52 hPa) could be measured by the sensor spot for the textiles. The permeability of the film was calculated with the oxygen permeability coefficient,  $P_{\text{O}_2}$ , determined using an adaptation of the ideal gas law (4) and the Fick's first law (5).

$$p_{\text{O}_2} \times V = n_{\text{O}_2} \times R \times T \quad (4)$$

$$J_{\text{O}_2} = -P_{\text{O}_2} \times \Delta c_{\text{O}_2} = \frac{1}{A} \times \frac{dn_{\text{O}_2}}{dt} \quad (5)$$

In Equation 4,  $p_{\text{O}_2}$  is the partial pressure of oxygen,  $V$  the volume of the chamber,  $n_{\text{O}_2}$  the oxygen amount in moles,  $R$  the gas constant, and  $T$  the absolute temperature. In Equation 5,  $J_{\text{O}_2}$  represents the flow of oxygen per unit area,  $\Delta c_{\text{O}_2}$  the difference in oxygen concentration between the filled chamber and the outside, and  $A$  the

permeation area. By combining these two equations, the oxygen permeability coefficient could be calculated by:

$$|P_{O_2}| = \frac{V}{A \times |\Delta P_{O_2}|} \times \frac{dp_{O_2}}{dt} \quad (6)$$

The oxygen permeability coefficients were calculated considering only the average of the calculated values between 1 and 13 min.

## Results and Discussion

### Structure of the coated textiles

The studied textiles consist of an ordered structural assembly of cellulosic fibers (TENCEL<sup>®</sup>, Cotton, Lenzing Viscose<sup>®</sup>, and Lenzing Modal<sup>®</sup>) having a white color. They were produced by interlacing warp fibers (longitudinal) and weft fibers (transversal) so that each warps fiber passes alternately under and over each weft fibers. This structural hierarchy can be well observed in Figure 2 A). After dissolution of the chitin in a mix-

ture composed of the ionic liquid BmimOAc and the co-solvent GVL, a chitin layer was formed on one side of the textiles by promoting its precipitation in ethanol [10]. Once the textiles were coated with chitin, they exhibited a thin transparent shiny film on the chitin side while the untreated side was visually not modified during the coating (Figure 1).

The morphology of the prepared materials was observed with SEM. An example of the obtained SEM images for the coated material viscose performed on the surface of both sides, i.e. chitin and textile layer, and the cross section is presented in Figure 2. On the one hand, it could be observed that the viscose network consisting of interlaced fibers was not damaged by the coating procedure. The chitin side, on the other hand, exhibited a homogeneous and smooth surface without crevices or flaws. The chitin layer covered the pores of the textile without penetrating inside. The cross section of the coated material displayed two distinct layers, i.e. the interlaced fibers representative

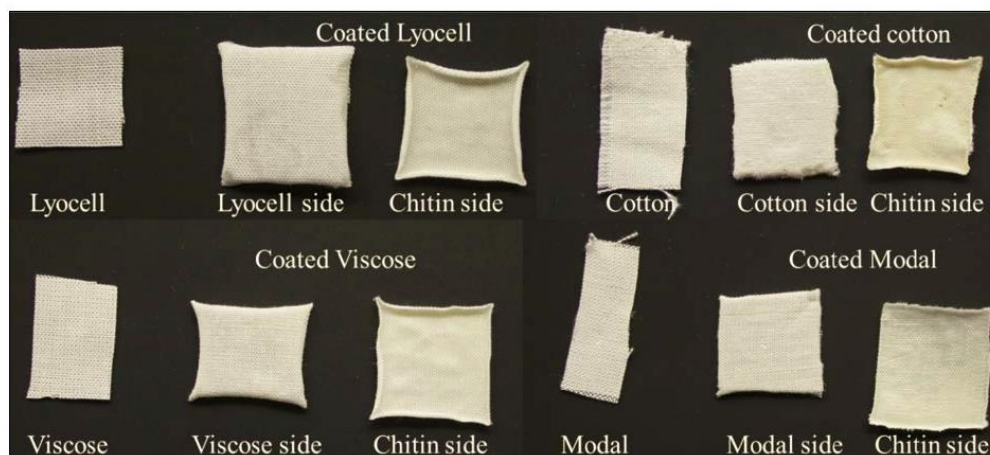


Figure 1: Appearance of untreated and chitin coated textiles.

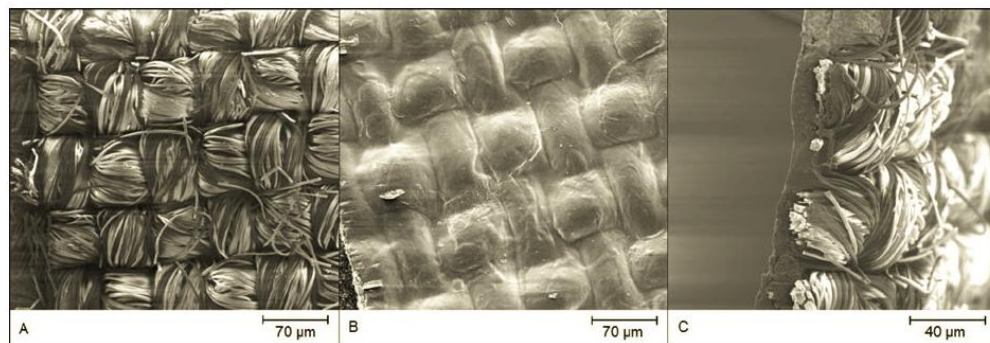
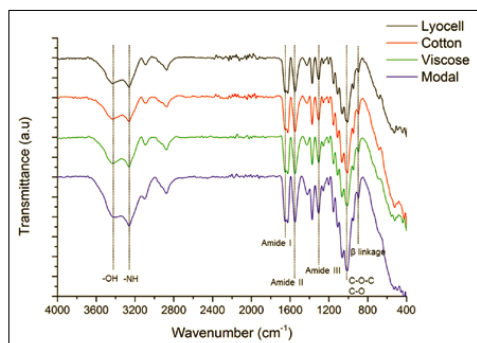


Figure 2: SEM images of the viscose textile coated with chitin obtained from (A) the viscose side, (B) the chitin side, and (C) the cross section.

of the textile side and a thin homogeneous chitin coat. The same observations were made also for all three other coated materials. The thickness of the chitin coat on all materials was estimated to be  $10 \pm 2 \mu\text{m}$  as inferred from the cross section SEM images. To confirm the presence of chitin on the coated side and to exclude degradation of the textiles, all materials were characterized by FTIR in ATR mode. Figure 3 shows the FTIR-ATR spectra of the chitin side for the four coated textiles. The IR curves were shifted by a



**Figure 3:** FTIR-ATR spectra of the chitin coated side for the prepared textiles.

constant value self-developed for visual clarity. Firstly, no differences appeared comparing all spectra. Secondly, the specific bands characteristic to chitin such as the amide I doublet band located at 1654 and 1625  $\text{cm}^{-1}$ , the amide II band at 1550  $\text{cm}^{-1}$  and the amide III band at 1307  $\text{cm}^{-1}$  could be detected for all materials. This means that the recovered chitin was not deacetylated. The other bands at 3430 and 3261  $\text{cm}^{-1}$  were attributed to the OH and NH stretching, at 3090  $\text{cm}^{-1}$  to the  $\text{CH}_3$  asymmetric stretching, and at 2875  $\text{cm}^{-1}$  to the  $\text{CH}_3$  symmetric,  $\text{CH}$ , and  $\text{CH}_2$  stretching [14]. CH deformation and C- $\text{CH}_3$  amide stretching vibrations were assignable to the peaks at 1428 and 1373  $\text{cm}^{-1}$ . The intense peaks at 1154-1010  $\text{cm}^{-1}$  corresponded to C-O-C and C-O stretching. The last peak at 896  $\text{cm}^{-1}$  confirmed the presence of  $\beta$  linkage in the molecule [14,15]. This indicated that chitin was successfully coated on the textiles and no obvious degradation occurred during the preparation.

Each starting material and its corresponding side on the coated textiles are compared by FTIR-ATR curves in Figure 4. Again, IR curves for the coated textiles were shifted for a better display. The spectrum for each textile side was similar to the spectrum for its non-

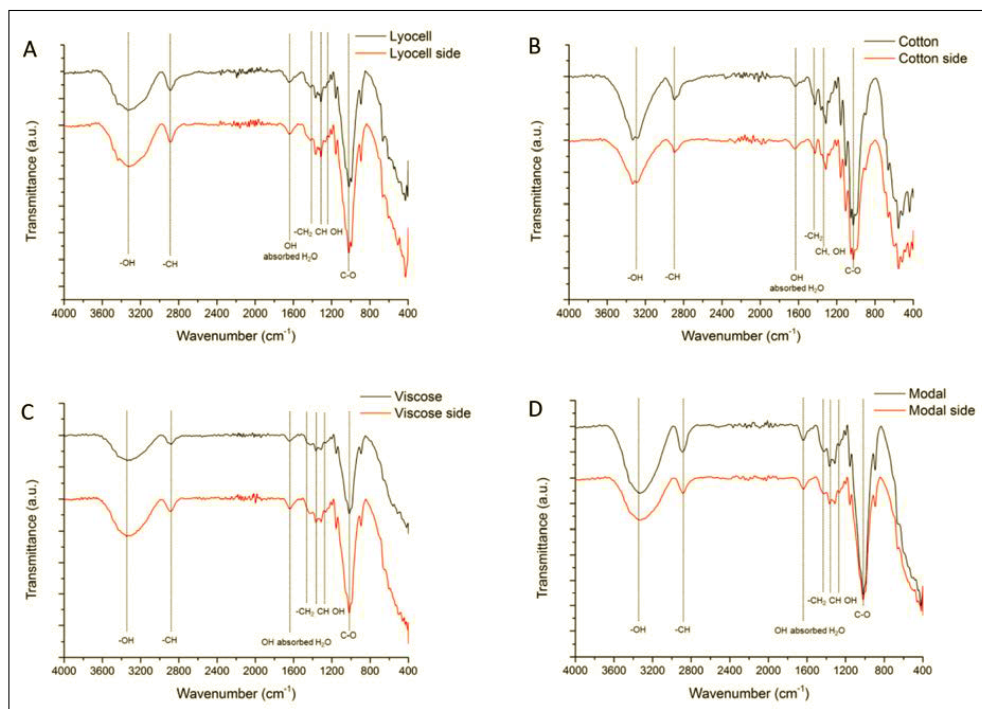


**Figure 4:** Comparative FTIR-ATR spectra of each reference textile, (A) lyocell, (B) cotton, (C) viscose, and (D) modal with its corresponding untreated side on the coated materials.

coated material independent of its crystalline structure, namely cellulose I for the natural cotton and cellulose II and amorphous cellulose for the man-made lyocell, viscose, and modal textiles. Thus, the cellulosic fibers were not chemically degraded during the coating process. In addition, the absence of the chitin characteristic bands confirmed the presence of chitin solely on the coated side of the prepared material as also observed under SEM.

### Evaluation of new functional properties

In order to evaluate the specific properties of these new materials, a comparison of the untreated textiles and the coated ones were performed regarding their wetting and permeation performance.

In a first step, we studied whether the chitin coat can act as a water barrier, since this biopolymer is a major structural component in the exoskeleton of marine crustaceans and contributes to their protection [3]. Therefore, wetting properties of the films were characterized using water contact angles measurements. Typically, contact angles lower than  $90^\circ$  correspond to favorable wetting of the surface (termed hydrophilic), whereas low wettability materials (hydrophobic) induce contact angles higher than  $90^\circ$  [16]. The relation between the water contact angles and the type of textile (coated and non-coated) is illustrated in Figure 5 A). Due to the high hydrophilic behavior of cellulosic fibers and the porous structure of the textiles, no water contact angle could be measured for the non-coated materials as the water drop was immediately absorbed. Only cotton induced a contact angle of  $85 \pm 5^\circ$  for a few seconds (10 s), probably due its highly ordered structure (cellulose I). For the coated materials, the water contact angle tended to be identical on almost all chitin sides and was approximately  $90^\circ$  ( $90 \pm 4^\circ$  for the coated Lyocell,  $91 \pm 3^\circ$  for the coated Cotton, and  $90 \pm 4^\circ$  for the coated Viscose). Only the coated modal textile exhibited a slight smaller value of  $84 \pm 3^\circ$ . These results proved that the chitin layers exhibit a poor degree of wetting towards water. After a long contact period on the surface of the chitin layer, a decrease of the water contact angles were detected and the absorption times were recorded (Figure 5 B). A complete absorption of a  $2 \mu\text{L}$  drop on all chitin layers was reached after ca. 20 min ( $24 \pm 3$  min for the coated Lyocell,  $22 \pm 6$  min for the coated Cotton,  $21 \pm 1$  min for the coated Viscose, and  $19 \pm 4$  min for the coated Modal). Accordingly, the formed chitin layer is not impermeable to water but significantly retards its infiltration.

Since the textile side of the coated materials immediately absorbed the water drop textile wettability properties were not changed during the process (Figure 5 B). Consequently, the chitin coat affected only the wet-

ting properties on one side of the coated materials, by making the textiles more hydrophobic and by slowing down the water penetration into the textiles, probably by plugging the holes and the reduced wetting angle towards the more hydrophobic chitin.

**Table 1:** Water permeability coefficient,  $P_{\text{H}_2\text{O}}$ , with corresponding standard deviations as a function of the type of materials.

Materials	$P_{\text{H}_2\text{O}}$ ( $\times 10^{-7}$ m/s)
Lyocell	$2.0 \pm 0.5$
Lyocell coated with chitin	$0.6 \pm 0.2$
Cotton	$1.6 \pm 0.4$
Cotton coated with chitin	$0.5 \pm 0.2$
Viscose	$1.7 \pm 0.7$
Viscose coated with chitin	$0.5 \pm 0.2$
Modal	$2.9 \pm 0.8$
Modal coated with chitin	$0.7 \pm 0.2$

To study the influence of chitin on the water diffusion through the materials, water permeability tests for all of the coated and non-coated materials were additionally performed under identical conditions. From these experiments, water permeability coefficients were calculated according to Equation 3 and are reported in Table 1. As expected, the permeability coefficients for all non-coated textiles were higher than the ones for the coated materials, namely by a factor of 3.3, 3.2, 3.4, and 4.1 for Lyocell, Cotton, Viscose, and Modal, respectively. The water transport was faster and easier through the unmodified textiles, because of their porous and hydrophilic nature of the textiles. As shown in Table 1, water permeability values for the coated textiles ranged from  $0.5$  to  $0.7 \times 10^{-7}$  m/s. This indicated that the chitin coat has the same water barrier properties independently of the nature of the textile and slow down the water permeation.

In order to explore other barrier effects of the chitin layer, gas (i.e.  $\text{O}_2$ ) permeability tests were carried out under dry conditions. Figure 6 (page 112) shows the evolution of the oxygen partial pressure,  $p_{\text{O}_2}$ , in the measurement cell as a function of time investigated for all materials. Oxygen permeability coefficients were calculated according to Equation 6 considering the quasi linear increase of the oxygen partial pressure and are reported in Table 2. For non-coated textiles,  $p_{\text{O}_2}$  identically increased from 0 to 51 hPa in 13 minutes. Furthermore, it has to be noticed that this  $p_{\text{O}_2}$  raise followed the same trend as in the case when no membrane was fixed on the top of the permeation chamber. Independently of the textile nature, all are highly permeable to oxygen

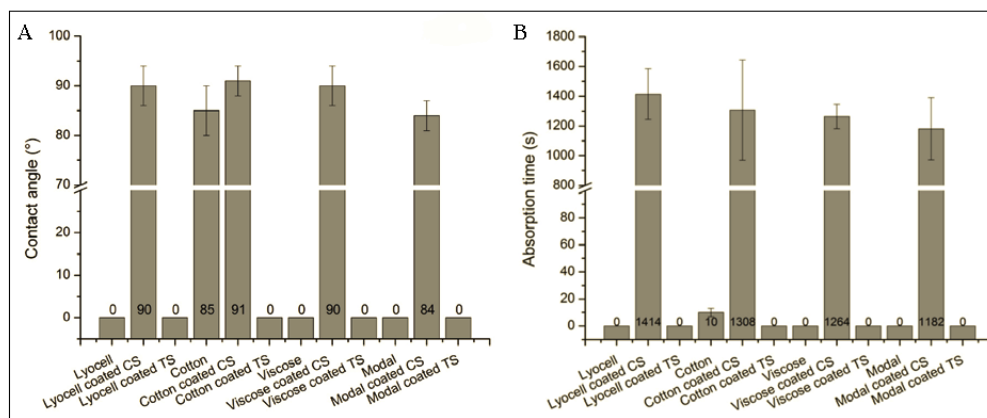


Figure 5: (A) Contact angle and (B) absorption time of a 2 µL water drop on the surface of the textile materials non-coated and coated with chitin (CS stands for Chitin Side and TS for Textile Side).

which can be explained by the presence of open pores. This generated high permeability coefficients for these materials in the range from 9.0 to 9.1 x10<sup>-4</sup> m/s (Table 2). In contrast, the oxygen diffusion through the coated materials was much slower as shown in Figure 6 B). After 13 minutes, p<sub>O<sub>2</sub></sub> values of 3.1, 3.0, 2.8, and 2.7 hPa were recorded for the coated Lyocell, Cotton, Viscose, and Modal, respectively. As a result, coated textiles show significant lower permeability coefficients, which were ranged from 0.40 to 0.46 x10<sup>-4</sup> m/s. Comparing these values to those obtained for the non-coated textiles, it can be concluded that oxygen respectively permeated through Lyocell, Cotton, Viscose, and Modal 19.8, 19.8, 21.4, and 22.8 times faster than through its corresponding coated materials.

Table 2: Oxygen permeability coefficients, P<sub>O<sub>2</sub></sub>, with corresponding standard deviations as a function of the type of materials.

Materials	P <sub>O<sub>2</sub></sub> (x10 <sup>-4</sup> m/s)
Without membrane	9.4 ± 0.4
Lyocell	9.1 ± 0.3
Lyocell with chitin	0.46 ± 0.02
Cotton	9.1 ± 0.4
Cotton with chitin	0.46 ± 0.02
Viscose	9.0 ± 0.3
Viscose with chitin	0.42 ± 0.01
Modal	9.1 ± 0.3
Modal with chitin	0.40 ± 0.01

To prove that these new functional properties were caused by chitin and not just by the plugging of the textiles pores, the same coating procedure was performed

with cellulose instead of chitin. To achieve this, a Lyocell textile was coated with microcrystalline cellulose under the same conditions as previously described. Unfortunately, it was not possible to reproduce a comparably thin 10 ± 2 µm cellulose layer. Therefore a quantitative comparison could not be done, especially for the permeability tests. However, it can be mentioned that cellulose coating induced a lower water contact angle of 54° instead of 90° for the chitin coating. The water drop was also two times faster absorbed by the cellulose layer than by the chitin one. Concerning the gas/water permeability properties of the cellulose coated Lyocell, it seemed that cellulose coating was more permeable to water but slightly less to oxygen than chitin coating. Further work has to be done to confirm these observations.

At the end of the coating process, the recycling of the ionic liquid was attempted for sustainability and profitability interests. Once chitin regenerated, the ethanol-based precipitation solutions were collected and submitted to a drying procedure detailed in the methods. Ethanol could be successfully removed under reduced pressure using a rotary evaporator. However, GVL was still present in the residue due to its remarkable low vapor pressure (0.65 kPa at 25 °C and 3.5 kPa at 80 °C) [17]. A second step was thus carried out to remove GVL by using a high vacuum setup. Analysis of the obtained extract by <sup>1</sup>H and <sup>13</sup>C NMR revealed that BmimOAc remained unaltered and no trace of ethanol or GVL was detected. The recovered IL was reused to dissolve successfully 2 wt% of chitin as described above in the dissolution experiment. Again, BmimOAc was then a second time recovered and reused without appreciable decrease of its efficiency.

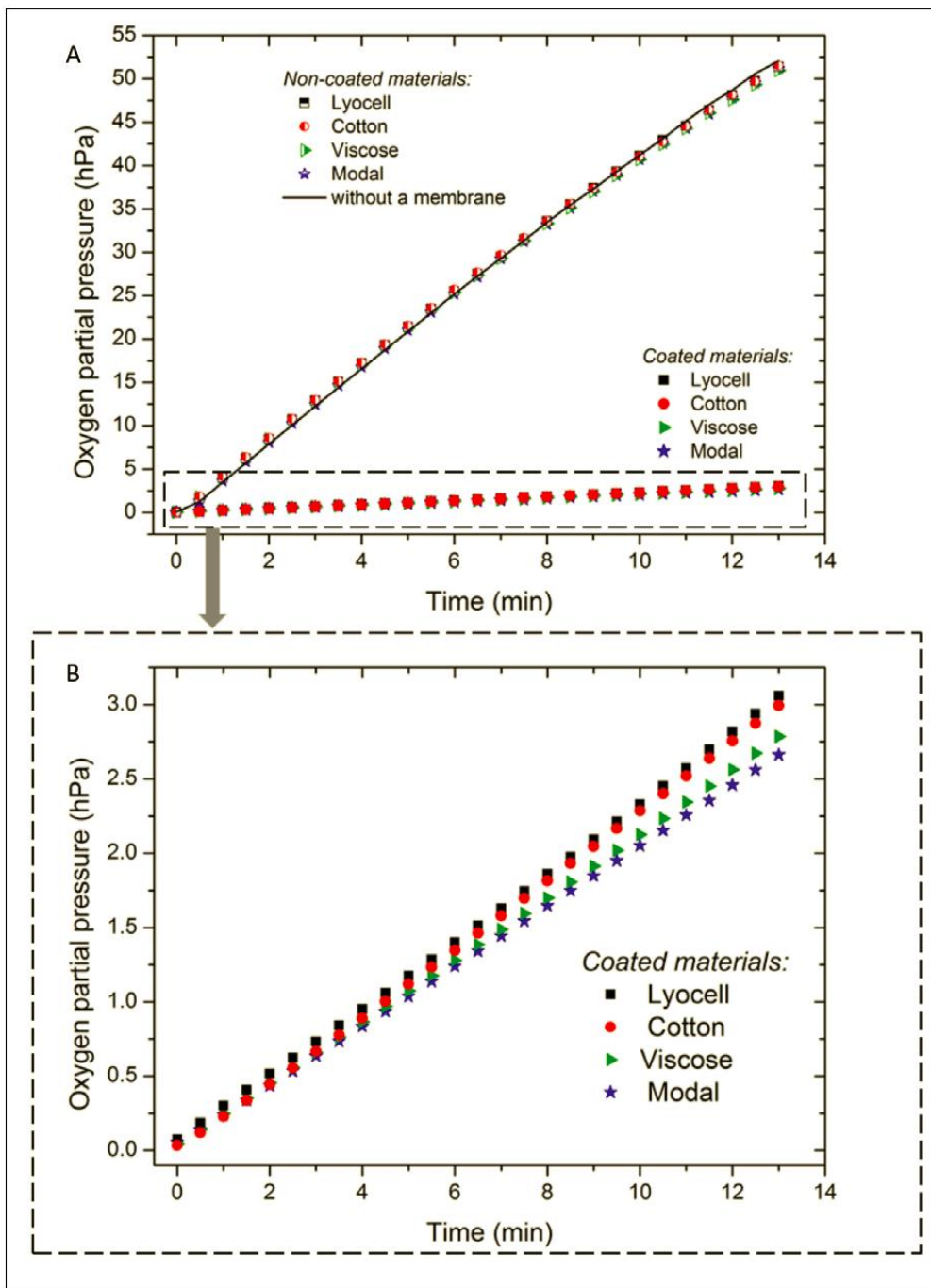


**Figure 6:** Oxygen partial pressure,  $p_{O_2}$ , over time measured in the  $O_2$  permeation chamber for (A) all the textile materials non-coated and coated with chitin and for (B) specific to the coated materials.

## Conclusions

Textiles made from TENCEL®, Lenzing Viscose®, Lenzing Modal® and cotton fibers were coated with chitin, a natural and antibacterial polymer, to produce new functional and renewable materials. The approach used therefore was the chitin regeneration on one surface of the textiles. Chitin was dissolved in the ionic liquid 1-butyl-3-methylimidazolium acetate with a bio-sourced solvent  $\gamma$ -valerolactone and precipitated with ethanol, after being in contact with the starting materials. Transparent chitin coats of 10  $\mu\text{m}$  thickness were successfully created on the textiles without penetration into the textiles. These new composite materials exhibited the unique properties of chitin on one side without degrading cellulose properties on the other side. The chitin coat influenced the properties of the resulting composite materials by making them more hydrophobic and by slowing down the penetration of water or  $\text{O}_2$  into the membrane. Further optimization, as for instance the increase of the thickness of the coat, could improve the barrier properties of these new materials, making them potential candidates for various applications as impermeable textiles for hygiene products. Finally, a procedure to recover the ionic liquid during the process was proposed for sustainable concerns.

## Acknowledgements

As part of the project ForCycle, this work was supported by the Bavarian State Ministry of the Environment and Consumer Protection.

## References

- [1] Mohanty, A. K.; Misra, M.; Drzal, L. T.: Sustainable Bio-Composites from Renewable Resources: Opportunities and Challenges in the Green Materials World. *Journal of Polymers and the Environment* 2002, 10, 19-26.
- [2] Klemm, D.; Heublein, B.; Fink, H.-P.; Bohn, A.: Cellulose: Fascinating biopolymer and sustainable raw material. *Angew. Chem., Int. Ed.* 2005, 44, 3358-3393.
- [3] Khor, E.: Chapter 5: the sources and production of chitin. In *Chitin: fulfilling a biomaterials promise*; Elsevier, 2014; pp 63-72.
- [4] Ravi Kumar, M. N. V.: A review of chitin and chitosan applications. *Reactive and Functional Polymers* 2000, 46, 1-27.
- [5] Islam, S.; Bhuiyan, M. A. R.; Islam, M. N.: Chitin and Chitosan: Structure, Properties and Applications in Biomedical Engineering. *J. Polym. Environ.* 2016, Ahead of Print.
- [6] Rinaudo, M.: Chitin and chitosan: Properties and applications. *Progress in Polymer Science* 2006, 31, 603-632.
- [7] Shen, L.; Patel, M. K.: Life cycle assessment of man-made cellulose fibers. *Lenzinger Ber.* 2010, 88, 1-59.
- [8] Kurita, K.: Chitin and Chitosan: Functional Biopolymers from Marine Crustaceans. *Mar. Biotechnol.* 2006, 8, 203-226.
- [9] Crini, G.; Guibal, É.; Morcellet, M.; Torri, G.; Badot, P.-M.: Chitine et chitosane. Préparation, propriétés et principales applications. In *Chitine et chitosane, du biopolymère à l'application*; Presses universitaires de Franche-Comté, 2009; pp 19-53.
- [10] Wu, Y.; Sasaki, T.; Irie, S.; Sakurai, K.: A novel biomass-ionic liquid platform for the utilization of native chitin. *Polymer* 2008, 49, 2321-2327.
- [11] Qin, Y.; Lu, X.; Sun, N.; Rogers, R. D.: Dissolution or extraction of crustacean shells using ionic liquids to obtain high molecular weight purified chitin and direct production of chitin films and fibers. *Green Chem.* 2010, 12, 968-971.
- [12] Jaworska, M. M.; Kozlecki, T.; Gorak, A.: Review of the application of ionic liquids as solvents for chitin. *J. Polym. Eng.* 2012, 32, 67-69.
- [13] Evans, D. F.; Wennerström, H.: 6. Bilayer systems. In *The Colloidal Domain: Where Physics, Chemistry, Biology, and Technology Meet*; Wiley, 1999; pp 328-331.
- [14] Pearson, F. G.; Marchessault, R. H.; Liang, C. Y.: Infrared spectra of crystalline polysaccharides. V. Chitin. *J. Polym. Sci.* 1960, 43, 101-16.
- [15] Muzzarelli, R. A. A.; Morganti, P.; Morganti, G.; Palombo, P.; Palombo, M.; Biagini, G.; Mattioli Belmonte, M.; Giantomassi, F.; Orlandi, F.; Muzzarelli, C.: Chitin nanofibrils/chitosan glycolate composites as wound medicaments. *Carbohydr. Polym.* 2007, 70, 274-284.
- [16] Yuan, Y.; Lee, T. R.: Contact Angle and Wetting Properties. In *Surface Science Techniques*; Springer Berlin Heidelberg, 2013; pp 3-34.
- [17] Horvath, I. T.; Mehdi, H.; Fabos, V.; Boda, L.; Mika, L. T.:  $\gamma$ -Valerolactone – a sustainable liquid for energy and carbon-based chemicals. *Green Chem.* 2008, 10, 238-242.



## 4 Conclusion

In this work, for the purpose to successful fabricate novel chitin/cellulose and chitin/lignin composite materials in a sustainable and environmental benign process. First, several different solvents such as a conventional polar solvent system, DES and ILs were investigated for their solubility to dissolve MCC and  $\alpha$ -chitin. The results illustrates that the complete dissolution of both chitin and MCC are only successfully attained in DMAc/LiCl and BmimOAc. On the otherside, AmimBr shows a partial solubility for chitin, whereas cellulose is insoluble. EmimOAc is able to dissolve MCC and not chitin. It is noted that neither chitin nor MCC present a solubility in both choline chloride/urea (molar ratio, 1:2) and choline chloride/thiourea (molar ratio, 1:2) under the selected experimental conditions.

Because the solvent system DMAc/LiCl is not only toxicity and non-biodegradability but also need a required activation procedure for the biopolymers before they are dissolved. BmimOAc, which can directly dissolving chitin and other two biopolymers, might be an alternative solvent. In order to improve the sustainability of BmimOAc, a bio co-solvent GVL was added in an appropriate amounts in BmimOAc. Compared to sole BmimOAc, the BmimOAc-GVL solvent system has a considerable improved capacity to dissolve chitin, MCC and Kraft lignin. For instance, compared to the other solvent systems, BmimOAc-GVL has an obvious shorter dissolution time (3 h) for the biopolymers. The reason for this phenomenon could be that GVL reduces the viscosity of BmimOAc, which is beneficial for the dissolution of biopolymers with a high molecular weight. Furthermore, the addition of GVL offers significant improvement for the environmentally friendly of the dissolution process by lower the processing temperature from 120 °C to 90 °C.

Chitin/cellulose composite materials were first prepared by regeneration from their mixtures with above mentioned solvent systems. However, it is found that chitin/cellulose composite materials could be only successfully regenerated from DMAc/LiCl and BmimOAc-GVL in this work. The result is consistent with the dissolution ability of the two solvent systems for the two biopolymers. Furthermore, the weak composite gel regenerated from AmimBr and EmimOAc confirmed the incomplete dissolution of chitin in AmimBr. Considering the unsuccessfully fabrication of the chitin/lignin composites via the melt compounding process. The solution process using BmimOAc-GVL solvent system is considered as a suitable method for fabrication of both chitin/cellulose and chitin/lignin composites. Furthermore, the successful recycling of the solvent is revealed that the

solution process using BmimOAc-GVL for the fabrication chitin based composites is sustainable and environmentally benign.

The properties of the regenerated chitin based materials from BmimOAc-GVL solvent system were evaluated by means of various analytical methods. The analytical results indicate that chitin is not converted into chitosan by dissolving in BmimOAc-GVL, which is critical for the use of intact unaltered chitin in composite materials. Furthermore, the mechanical investigation illustrates that increasing the chitin content is beneficial for achieving elastic properties of the composite chitin/cellulose material. The chitin/cellulose composite materials with acceptable regularity shapes and good mechanical properties can be attained by drying with compressed air. In addition, the flexibility of the composite chitin/lignin films could be attributed to the presence of chitin. The obtained lignin/chitin films exhibits linear dimensional changes after drying, which decreased with the increasing concentration of chitin.

The evaluation of the modification of the chitin/cellulose composites was performed on chitin coated cellulosic materials. Chitin coatings on the surface of wood as well as on single-side of cellulosic textiles were successfully prepared from BmimOAc-GVL. The analytical results show that the chitin thin layer induces a specific hydrophobicity on the surfaces of wood and the cellulosic textiles. In addition, the chitin coating also slows down the penetration of water and oxygen into the coated materials, which suggests a potential application of chitin as a promising water and oxygen barrier.

The investigation of chitin/lignin composite as a biofilm sorbent was performed for Fe(III) and Cu(II) aqueous solutions at room temperature. It is observed that chitin/lignin composite film do not only shows a considerable adsorption/desorption capacity on Fe(III) and Cu(II) ions from aqueous solutions but also maintain an acceptable stability in the metal ion solutions. The adsorption mechanism of the chitin/lignin composite film is evaluated to follow a pseudo-second-order kinetic model. Furthermore, the result indicates that two mechanisms such as adsorption and ion-exchange are responsible for metal ion uptake in the composite films. The adsorption isotherms of the chitin/lignin composite film for both Fe(III) and Cu(II) can be described according to the Langmuir model. In addition, the chitin/lignin composite film shows readsorption ability for the metal ions, which indicates its stability and reusability as a biofilm sorbent.

This thesis offers possibilities and opportunities for the further development of high value added chitin based composite materials with environmental benign processes. Chitin-based composite materials show a bright future as a promising alternative to traditional petroleum based materials.

For instance, the obtained chitin/cellulose composite shows potential applications as biodegradable materials for packaging, medical devices or textiles. Chitin/lignin composite can be utilized as a biosorbent film in water purification. In order to overcome the limitations of the solubility of chitin and other biopolymers and scale-up of their fabrication from laboratory to industry, considerable efforts should be conducted for their dissolution, advanced sustainable processes, etc. Especially, an approach or solvent, which can dissolve chitin in large amount without deacetylation it into chitosan, would preferable. Since chitin is a promising renewable resource with high performance materials, the chitin based composite materials are expected to be increasingly explored and developed with facile and environmental benign processes in the near future.



## References:

1. Astudillo, J.C., et al., Detached aquaculture buoys in the SE Pacific: potential dispersal vehicles for associated organisms. *Aquatic Biology*, 2009. 5(3): p. 219-231.
2. Carpenter, E.J. and K. Smith, Plastics on the Sargasso Sea surface. *Science*, 1972. 175(4027): p. 1240-1241.
3. Jambeck, J.R., et al., Plastic waste inputs from land into the ocean. *Science*, 2015. 347(6223): p. 768-771.
4. Andrady, A.L., Microplastics in the marine environment. *Marine pollution bulletin*, 2011. 62(8): p. 1596-1605.
5. Ray, P., et al., Renewable Green Platform Chemicals for Polymers. *Molecules*, 2017. 22(3).
6. Hench, L.L., Biomaterials: a forecast for the future. *Biomaterials*, 1998. 19(16): p. 1419-1423.
7. Khalaf, M.N., *Green Polymers and Environmental Pollution Control*. 2016: CRC Press.
8. Radzuan, N.A.M., et al., Die configuration effects on electrical conductivity of polypropylene reinforced milled carbon fiber. *Technology*, 1995. 53(2): p. 125-131.
9. Mostafa, N., et al., Production of biodegradable plastic from agricultural wastes. *Arabian journal of chemistry*, 2018. 11(4): p. 546-553.
10. Faruk, O., et al., Progress report on natural fiber reinforced composites. *Macromolecular Materials and Engineering*, 2014. 299(1): p. 9-26.
11. Mohanty, A., M.a. Misra, and G. Hinrichsen, Biofibres, biodegradable polymers and biocomposites: An overview. *Macromolecular materials and Engineering*, 2000. 276(1): p. 1-24.
12. Huang, S.J., Polymer waste management—biodegradation, incineration, and recycling. *Journal of Macromolecular Science, Part A: Pure and Applied Chemistry*, 1995. 32(4): p. 593-597.
13. Dhand, V., et al., A short review on basalt fiber reinforced polymer composites. *Composites Part B: Engineering*, 2015. 73: p. 166-180.
14. Saito, T., A cost-effective P/M titanium matrix composite for automobile use. *Advanced Performance Materials*, 1995. 2(2): p. 121-144.
15. Li, J., et al., Improved fatigue performance for wood-based structural panels using slot and tab construction. *Composites Part A: Applied Science and Manufacturing*, 2016. 82: p. 235-242.
16. Sun, L., et al., Thermal decomposition of fire-retarded wood flour/polypropylene composites. *Journal of Thermal Analysis and Calorimetry*, 2016. 123(1): p. 309-318.
17. Mohanty, A., M. Khan, and G. Hinrichsen, Influence of chemical surface modification on the properties of biodegradable jute fabrics—polyester amide composites. *Composites Part A: Applied Science and Manufacturing*, 2000. 31(2): p. 143-150.
18. John, M.J. and S. Thomas, Biofibres and biocomposites. *Carbohydrate polymers*, 2008. 71(3): p. 343-364.

- 19.Kalia, S., B. Kaith, and I. Kaur, Pretreatments of natural fibers and their application as reinforcing material in polymer composites—a review. *Polymer Engineering & Science*, 2009. 49(7): p. 1253-1272.
- 20.Ciechanska, D., Multifunctional bacterial cellulose/chitosan composite materials for medical applications. *Fibres Text East Eur*, 2004. 12(4): p. 69-72.
- 21.Rinaudo, M., Chitin and chitosan: Properties and applications. *Progress in Polymer Science*, 2006. 31(7): p. 603-632.
- 22.Muzzarelli, R.A., Natural chelating polymers; alginic acid, chitin and chitosan, in *Natural chelating polymers; alginic acid, chitin and chitosan*. 1973, Pergamon Press.
- 23.Wysokowski, M., et al., Poriferan chitin as a versatile template for extreme biomimetics. *Polymers*, 2015. 7(2): p. 235-265.
- 24.Herrera, N., et al., Plasticized polylactic acid nanocomposite films with cellulose and chitin nanocrystals prepared using extrusion and compression molding with two cooling rates: Effects on mechanical, thermal and optical properties. *Composites Part A: Applied Science and Manufacturing*, 2016. 83: p. 89-97.
- 25.Takegawa, A., et al., Preparation of chitin/cellulose composite gels and films with ionic liquids. *Carbohydrate Polymers*, 2010. 79(1): p. 85-90.
- 26.Wysokowski, M., et al., Modification of Chitin with Kraft lignin and Development of New Biosorbents for Removal of Cadmium(II) and Nickel(II) Ions. *Marine Drugs*, 2014. 12(4): p. 2245.
- 27.Pillai, C.K.S., W. Paul, and C.P. Sharma, Chitin and chitosan polymers: Chemistry, solubility and fiber formation. *Progress in Polymer Science*, 2009. 34(7): p. 641-678.
- 28.Duan, Y., et al., Cellulose and chitin composite materials from an ionic liquid and a green co-solvent. *Carbohydrate Polymers*, 2018.
- 29.Kadokawa, J.-i., et al., Facile Preparation of Chitin/Cellulose Composite Films Using Ionic Liquids. *Journal of Polymers and the Environment*, 2012. 20(1): p. 37-42.
- 30.Wu, Y., et al., A novel biomass-ionic liquid platform for the utilization of native chitin. *Polymer*, 2008. 49(9): p. 2321-2327.
- 31.Kurita, K., Controlled functionalization of the polysaccharide chitin. *Progress in Polymer Science*, 2001. 26(9): p. 1921-1971.
- 32.Karrer, P. and A. Hofmann, Polysaccharide XXXIX. Über den enzymatischen Abbau von Chitin und Chitosan I. *Helvetica Chimica Acta*, 1929. 12(1): p. 616-637.
- 33.Muzzarelli, R.A., *Chitin*. 2013: Elsevier.
- 34.Odier, A., Mémoire sur la composition chimique des parties cornées des insectes. *Mem. Soc. Hist. Paris*, 1823. 1: p. 29-42.
- 35.Cárdenas, G., et al., Chitin characterization by SEM, FTIR, XRD, and <sup>13</sup>C cross polarization/mass angle spinning NMR. *Journal of Applied Polymer Science*, 2004. 93(4): p. 1876-1885.
- 36.El-Nesr, E., et al., Chitin and chitosan extracted from irradiated and non-irradiated shrimp wastes (Comparative Analysis Study). *Arab Journal of Nuclear Science and Applications*, 2013. 46(1): p. 53-66.

37. Kumar, M.N.R., A review of chitin and chitosan applications. *Reactive and functional polymers*, 2000. 46(1): p. 1-27.
38. Mogilevskaya, E., et al., The crystal structure of chitin and chitosan. *Polymer Science Series A*, 2006. 48(2): p. 116-123.
39. Gosselink, R., et al., Characterisation and application of NovaFiber lignin. *Industrial Crops and Products*, 2004. 20(2): p. 191-203.
40. Yen, M.-T., J.-H. Yang, and J.-L. Mau, Physicochemical characterization of chitin and chitosan from crab shells. *Carbohydrate Polymers*, 2009. 75(1): p. 15-21.
41. Horton, D. and D. Lineback, Deacetylation Chitosan from Chitin. In; Whistler RL, Wolfson ML, Eds. *Methods in Carbohydrate Chemistry*. New York: Academic Press, 1965. 403.
42. Park, B.K. and M.-M. Kim, Applications of chitin and its derivatives in biological medicine. *International journal of molecular sciences*, 2010. 11(12): p. 5152-5164.
43. Kurita, K., Chitin and chitosan: functional biopolymers from marine crustaceans. *Marine Biotechnology*, 2006. 8(3): p. 203.
44. Wei, L. and A. McDonald, A review on grafting of biofibers for biocomposites. *Materials*, 2016. 9(4): p. 303.
45. Barber, P.S., et al., Coagulation of Chitin and Cellulose from 1- Ethyl- 3- methylimidazolium Acetate Ionic- Liquid Solutions Using Carbon Dioxide. *Angewandte Chemie*, 2013. 125(47): p. 12576-12579.
46. Pu, Y., N. Jiang, and A.J. Ragauskas, Ionic liquid as a green solvent for lignin. *Journal of Wood Chemistry and Technology*, 2007. 27(1): p. 23-33.
47. King, C., et al., A platform for more sustainable chitin films from an ionic liquid process. *Green Chemistry*, 2017. 19(1): p. 117-126.
48. Khor, E. and L.Y. Lim, Implantable applications of chitin and chitosan. *Biomaterials*, 2003. 24(13): p. 2339-2349.
49. Ardizzone, S., et al., Microcrystalline cellulose powders: structure, surface features and water sorption capability. *Cellulose*, 1999. 6(1): p. 57-69.
50. Klemm, D., et al., Cellulose: fascinating biopolymer and sustainable raw material. *Angewandte Chemie International Edition*, 2005. 44(22): p. 3358-3393.
51. Klemm, D., et al., *Comprehensive cellulose chemistry. Volume 1: Fundamentals and analytical methods*. 1998: Wiley-VCH Verlag GmbH.
52. Klemm, D., et al., Cellulose: Fascinating Biopolymer and Sustainable Raw Material. *Angewandte Chemie International Edition*, 2005. 44(22): p. 3358-3393.
53. Varshney, V. and S. Naithani, Chemical functionalization of cellulose derived from nonconventional sources, in *Cellulose Fibers: Bio-and Nano-Polymer Composites*. 2011, Springer. p. 43-60.
54. Shokri, J. and K. Adibkia, Application of Cellulose and Cellulose Derivatives in Pharmaceutical Industries. *Cellulose - Medical, Pharmaceutical and Electronic Applications*. 2013.
55. Nevell, T.P. and S.H. Zeronian, *Cellulose chemistry and its applications*. 1985.

56. Siqueira, G., J. Bras, and A. Dufresne, Cellulosic bionanocomposites: a review of preparation, properties and applications. *Polymers*, 2010. 2(4): p. 728-765.
57. Huber, T., et al., A critical review of all-cellulose composites. *Journal of Materials Science*, 2012. 47(3): p. 1171-1186.
58. Rowell, R.M., *Handbook of wood chemistry and wood composites*. 2012: CRC press.
59. Park, S., et al., Cellulose crystallinity index: measurement techniques and their impact on interpreting cellulase performance. *Biotechnology for Biofuels*, 2010. 3(1): p. 1-10.
60. Thoorens, G., et al., Microcrystalline cellulose, a direct compression binder in a quality by design environment—A review. *International Journal of Pharmaceutics*, 2014. 473(1-2): p. 64-72.
61. Atalla, R.H. and D.L. Vanderhart, Native cellulose: a composite of two distinct crystalline forms. *Science*, 1984. 223(4633): p. 283-285.
62. Dufresne, A., Polymer nanocomposites from biological sources. *Encyclopedia of nanoscience and nanotechnology*, 2010: p. 219-250.
63. Nishiyama, Y., et al., Crystal structure and hydrogen bonding system in cellulose Ia from synchrotron X-ray and neutron fiber diffraction. *Journal of the American Chemical Society*, 2003. 125(47): p. 14300-14306.
64. O'sullivan, A.C., Cellulose: the structure slowly unravels. *Cellulose*, 1997. 4(3): p. 173-207.
65. Zugenmaier, P., Conformation and packing of various crystalline cellulose fibers. *Progress in polymer science*, 2001. 26(9): p. 1341-1417.
66. Terinte, N., R. Ibbett, and K.C. Schuster, Overview on native cellulose and microcrystalline cellulose I structure studied by X-ray diffraction (WAXD): Comparison between measurement techniques. *Lenzinger Berichte*, 2011. 89(1): p. 118.
67. Gaonkar, S. and P. Kulkarni, Improved method for the preparation of microcrystalline cellulose from water hyacinth. *Textile Dyer Printer*, 1987. 20(26): p. 19-22.
68. Tobyn, M.J., et al., Physicochemical comparison between microcrystalline cellulose and silicified microcrystalline cellulose. *International journal of pharmaceutics*, 1998. 169(2): p. 183-194.
69. El-Sakhawy, M. and M.L. Hassan, Physical and mechanical properties of microcrystalline cellulose prepared from agricultural residues. *Carbohydrate polymers*, 2007. 67(1): p. 1-10.
70. Mathew, A.P., K. Oksman, and M. Sain, Mechanical properties of biodegradable composites from poly lactic acid (PLA) and microcrystalline cellulose (MCC). *Journal of applied polymer science*, 2005. 97(5): p. 2014-2025.
71. Gong, W., et al., Lignin from bamboo shoot shells as an activator and novel immobilizing support for  $\alpha$ -amylase. *Food chemistry*, 2017. 228: p. 455-462.
72. dos Santos, P.S., et al., Characterisation of Kraft lignin separated by gradient acid precipitation. *Industrial Crops and Products*, 2014. 55: p. 149-154.
73. Sarkanen, K.V. and C.H. Ludwig, *Lignins. Occurrence, formation, structure, and reactions*. 1971.
74. Chakar, F.S. and A.J. Ragauskas, Review of current and future softwood Kraft lignin process chemistry. *Industrial Crops and Products*, 2004. 20(2): p. 131-141.

75. Baucher, M., et al., Biosynthesis and genetic engineering of lignin. *Critical reviews in plant sciences*, 1998. 17(2): p. 125-197.
76. Campbell, M.M. and R.R. Sederoff, Variation in Lignin Content and Composition (Mechanisms of Control and Implications for the Genetic Improvement of Plants). *Plant physiology*, 1996. 110(1): p. 3.
77. Kai, D., et al., Towards lignin-based functional materials in a sustainable world. *Green Chemistry*, 2016. 18(5): p. 1175-1200.
78. Hatakeyama, H., et al., Water absorbent polyurethane composites derived from molasses and lignin filled with microcrystalline cellulose. *Journal of Materials Science*, 2012. 47(20): p. 7254-7261.
79. Smook, G., *Handbook for Pulp and Paper Technologists*. 1992 Angus Wilde Publications. 1992, Vancouver.
80. Bernardini, J., et al., Flexible polyurethane foams green production employing lignin or oxypropylated lignin. *European Polymer Journal*, 2015. 64: p. 147-156.
81. Angela, P., F. John, and K. Suzana, Characterization of Fractions Obtained from Two Industrial Softwood Kraft lignins. *ACS sustainable chemistry*, 2015.
82. Passoni, V., et al., Fractionation of industrial softwood Kraft lignin: Solvent selection as a tool for tailored material properties. *ACS Sustainable Chemistry & Engineering*, 2016. 4(4): p. 2232-2242.
83. Jääskeläinen, A.-S., et al., Aqueous organic solvent fractionation as means to improve lignin homogeneity and purity. *Industrial crops and products*, 2017. 103: p. 51-58.
84. Khuu, R., S. Joshua, and J. Ragauskas, Fractionation of Organosolv Lignin Using Acetone: Water and Properties of the Obtained Fractions. *ACS sustainable chemistry*, 2017.
85. Sarkanen, K., Acid-catalyzed delignification of lignocellulosics in organic solvents, in *Progress in biomass conversion*. 1980, Elsevier. p. 127-144.
86. El Hage, R., et al., Characterization of milled wood lignin and ethanol organosolv lignin from miscanthus. *Polymer Degradation and Stability*, 2009. 94(10): p. 1632-1638.
87. Jiang, J.E., et al., Relationship between residual lignin structure and pulp bleachability. 1996.
88. Lee, Y.-Y. and B.-H. Lee, Solvent-phase thermal cracking of lignin for production of potential liquid fuels. *Journal of Industrial and Engineering Chemistry*, 1998. 4(4): p. 334-339.
89. Zhou, C.-G., et al., Remarkable performance of magnetized chitosan-decorated lignocellulose fiber towards biosorptive removal of acidic azo colorant from aqueous environment. *Reactive and Functional Polymers*, 2016. 100: p. 97-106.
90. Yang, S., et al., Lignin-phenol-formaldehyde resin adhesives prepared with biorefinery technical lignins. *Journal of Applied Polymer Science*, 2015. 132(36).
91. Toriz, G., F. Denes, and R. Young, Lignin- polypropylene composites. Part 1: Composites from unmodified lignin and polypropylene. *Polymer Composites*, 2002. 23(5): p. 806-813.
92. Liu, R., et al., Comparison on properties of lignocellulosic flour/polymer composites by using wood, cellulose, and lignin flours as fillers. *Composites Science and Technology*, 2014. 103: p. 1-7.
93. Mousavioun, P., P.J. Halley, and W.O. Doherty, Thermophysical properties and rheology of PHB/lignin blends. *Industrial crops and products*, 2013. 50: p. 270-275.

94. Thakur, V.K., M.K. Thakur, and R.K. Gupta, Graft copolymers of natural fibers for green composites. *Carbohydrate polymers*, 2014. 104: p. 87-93.
95. Stewart, D., Lignin as a base material for materials applications: Chemistry, application and economics. *Industrial crops and products*, 2008. 27(2): p. 202-207.
96. Chung, Y.-L., et al., A renewable lignin–lactide copolymer and application in biobased composites. *ACS Sustainable Chemistry & Engineering*, 2013. 1(10): p. 1231-1238.
97. Thakur, V., M. Thakur, and A. Singha, Free radical–induced graft copolymerization onto natural fibers. *International Journal of Polymer Analysis and Characterization*, 2013. 18(6): p. 430-438.
98. Thakur, V.K., et al., Progress in green polymer composites from lignin for multifunctional applications: a review. *ACS Sustainable Chemistry & Engineering*, 2014. 2(5): p. 1072-1092.
99. Fowler, P.A., J.M. Hughes, and R.M. Elias, Biocomposites: technology, environmental credentials and market forces. *Journal of the Science of Food and Agriculture*, 2006. 86(12): p. 1781-1789.
100. Zhang, Y., et al., Formation and Characterization of Cellulose Membranes from N- Methylmorpholine- N- oxide Solution. *Macromolecular Bioscience*, 2001. 1(4): p. 141-148.
101. Ishii, D., et al., Investigation of the Structure of Cellulose in LiCl/DMAc Solution and Its Gelation Behavior by Small- Angle X- Ray Scattering Measurements. *Macromolecular bioscience*, 2006. 6(4): p. 293-300.
102. Bouyer, D., et al., Influence of mass transfer on gelation time using VIPS-gelation process for chitin dissolved in LiCl/NMP solvent—Modelling and experimental study. *Chemical Engineering Journal*, 2010. 157(2-3): p. 605-619.
103. Ostlund, Å., et al., Dissolution and gelation of cellulose in TBAF/DMSO solutions: the roles of fluoride ions and water. *Biomacromolecules*, 2009. 10(9): p. 2401-2407.
104. Tamura, H., H. Nagahama, and S. Tokura, Preparation of chitin hydrogel under mild conditions. *Cellulose*, 2006. 13(4): p. 357-364.
105. Shen, X., et al., Hydrogels based on cellulose and chitin: fabrication, properties, and applications. *Green Chemistry*, 2016. 18(1): p. 53-75.
106. Abbott, A.P., et al., Novel solvent properties of choline chloride/urea mixtures. *Chemical Communications*, 2003(1): p. 70-71.
107. Cai, J. and L. Zhang, Rapid dissolution of cellulose in LiOH/urea and NaOH/urea aqueous solutions. *Macromolecular Bioscience*, 2005. 5(6): p. 539-548.
108. Marson, G.A. and O.A. El Seoud, Cellulose dissolution in lithium chloride/N,N-dimethylacetamide solvent system: relevance of kinetics of decrystallization to cellulose derivatization under homogeneous solution conditions. *J Polym Sci Polym Chem*, 1999. 37.
109. Mukesh, C., et al., Choline chloride–thiourea, a deep eutectic solvent for the production of chitin nanofibers. *Carbohydrate polymers*, 2014. 103: p. 466-471.
110. Fukaya, Y., et al., Cellulose dissolution with polar ionic liquids under mild conditions: required factors for anions. *Green Chemistry*, 2008. 10(1): p. 44-46.
111. Wang, H., G. Gurau, and R.D. Rogers, Ionic liquid processing of cellulose. *Chemical Society Reviews*, 2012. 41(4): p. 1519-1537.

112. Prasad, K., et al., Weak gel of chitin with ionic liquid, 1-allyl-3-methylimidazolium bromide. *International Journal of Biological Macromolecules*, 2009. 45(3): p. 221-225.
113. Krossing, I., et al., Why are ionic liquids liquid? A simple explanation based on lattice and solvation energies. *J. Am. Chem. Soc.*, 2006. 128(Copyright (C) 2015 American Chemical Society (ACS). All Rights Reserved.): p. 13427-13434.
114. Forsyth, S.A., J.M. Pringle, and D.R. MacFarlane, Ionic Liquids-An Overview. *Aust. J. Chem.*, 2004. 57(Copyright (C) 2015 American Chemical Society (ACS). All Rights Reserved.): p. 113-119.
115. Holbrey, J.D., Industrial applications of ionic liquids. *Chim. Oggi*, 2004. 22(Copyright (C) 2015 American Chemical Society (ACS). All Rights Reserved.): p. 35-37.
116. Rogers, R.D., K.R. Seddon, and Editors, *Ionic Liquids: Industrial Applications for Green Chemistry*. (Proceedings of a Symposium held 1-5 April 2001 in San Diego, California.) [In: ACS Symp. Ser., 2002; 818]. 2002: American Chemical Society. 474 pp.
117. Wang, H., G. Gurau, and R.D. Rogers, Ionic liquid processing of cellulose. *Chem. Soc. Rev.*, 2012. 41(Copyright (C) 2014 American Chemical Society (ACS). All Rights Reserved.): p. 1519-1537.
118. Muzzarelli, R.A.A., Biomedical exploitation of chitin and chitosan via mechano-chemical disassembly, electrospinning, dissolution in imidazolium ionic liquids, and supercritical drying. *Mar. Drugs*, 2011. 9(Copyright (C) 2015 American Chemical Society (ACS). All Rights Reserved.): p. 1510-1533.
119. Prasad, K., et al., Weak gel of chitin with ionic liquid, 1-allyl-3-methylimidazolium bromide. *Int. J. Biol. Macromol.*, 2009. 45(Copyright (C) 2015 American Chemical Society (ACS). All Rights Reserved.): p. 221-225.
120. Pinkert, A., et al., Ionic liquids and their interaction with cellulose. *Chem. Rev. (Washington, DC, U. S.)*, 2009. 109(Copyright (C) 2015 American Chemical Society (ACS). All Rights Reserved.): p. 6712-6728.
121. Sun, X., et al., The dissolution behavior of chitosan in acetate-based ionic liquids and their interactions: from experimental evidence to density functional theory analysis. *RSC Adv.*, 2014. 4(Copyright (C) 2015 American Chemical Society (ACS). All Rights Reserved.): p. 30282-30291.
122. Wang, W.-T., et al., Dissolution Behavior of Chitin in Ionic Liquids. *J. Macromol. Sci., Part B: Phys.*, 2010. 49(Copyright (C) 2015 American Chemical Society (ACS). All Rights Reserved.): p. 528-541.
123. Stolte, S., et al., Effects of different head groups and functionalised side chains on the aquatic toxicity of ionic liquids. *Green Chemistry*, 2007. 9(11): p. 1170-1179.
124. Wood, N. and G. Stephens, Accelerating the discovery of biocompatible ionic liquids. *Physical Chemistry Chemical Physics*, 2010. 12(8): p. 1670-1674.
125. Klapiszewski, Ł., et al., Preparation and characterization of multifunctional chitin/lignin materials. *Journal of Nanomaterials*, 2013. 2013: p. 12.
126. Bartczak, P., et al., Treatment of model solutions and wastewater containing selected hazardous metal ions using a chitin/lignin hybrid material as an effective sorbent. *Journal of environmental management*, 2017. 204: p. 300-310.
127. Salman, M., M. Athar, and U. Farooq, Biosorption of heavy metals from aqueous solutions using indigenous and modified lignocellulosic materials. *Reviews in Environmental Science and Bio/Technology*, 2015. 14(2): p. 211-228.

128. Alomá, I., et al., Removal of nickel (II) ions from aqueous solutions by biosorption on sugarcane bagasse. *Journal of the Taiwan Institute of Chemical Engineers*, 2012. 43(2): p. 275-281.
129. Shankar, S., et al., Preparation, characterization, and antimicrobial activity of chitin nanofibrils reinforced carrageenan nanocomposite films. *Carbohydrate Polymers*, 2015. 117: p. 468-475.
130. Freyburger, A., Novel bio-based materials from cellulose and chitin. PhD Thesis, Universität Regensburg, 2018.
131. Röder, T., et al., Solutions of cellulose in N,N-dimethylacetamide/lithium chloride studied by light scattering methods. *Polymer*, 2001. 42(16): p. 6765-6773.
132. Dupont, A.-L., Cellulose in lithium chloride/N,N-dimethylacetamide, optimisation of a dissolution method using paper substrates and stability of the solutions. *Polymer*, 2003. 44(15): p. 4117-4126.
133. Alonso, D.M., S.G. Wettstein, and J.A. Dumesic, Gamma-valerolactone, a sustainable platform molecule derived from lignocellulosic biomass. *Green Chemistry*, 2013. 15(3): p. 584-595.
134. Sharma, M., et al., Dissolution of  $\alpha$ -chitin in deep eutectic solvents. *Rsc Advances*, 2013. 3(39): p. 18149-18155.
135. Tang, X., et al., Green processing of lignocellulosic biomass and its derivatives in deep eutectic solvents. *ChemSusChem*, 2017. 10(13): p. 2696-2706.
136. Swatloski, R.P., J.D. Holbrey, and R.D. Rogers, Ionic liquids are not always green: hydrolysis of 1-butyl-3-methylimidazolium hexafluorophosphate. *Green Chemistry*, 2003. 5(4): p. 361-363.
137. Vigier, K.D.O., G. Chatel, and F. Jerome, Contribution of deep eutectic solvents for biomass processing: opportunities, challenges, and limitations. *ChemCatChem*, 2015. 7(8): p. 1250-1260.
138. Fukumoto, K., M. Yoshizawa, and H. Ohno, Room temperature ionic liquids from 20 natural amino acids. *Journal of the American Chemical Society*, 2005. 127(8): p. 2398-2399.
139. Forsyth, S.A., J.M. Pringle, and D.R. MacFarlane, Ionic Liquids; An Overview. *Australian Journal of Chemistry*, 2004. 57(2): p. 113-119.
140. Pang, J.-H., et al., Fabrication and Characterization of Regenerated Cellulose Films Using Different Ionic Liquids. *Journal of Spectroscopy*, 2014. 2014: p. 8.
141. Nelson, M.L. and R.T. O'Connor, Relation of certain infrared bands to cellulose crystallinity and crystal latticed type. Part I. Spectra of lattice types I, II, III and of amorphous cellulose. *Journal of Applied Polymer Science*, 1964. 8(3): p. 1311-1324.
142. Vogler, E.A., Structure and reactivity of water at biomaterial surfaces. *Advances in colloid and interface science*, 1998. 74(1): p. 69-117.
143. García-González, C., et al., Supercritical drying of aerogels using CO<sub>2</sub>: Effect of extraction time on the end material textural properties. *The Journal of Supercritical Fluids*, 2012. 66: p. 297-306.
144. Mantanis, G. and R. Young, Wetting of wood. *Wood science and Technology*, 1997. 31(5): p. 339.

## Appendices

### Appendix 1. Fabrication of chitin based composites

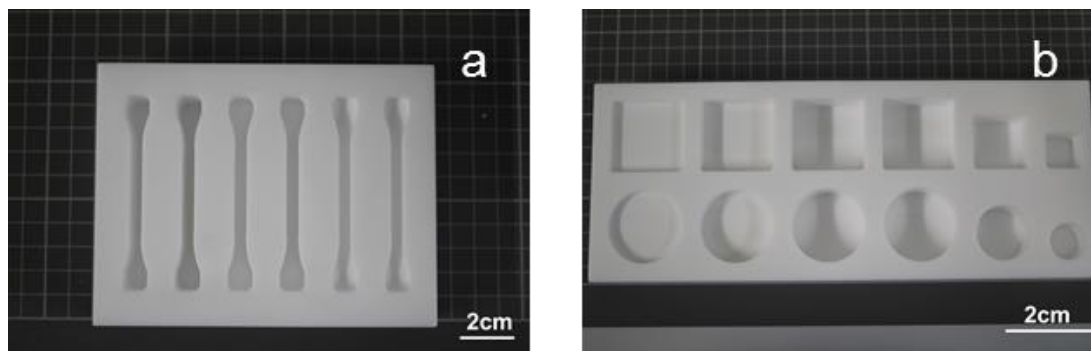


**Figure A.1:** Teflon mould for preparing the chitin based composite gel (a) and film (b).

### Appendix 2. Dissolution of chitin and lignin in BmimOAc-GVL

The dissolution of Kraft lignin in BmimOAc-GVL was confirmed using a light microscope (Leitz, Germany).

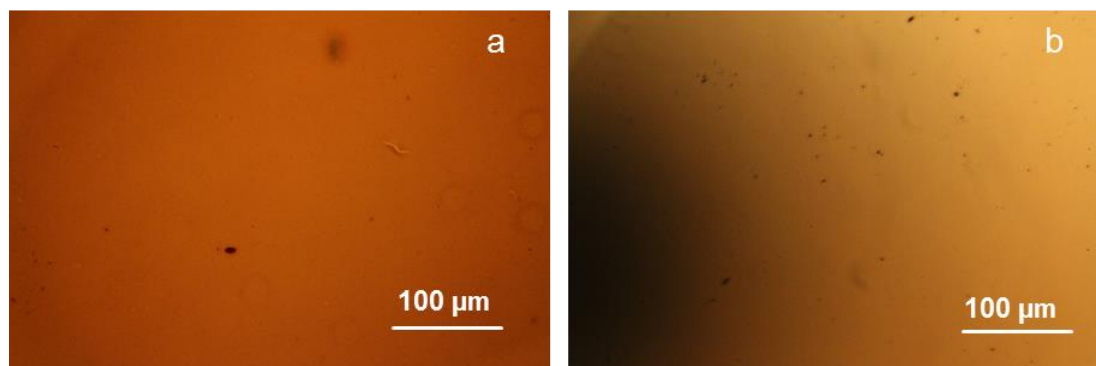


**Figure A.2:** Light microscopy images of mixtures containing (a) 30 wt%, (b) 35 wt% Kraft lignin in BmimOAc-GVL (mass ratio: 4:1) under the selected experimental conditions.



## **Acknowledgement**

I would like to take this opportunity to express my sincere gratitude to all those who contributed to the creation of this work with their kind support. Especially appreciate on my supervisor Prof. Cordt Zollfrank for giving the opportunity and endless support of the work, the constant and motivating promotion as well as the creation of a productive work environment.

I would like to thank my mentor Prof. Werner Kunz, an expert in solution chemistry from Institute of Physical and Theoretical Chemistry, University of Regensburg, for his great mentorship and guidance. Meantime, as one of the dissertation project member, he also supplied me invaluable advice and insightful comments. I am also grateful to my project partner Dr. Auriane Freyburger, for the contribution on this work and pleasant cooperation.

I would also like to express my appreciation for the all the colleagues in the Department of Biogenic Polymers at the Technical University of Munich for their kindly and continued support. With a special mention to Sabine Kugel, Steffi Deuerling, Maria Haslböck, Jörg Dörrstein, Matthias Langhansl, Maximilian Rothammer, Korbinian Sommer and Dr. Daniel Van Opdenbosch for their friendly contribution in various projects related to this dissertation. Furthermore, I would like to thanks to Petra Peklo for the help with administrative tasks and Sabine Witzel for the help with laboratory organization as well as Christina Sagmeister from Professorship Chemical Process Engineering for technical assistance of this work. I am very lucky to be in such a warm and active group. Without your help, this work could not be possible to completion. Moreover, because of you, my experience of PhD study was full of exciting and fun and it would be one of the best memories of my life.

Many thanks also giving to the Bavarian State Ministry of the Environment and Consumer Protection and TUM Graduate School for their financial supports.

Last but not least, I would like to express my deepest gratitude to my family and friends for their warm love, continued patience and endless support. Especially on my son Modi, his love and understanding are the motivation for me to achieve my goal.

Yaqing Duan